Sede Amministrativa: Università degli Studi di Padova

Dipartimento di Scienze Biomediche

CORSO DI DOTTORATO DI RICERCA IN: BIOSCIENZE E BIOTECNOLOGIE
CURRICOLO: BIOCHIMICA E BIOFISICA
CICLO: XXIX

Mitochondrial ROS formation catalyzed by monoamine oxidase is causally related to inflammation, fibrosis and diastolic dysfunction in type 1 diabetic hearts

Tesi redatta con il contributo finanziario dell'EU FP7-PEOPLE-2012-ITN Marie Sklodowska Curie, titolo del progetto: "RADical reduction of OXidative stress in cardiovascular diseases (RADOX)"

Coordinatore: Prof. Paolo Bernardi
Supervisore: Prof. Fabio Di Lisa
Co-Supervisore: Dr. Nina Kaludercic

Dottorando: Soni Deshwal

ACKNOWLEDGEMENTS

This thesis would not have been possible without a number of people who assisted me in my research, helped me learn important skills and gave me valuable advice.

First and foremost I would like to express my deepest gratitude to my supervisor, **Prof. Fabio Di Lisa**, without his guidance and persistent help this study would not have been possible. From the beginning till the end he taught me a lot about mitochondrial and cardiovascular field and continuously encouraged me to present my work in several international conferences. He exposed me to the great scientific community and always supported me academically and emotionally throughout my stay in his laboratory.

Besides my supervisor, I would like to thank my co-supervisor, **Dr. Nina Kaludercic**, who guided me and showed me always the right direction during my PhD. She helped me in learning all the technical skills and interpreting data which were required to complete this study. She not only supported me as a tutor but also as a friend during my stay in Padova. She always helped me and encouraged in my hard times and motivated me to finish what I started. Without her help and guidance it would not have been possible to conduct this research and write this thesis.

I thank all my colleagues and lab members, especially **Dr. Moises Di Sante**, for the stimulating discussions, for all the feedback that I received on my writing and for all the fun we had during these years. I would also like to thank all my friends in Padova and abroad, who gave me memorable moments, moral support and encouragement to successfully write this thesis and stay motivated to further continue my career in the research. I am also thankful to **RADOX ITN** and **Marie Skłodowska-Curie fellowship** for providing me financial support and a giving me a great opportunity to meet other amazing fellows in the network.

Last but not the least, my greatest thanks to my parents, sister and brother for giving me love, encouragement and for supporting me in my decision to come abroad and pursue my passion for science. Words cannot express how grateful I am to my loving partner, Vito Pellegrini, for all the support, patience and unconditional love that he gave me during all these years. Thank you.

INDEX

1. ABBREVIATIONS

12/15-LO	12/15-lipoxygenase
15-S-HETE	15-(S)-Hydroxyeicosatetraeonic acid
ADP	Adenosine di-phosphate
AGEs	Advanced glycation end products
ALDH	Aldehyde dehydrogenase
AMP	Adenosine monophosphate
AMPK	Adenosine monophosphate-activated protein kinase
ATF4	Activating-transcription factor 4
ATF6	Activating-transcription factor 6
ATP	Adenosine triphosphate
BiP	Binding immunoglobulin protein
CAMKII	Calcium activates Ca^{2+}/calmodulin-dependent protein kinase II
CHOP	C/EBP homologous protein
ECM	Extra-cellular matrix
eIF2α	Eukaryotic translation initiation factor 2α
ER	Endoplasmic reticulum
ERAD	ER-associated degradation pathway
ERK	Extracellular signal regulated kinase
ETC	Electron transport chain
FAD	Flavin adenine dinucleotide
FCCP	Carbonyl cyanide-4-phenylhydrazone
GADD34	Growth arrest and DNA damage 34
GFAD	Glutamine-fructose-6-phosphate amidotransferase
GLUT	Glucose transporter
GRP78	78 kDa glucose-regulated protein
H_2O_2	Hydrogen peroxide
HBSS	Hank's balanced salt solution
HFpEF	Heart failure with preserved ejection fraction
HG	High glucose

HLA	Human leukocyte antigen
HM	High mannitol
HNE	Hydroxynonenal
IMM	Inner mitochondrial membrane
I/R	Ischemia/reperfusion
IL-1β	Interleukin-1β
IR	Insulin receptor
IRE-1	Inositol-requiring kinase-1
IRS	Insulin receptor substrates
KO	Knockout
LV	Left ventricle
MAMs	Mitochondria associated membranes
MAO	Monomaine oxidase
MEM	Minimum essential media
Mn-SOD	Manganese-superoxide dismutase
MPTP	Mitochondrial permeability transition pore
MRI	Magnetic resonance imaging
mTOR	Mammalian target of rapamycin
MTR	MitoTracker Red CM-H_2XROS
NADPH	Nicotinamide adenine dinucleotide phosphate
NF-κB	Nuclear factor kappa-light-chain-enhancer of activated B cells
NG	Normal glucose
NLRP3	Nucleotide-binding oligomerization domain-like receptors with pyrin domain
NOS	Nitric oxide synthase
Nox	NADPH oxidase
Nrf2	Nuclear factor (erythroid-derived 2)-like-2 factor
NRVMs	Neonatal rat ventricular myocytes
OGT	O-GlcNAc transferase
OMM	Outer mitochondrial membrane
PERK	Protein kinase R-like ER kinase
PI3K	Phosphoinositide 3-kinase

PIP2	Phosphatidylinositol 4,5-bisphosphate
PIP3	Phosphatidylinositol 3,4,5-trisphosphate
PKB	Protein kinase B
PV	Pressure volume
RAGE	Receptor for advance glycation end products
ROS	Reactive oxygen species
S1P	Sphingosine-1-phosphate
SERCA	Sarco/ER Ca^{2+} ATPase
SGLT	Sodium/glucose cotransporter family
SIRT1	Sirtuin 1
STZ	Streptozotocin
T1D	Type 1 diabetes
T2D	Type 2 diabetes
TAC	Transverse aortic constriction
TGF-β	Transforming growth factor-β
TMRM	Tetramethylrhodamine
TNFα	Tumor necrosis factor α
TUDCA	Tauroursodeoxycholic acid
UPR	Unfolded protein response
WT	Wild type
XBP1	X-box-binding protein 1
XO	Xanthine oxidase
ΔΨm	Mitochondrial membrane potential

2. SOMMARIO

Le malattie cardiovascolari sono le principali cause di morte tra i pazienti diabetici. Tra i vari meccanismi che contribuiscono allo sviluppo della cardiomiopatia diabetica, lo stress ossidativo ha ricevuto un'attenzione clinica e sperimentale significativa. Tuttavia, l'uso di terapie antiossidanti in studi clinici su larga scala è risultato inefficace nel trattamento di questi disturbi patologici. Nel complesso, questi studi indicano una reale necessità di sviluppare strategie terapeutiche volte a inibire specifiche fonti di specie reattive dell'ossigeno (ROS). Lo scopo di questa tesi è stato quello di valutare il ruolo delle monoammino ossidasi (MAO), enzimi mitocondriali localizzati nella membrana esterna, nello stress ossidativo e nella disfunzione mitocondriale in cardiomiociti esposti ad elevate concentrazione di glucosio (in vitro) ed il loro contributo in vivo nei danni cardiaci in un modello di T1D.

Inizialmente, abbiamo valutato la formazione di ROS e la funzione mitocondriale in cardiomiociti primari trattati con alti livelli di glucosio (HG) e/o interleuchina-1β (IL-1β), una citochina pro-infiammatoria presente in livelli elevati in pazienti diabetici. Le cellule esposte a questi stimoli mostrano un aumento della formazione di ROS, accompagnata da disfunzione mitocondriale, come determinato dal minore potenziale di membrana mitocondriale. La pargilina, un inibitore MAO, previene completamente queste alterazioni, suggerendo che HG e IL-1β inducano la formazione di ROS e le disfunzione mitocondriale MAO-dipendente.

Inoltre, per valutare se l'attività della MAO sia coinvolta nell'interazione tra i mitocondri ed il reticolo endoplasmatico (ER) e se possa determinare l'attivazione del'Unfolded Protein Response (UPR), in questo modello abbiamo misurato marcatori di stress dell'ER. È interessante notare come, in cardiomiociti adulti, l'espressione della proteina transcription factor 4 (ATF4), della growth arrest and DNA damage-inducible protein (GADD34), 78 kDa glucose-regulated protein (GRP78) e i livelli di fosforillazione di IRE1α (inositol-requiring enzyme 1α) siano significativamente elevati, il che dimostra la chiara presenza di stress del reticolo (ER). La somministrazione di pargilina previene e blocca queste alterazioni, suggerendo che MAO sia coinvolto nel processo di UPR indotto dalla combinazione di alto glucosio e IL-1β. Inoltre questi dati suggeriscono che, almeno in queste condizioni, la formazione di ROS MAO-dipendente è a monte dello stress del reticolo (ER) e svolge un

ruolo importante nell'interazione tra mitocondri, infiammazione del reticolo in cardiomiociti esposti a condizioni simulanti il diabete.

Dato il coinvolgimento della MAO nel danno cellulare causato da HG e IL-1β, abbiamo valutato il suo ruolo nella disfunzione cardiaca in modelli murini di diabete di tipo 1 (T1D) indotta da trattamento con streptozotocina (STZ). La rigidità diastolica, un indice di disfunzione diastolica, era significativamente aumentata nei topi STZ, mentre la frazione di eiezione, un indice di funzione sistolica, è rimasta invariata. Inoltre, i marcatori di stress ossidativo (4-idrossinonenale) e UPR (ATF4 e GADD34) sono risultati significativamente aumentati nei cuori STZ rispetto al controllo. È importante sottolineare come i topi diabetici trattati con la pargilina, inibitore specifico per MAO, abbiano mostrato una funzione diastolica preservata e l'assenza di stress ossidativo e dell' ER. In accordo con studi precedenti dove si dimostra come la fibrosi è una delle caratteristiche principali nella cardiomiopatia diabetica, i cuori dei topi diabetici evidenziano una maggiore deposizione di collagene. È interessante notare che la somministrazione di pargilina ha impedito questa alterazione, suggerendo che l'attività MAO rivesta un ruolo cruciale nella progressione della fibrosi in questi animali. Al fine di determinare se la fibrosi MAO-mediata sia dovuta al rilascio di fattori pro-infiammatori e pro-fibrotici da mastociti cardiaci, abbiamo valutato la loro degranulazione. Abbiamo osservato che, la degranulazione dei mastociti è aumentata di quasi 2 volte nei cuori diabetici rispetto ai topi di controllo. L'inibizione MAO ha completamente bloccato l'attivazione dei mastociti nei topi diabetici. Questi dati indicano un ruolo completamente nuovo di questi flavoenzimi nell'attivare mastociti cardiaci alla base del rimodellamento della matrice extracellulare, nella fibrosi e in ultima analisi, nella disfunzione del ventricolo sinistro (LV) in T1D.

Complessivamente, questi risultati dimostrano non solo come le MAO contribuisca alla formazione di ROS e alla disfunzione mitocondriale indotta da HG e dall'infiammazione, ma anche che queste specie reattive perturbano la funzione dell'ER e portano all'attivazione dell'UPR. Inoltre, abbiamo dimostrato come questi flavoenzimi svolgano un ruolo importante nella formazione di un circolo vizioso tra stress ossidativo e infiammazione, che è probabilmente la causa della fibrosi cardiaca e della disfunzione diastolica ventricolare sinistra nei topi diabetici. Gli inibitori MAO sono clinicamente disponibili e vengono utilizzati per il trattamento di diverse malattie neurologiche e neurodegenerative. I risultati del

nostro studio suggeriscono come l'inibizione MAO potrebbe essere una strategia terapeutica promettente anche per il trattamento delle complicazioni cardiovascolari nel diabete.

3. SUMMARY

Cardiovascular disease is the leading cause of death among diabetic patients. Amongst various mechanisms proposed to contribute to the development of diabetic cardiomyopathy, oxidative stress has received significant experimental and clinical evaluation. However, large scale clinical trials using antioxidant therapies for the treatment of these pathological disorders have been ineffective. Collectively, these studies point towards a serious need to develop therapeutic strategies aimed at inhibiting specific sources of reactive oxygen species (ROS). In the present thesis, we investigated the role of monoamine oxidases (MAOs), outer mitochondrial enzymes that generate H_2O_2, in oxidative stress and mitochondrial dysfunction in cardiomyocytes exposed to diabetic milieu and cardiac damage in type 1 diabetes (T1D) mice in vivo.

Initially, we assessed ROS formation and mitochondrial function in primary cardiomyocytes treated with high glucose (HG) and/or interleukin-1β (IL-1β), a pro-inflammatory cytokine found to be elevated in diabetic patients. Cells exposed to these stimuli displayed an increase in ROS formation which was accompanied by mitochondrial dysfunction as documented by decreased mitochondrial membrane potential. MAO inhibitor pargyline completely prevented these alterations, suggesting that HG and IL-1β induce ROS formation and mitochondrial dysfunction in a MAO-dependent manner. Moreover, to study whether MAO activity is also involved in endoplasmic reticulum (ER)-mitochondria cross-talk and activation of unfolded protein response (UPR), we assessed markers of ER stress in this model. Interestingly, in adult cardiomyocytes, protein expression of activating transcription factor 4 (ATF4), growth arrest and DNA damage-inducible protein (GADD34), 78 kDa glucose-regulated protein (GRP78) and phosphorylation levels of IRE1α (inositol-requiring enzyme 1α) were significantly upregulated, marking the clear occurrence of ER stress. Pargyline administration abrogated these changes, suggesting that MAO is involved in HG and IL-1β induced UPR. Moreover, this suggests that, at least in this setting, MAO-dependent ROS formation is upstream of ER stress, and play an important role in the cross-talk between mitochondria, inflammation and ER stress occurring in cardiomyocytes exposed to diabetic milieu.

Given the involvement of MAO in HG and IL-1β induced cell damage, we investigated its role in cardiac dysfunction in streptozotocin (STZ)-induced T1D. We found that diastolic stiffness, an index of diastolic dysfunction, was significantly increased in STZ mice, whereas ejection fraction, an index of systolic function, remained unchanged. Moreover, markers of oxidative stress (4-hydroxynonenal) and UPR (ATF4 and GADD34) were significantly increased in STZ hearts as compared to controls. Importantly, STZ mice treated with MAO inhibitor pargyline displayed preserved diastolic function and absence of ER and oxidative stress. In agreement with previous reports showing that fibrosis is one of the major features of diabetic cardiomyopathy, we found that hearts from STZ-treated mice displayed increased collagen deposition. Interestingly, pargyline administration prevented this alteration, suggesting that MAO activity plays a crucial role in the progression of fibrosis in these animals. To understand whether MAO-mediated fibrosis was due to release of pro-inflammatory and pro-fibrotic factors from cardiac mast cells, we assessed mast cell degranulation. Indeed, mast cell degranulation increased by almost 2-fold in STZ hearts as compared to control mice. MAO inhibition completely blocked the activation of mast cells in diabetic mice. These data indicate the novel role of these flavoenzymes in activating cardiac mast cell thereby leading to the remodeling of the extracellular matrix, fibrosis and ultimately, left ventricle (LV) dysfunction in T1D.

Collectively, these results demonstrate that MAOs not only contribute to HG and inflammation induced mitochondrial ROS formation and dysfunction, but they also perturb ER function leading to the activation of UPR. Moreover, we showed that these flavoenzymes play a major role in the formation of a vicious cycle between oxidative stress and inflammation, which is likely the underlying cause of cardiac fibrosis and LV diastolic dysfunction in T1D mice. MAO inhibitors are clinically available and are being used for the treatment of several neurological and neurodegenerative diseases. Results from our study suggest that MAO inhibition could be a promising therapeutic strategy also for the treatment of cardiovascular complications in diabetes.

4. INTRODUCTION

4.1 DIABETES

Diabetes is a chronic condition associated with high levels of glucose in the blood. Pancreatic β-cells release peptide hormone insulin in the blood stream to maintain the levels of glucose in the blood. This hormone triggers the uptake of glucose, fatty acids and amino acids into liver, adipose tissue and muscle and promotes the storage of these nutrients in the form of glycogen, lipids and proteins, respectively [1]. In diabetic or pre-diabetic conditions, either the pancreatic islets do not secrete insulin or the body cells become insulin resistant, leading to high blood sugar.

The common symptoms of diabetes include

- Hunger and fatigue
- Frequent urination (polyuria)
- Extreme hunger even after eating adequate amounts of food (type 1)
- Slow healing
- Weight loss (type 1), obesity (type 2)
- Blurry vision
- Tingling in the hands and/or feet
- Sometimes dry mouth, itchy skin

The number of people affected by diabetes is rapidly increasing. As shown in Figure 1, according to IDF (International Diabetes Federation) one in eleven adults has diabetes and this ratio is expected to further increase in coming years. These statistics clearly indicate a need for the better understanding of the pathophysiology of this disease.

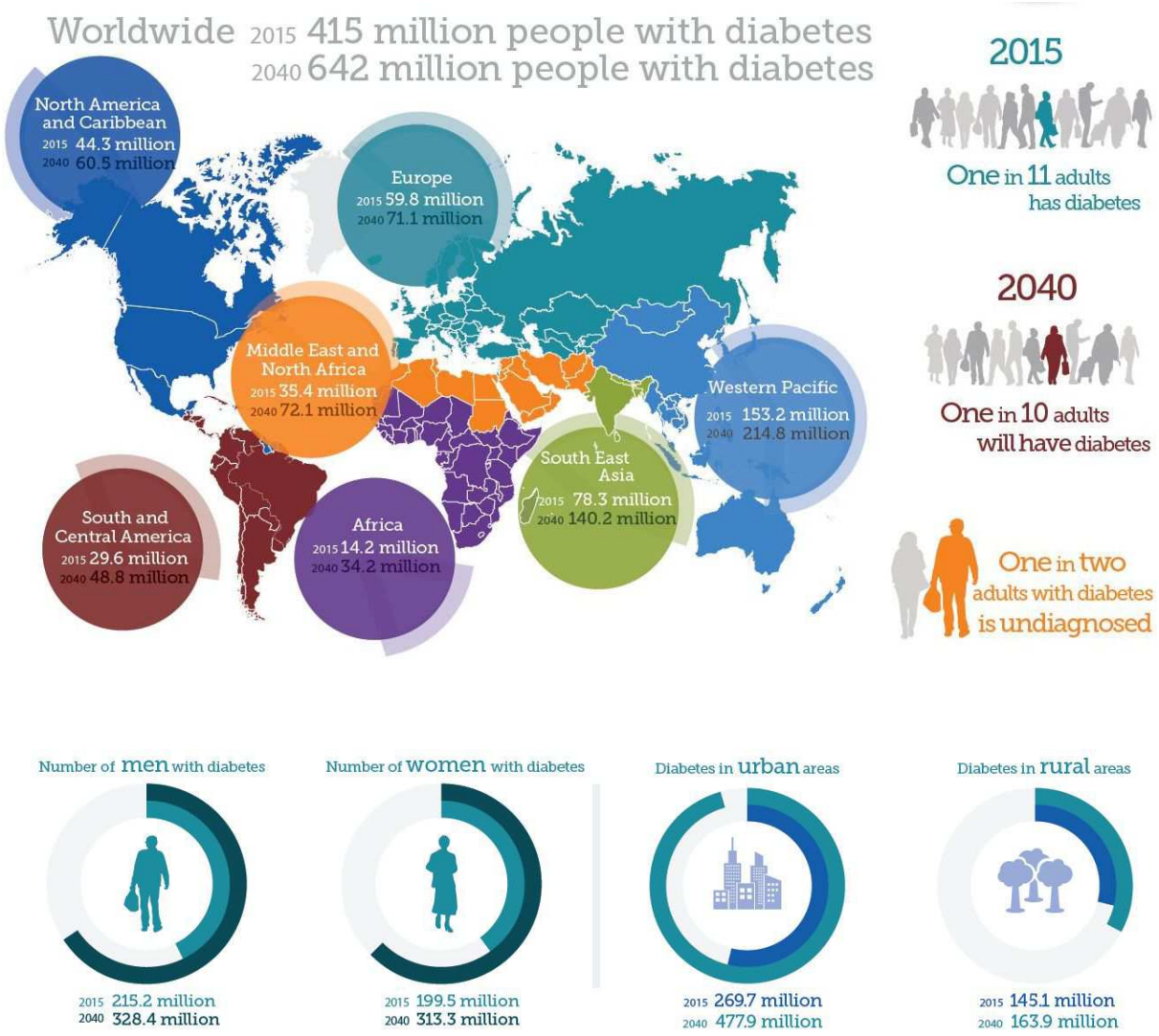

Figure 1. Global prevalence of diabetes. The figure shows the distribution of diabetic people in different geographical locations in the year 2015 and expected numbers for the year 2040. Source: International Diabetes Federation. IDF Diabetes Atlas, 7th edition, 2015. http://ww.idf.org/diabetesatlas

The two main types of diabetes are type 1 diabetes (T1D) and type 2 diabetes (T2D). A third type, gestational diabetes, develops only during pregnancy and is less common.

T1D, previously known as 'Insulin-dependent diabetes mellitus', is a condition in which destruction of pancreatic β-cells leads to insulin deficiency. It accounts for 5-10 percent of all the cases of diabetes and it is known as an autoimmune disorder [2]. A recent study reviewed several environmental risk factors including intestinal microbiota, dietary factors and viral infections that might contribute to the development and progression of T1D [3]. Besides environmental factors, the risk of developing T1D is increased by certain variants

of the *HLA-DQA1*, *HLA-DQB1*, and *HLA-DRB1* genes [4]. These genes belong to the family of human leukocyte antigen (HLA) complex. HLA complex genes encode for glycoproteins that are found on cell surface and help immune system to distinguish body's own proteins from proteins made by foreign invaders such as viruses and bacteria. In T1D, the immune system loses the ability to distinguish between these proteins and thus, destroys body's own pancreatic β-cells. So far, daily insulin injection and islet transplantation have been demonstrated to effectively maintain glucose homeostasis in T1D patients [5, 6]. However, islet transplantation is very limited due to the scarcity of donated islets. In this regard, several groups have made progress towards the production of β-cells in vitro from pluripotent stem cells or somatic cell types including α cells, pancreatic exocrine cells, gastrointestinal stem cells, fibroblasts and hepatocytes [5, 7, 8].

T2D is a metabolic disorder characterized by hyperglycemia, insulin resistance, and relative insulin deficiency [9]. Genes and environment together are important determinants of insulin resistance and β-cell dysfunction in T2D. Several gene loci including *PPARG* have been associated with obesity, insulin resistance and β-cell function [10]. Apart from increased caloric intake and decreased energy expenditure, other factors, such as dietary fat (particularly saturated fat), ageing, ethnicity and microbiome, seem to be important in T2D development [10, 11]. Several oral and injectable drugs, such as metformin, miglitol, alogliptin and pramlintide, are used for the treatment of T2D [10, 12], but these treatments are not able to maintain β-cell function. Therefore, new therapeutic targets, including AMP-activated protein kinase (AMPK), sirtuin 1 (SIRT1), fibroblast growth factor 21, forkhead box protein O1 and interleukin-1β (IL-1β) receptor antagonist have been proposed for the treatment of T2D [10].

4.1.1 Glucose uptake

Glucose is an important fuel for all the tissues in the body and normal glucose metabolism is vital for health. Glucose transport is mediated by two families of glucose transporters, facilitative glucose transporter family (GLUT) and Na^+/glucose cotransporter family (SGLT) [13]. SGLT transports glucose into the cell using the electrochemical gradient of Na^+ [13]. GLUT and SGLT families consist of thirteen members (GLUT1-12 and H^+-myo-

inositol transporter) and six members (SGLT1-6), respectively [14]. Expression of different isoforms of both the GLUT and SGLT families has been shown to be cell type specific [14].

Among all the reported glucose transporters, GLUT1-4 have been extensively studied. GLUT1 is known as the most ubiquitously distributed isoform in a variety of human tissues; in particular, it is shown to be expressed in endothelial and epithelial-like barriers of the brain, eye, peripheral nerve, placenta and lactating mammary gland [15]. Besides glucose, other substrates of GLUT1 include galactose, mannose and glucosamine [15]. GLUT2 has a low affinity for glucose and a high affinity for glucosamine and its expression mainly occurs in the kidney and intestinal absorptive epithelial cells where it is located in the basolateral membrane [14]. Besides kidney, GLUT2 is also expressed in liver, pancreas and brain. In hepatocytes it is involved in the release of gluconeogenesis-synthesized glucose into the blood. GLUT3 transports galactose, mannose, maltose, xylose and dehydroascorbic acid in addition to glucose [14]. Although GLUT3 mRNA is present in several human tissues, GLUT3 protein is mainly detected in the brain and it is therefore considered as neuro-specific glucose transporter [15]. GLUT4 is the insulin-sensitive transporter of this family and its role has been extensively studied in diabetes. Its expression is highest in insulin-sensitive tissues including brown and white adipose tissue, skeletal and cardiac muscle [15]. It has a similar affinity for glucose as GLUT1 (K_m of 5-6 mM), and can also transport glucosamine and ascorbic acid [14, 15].

4.1.1.1 Glucose transporter type 4 translocation and insulin signaling

Inside the cell GLUT4 continuously undergoes a process known as regulated recycling, in which endocytosis, sorting into specialized vesicles, exocytosis, tethering, docking and fusion of the protein are tightly regulated [16]. In the absence of insulin, most of the GLUT4 is stored in the cytoplasmic vesicles within the cell [16]. Both insulin and exercise acutely stimulate GLUT4 recruitment to the cell surface of muscle and adipose cells, but the signaling mechanisms initiated by these two physiological stimuli are different. Insulin stimulates the translocation of GLUT4 to the plasma membrane via targeted exocytosis and at the same time attenuates the endocytosis process [17]. Thus, the amount of glucose that is transported into adipose and muscle cells depends upon GLUT4 density on the plasma membrane and the amount of time that the transporter is maintained at that site.

Insulin activates the insulin receptor (IR) tyrosine kinase which phosphorylates and recruits different substrates, such as proteins from family of insulin receptor substrates (IRS) (Figure 2) [18]. Phosphorylated IRS display binding sites for numerous signaling partners, among which the recruitment of phosphoinositide 3-kinase (PI3K) has a major role in insulin signaling. PI3K catalyzes the phosphorylation of phosphatidylinositol 4,5-bisphosphate (PIP2) to phosphatidylinositol 3,4,5-trisphosphate (PIP3) [19]. PIP3 is dephosphorylated and converted back to PIP2 by phosphatase and tensin homolog (PTEN) [19]. Dysfunction of either PI3K or PTEN has been linked to various diseases including cancer and diabetes [19]. PIP3 triggers the activation of the protein kinase B (PKB), also known as Akt, through the actions of two intermediate protein kinases, PDK 1 (pyruvate dehydrogenase lipoamide kinase isozyme 1) and rapamycin-insensitive companion of mammalian target of rapamycin (Rictor/mTOR) [18]. Akt2 isoform appears to control GLUT4 trafficking in adipose and muscle cells and glucose output regulated by insulin signaling in liver [15]. Although several Akt2 substrates responsible for insulin-dependent effects on GLUT4 trafficking machinery have been identified, only a few have been extensively studied. These include the GTPase activating protein AS160, which contains multiple Akt2 phosphorylation sites and catalyzes the inactivation of Rab proteins 2A, 8A, 10 and 14 in vitro [15, 16]. Rab proteins are known to be critical organizers of intracellular membrane trafficking. However, AS160 knockdown partially inhibits insulin-dependent translocation of GLUT4 suggesting that unknown Akt2 substrate proteins must contribute to overall GLUT4 regulation by insulin [15, 16].

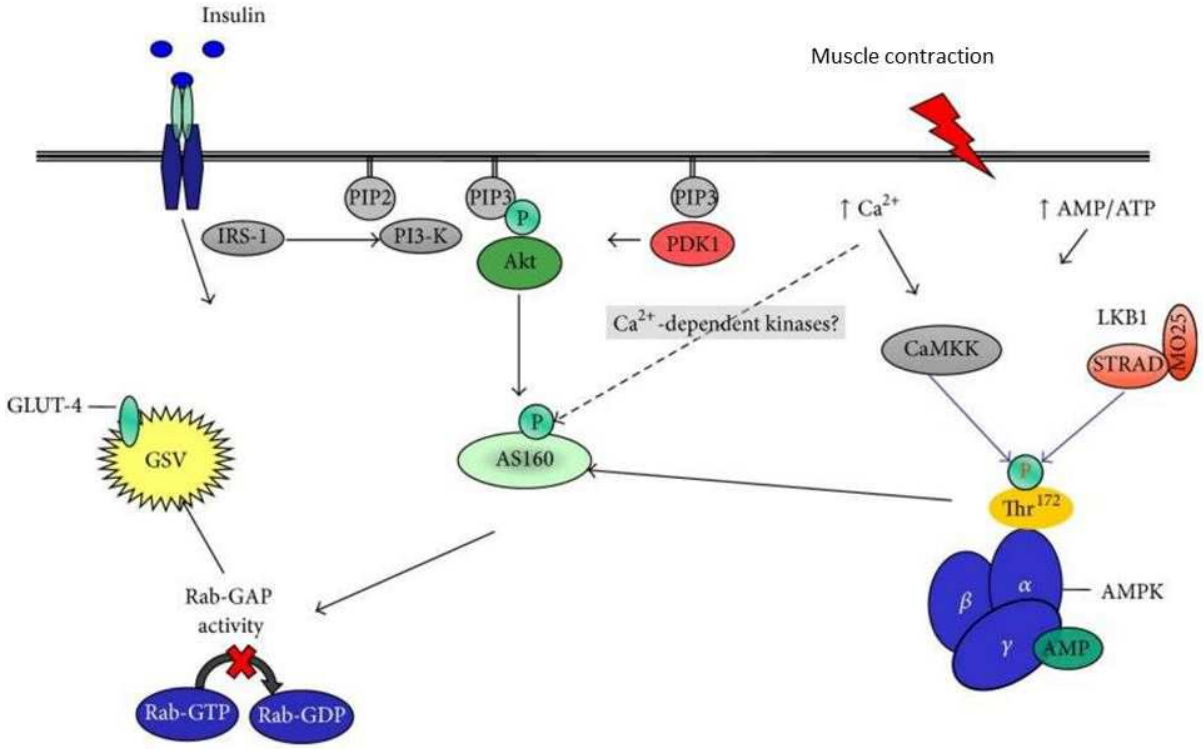

Figure 2. Insulin- and muscle contraction-mediated GLUT4 translocation. Insulin signaling through PI3K and muscle contraction through activation of AMPK mediate GLUT4 translocation to the cellular plasma membrane. AMPK activity is regulated by both increased AMP/ATP ratio and elevated intracellular calcium concentrations. Both PI3K and AMPK pathways result in the phosphorylation Akt2 substrate AS160 that mediates GLUT4 translocation. GLUT4: glucose transporter type 4, PI3K: phosphoinositide 3-kinase, AMPK: adenosine monophosphate-activated protein kinase, ATP: adenosine tri-phosphate. From Mackenzie et al., 2014 [20].

In addition to insulin-mediated pathway, AS160 phosphorylation can be induced by muscle contraction through a PI3K independent mechanism (Figure 2). Contraction-induced AS160 phosphorylation is mediated by adenosine monophosphate-activated protein kinase (AMPK), providing a potential intersection for insulin and exercise-mediated signaling to GLUT4 [16]. Muscle contraction results in a transient increase in Ca^{2+} levels along with an increase in AMP/adenosine tri-phosphate (ATP) ratio leading to AMPK activation. Calcium activates Ca^{2+}/calmodulin-dependent protein kinase II (CAMKII), which then contributes to AMPK activation through upstream kinases CaMKKα and β, at least in cultured cell lines and ex vivo brain slices [15, 16, 21]. Muscle glycogen appears to be a negative regulator of AMPK activity [21]. It has been demonstrated that in rat skeletal muscle glycogen suppresses

AMPK signaling, thus providing a negative feedback mechanism for AMPK-mediated glucose uptake [22]. However, downstream targets of this protein kinase involved in GLUT4 translocation are not yet known. Nevertheless, it has been demonstrated that simultaneous inhibition of AMPK and Akt activity is not able to completely prevent GLUT4 translocation to plasma membrane, suggesting that additional signals are involved in insulin-induced glucose uptake.

Besides insulin and muscle contraction, several other stress signals are also known to enhance glucose uptake in skeletal muscle. For instance, hypoxia, inhibitors of glycolysis and electron transport, and uncoupling of oxidative phosphorylation increase glucose uptake at least partially through AMPK and modulation of the AMP/ATP ratio (Figure 2) [16, 23].

4.1.2 Complications associated with diabetes

Chronic hyperglycemia is a life threatening risk factor that results in organ and tissue damage in the long term. One of the acute metabolic complications associated with mortality includes diabetic ketoacidosis occurring mainly in T1D [23]. The long-term vascular complications associated with diabetes are divided into two groups, (i) microvascular disease, resulting from the damage of small blood vessels and (ii) macrovascular disease, resulting from the damage of the arteries. Hyperglycemia-associated vascular complications are the major source of morbidity and mortality in both T1D and T2D. Thus, it is important for researchers and physicians to understand the relationship between diabetes and vascular disease because the prevalence of diabetes continues to increase all over the world. Microvascular complications include retinopathy, nephropathy and neuropathy. The major macrovascular complications include coronary artery disease, peripheral arterial disease, and stroke. Moreover, there is also myocardial dysfunction that is one of the deadliest complications associated with diabetes [23]. Other chronic complications of diabetes include depression, dementia and sexual dysfunction.

4.2 DIABETIC CARDIOMYOPATHY

Diabetic cardiomyopathy is a result of diabetes-induced changes in the structure and function of the heart and it is diagnosed only if there is cardiac dysfunction in the absence of coronary artery disease [24]. Cardiovascular disease is the leading cause of mortality and morbidity in diabetic patients [24]. Thus, a better understanding of its pathophysiology is necessary for early diagnosis and the development of treatment strategies.

Previous studies using magnetic resonance imaging (MRI) demonstrated that hyperglycemia and insulin resistance are associated with an increase in left ventricle (LV) mass and LV-mass to LV end-diastolic volume ratio [25, 26]. It has been frequently observed that, in diabetic patients, diastolic dysfunction occurs at early stages and precedes systolic dysfunction [25, 27, 28]. LV diastolic dysfunction is detected in almost 63% of the diabetic patients [29]. Diastole is the part of cardiac cycle that occurs when the ventricles are relaxing and filling with blood. During diastole, the pressure in the ventricles drops and mitral valve opens causing the accumulated blood from left atrium to flow into the ventricle [28]. Impairment in this process, such as increase in ventricle stiffness and decrease in ventricle relaxation, leads to diastolic dysfunction [30, 31]. Thus, the inability of the ventricle to accept an adequate amount of blood at normal diastolic pressure leads to diastolic heart failure. When this occurs in the absence of systolic dysfunction (Figure 3), it is commonly referred to as heart failure with preserved ejection fraction (HFpEF) [32].

Diastolic heart failure can also be accompanied by systolic heart failure (Figure 3). Systole is a period of cardiac cycle when the ventricles contract. During systole, pressure in the ventricles increases and when it exceeds the pressure in the atria, tricuspid and mitral vales close [33]. The pressure in the ventricles keeps increasing and reaches its maximum until the pulmonary and aortic valves open in the ejection phase [34]. In this phase, blood flows through pulmonary artery and aorta from right and left ventricles, respectively. Thus, ejection fraction is the measurement of the pumping efficiency of the heart, i.e. the fraction of blood that is ejected by the ventricles with each cardiac cycle [35]. Normal ejection fraction ranges from 50 to 70%, while values below 40% indicate presence of systolic heart failure.

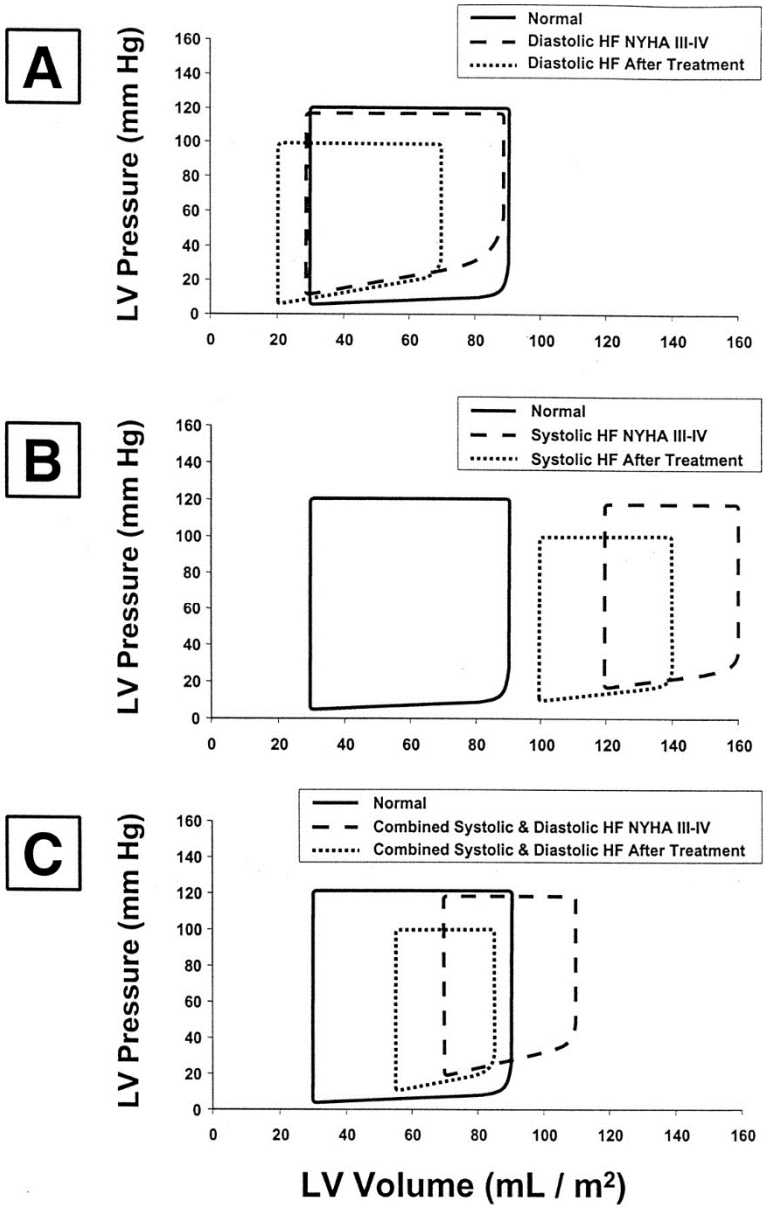

Figure 3. PV loop showing diastolic and systolic function. The figure shows PV loops for diastolic heart failure (A), systolic heart failure (B) and combination of diastolic and systolic heart failure (C) as compared to normal. PV: pressure-volume. From Zile et al., 2002 [36]

At an early stage, diabetic cardiomyopathy manifests as diastolic dysfunction with preserved ejection fraction [37]. In some patients, diastolic dysfunction may progress to compromised systolic function resulting in heart failure with reduced ejection fraction [37]. The mortality rate is 15-20% in diabetic patients with systolic dysfunction [38]. Although the exact mechanism of diabetes associated LV dysfunction is not known, it appears that hyperglycemia initiates a series of adaptive and maladaptive processes contributing to the development of heart failure.

4.2.1 Hyperglycemia-induced pathways associated with vascular complications in diabetes

Diabetic cardiomyopathy is a multi-factorial disease. Several mechanisms, including oxidative stress, inflammation, endoplasmic reticulum (ER) stress, metabolic derangements, abnormalities in ion homeostasis, alterations in structural proteins, apoptosis and fibrosis have been proposed to trigger diabetes-induced cardiac damage (Figure 4) [39]. Amongst these various mechanisms proposed, an increase in reactive oxygen species (ROS) formation has gained significant experimental and clinical evaluation [37, 40]. Hyperglycemia can increase ROS production by several pathways, including polyol pathway, formation of advanced glycation end products (AGEs), activation of protein kinase C (PKC), glucose auto-oxidation, and activation of the 12/15-lipoxygenases (12/15-LO) pathway [39].

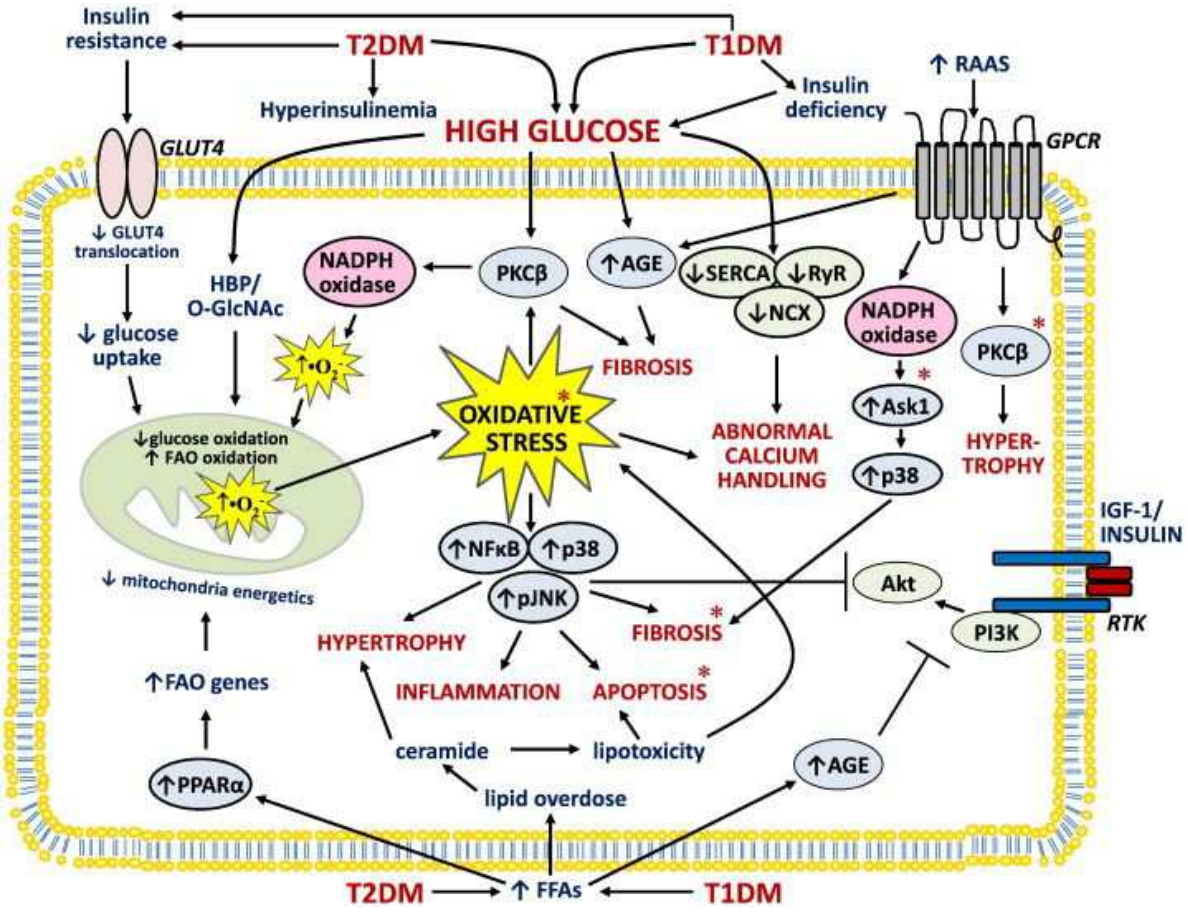

Figure 4. Mechanisms involved in the development of diabetic cardiomyopathy. High glucose in T1DM and T2DM results in PKC activation, glucose auto-oxidation, AGE formation, abnormal calcium handling and ROS formation. Activation of these pathways leads to energy depletion, increased fibrosis, apoptosis, hypertrophy and impaired LV contractile function and relaxation. AGEs:

advanced glycation end-products, ASK1: apoptotic signal regulating kinase-1, FAO: fatty acid oxidation, GLUT-4: glucose transporter-4, GPCR: G protein coupled receptor, HBP: hexosamine biosynthesis pathway, IGF-1: insulin-like growth factor-1, LV: left ventricle, JNK: c-Jun N-terminal kinase, NADPH: nicotinamide adenine dinucleotide phosphate, NCX: sodium–calcium exchanger, O-GlcNAc: O-linked β-N-acetylglucosamine, PI3K: phosphoinositide-3 kinase, PKCβ: protein kinase C-β, RTK: receptor tyrosine kinase, RyR: ryanodine receptor, SERCA: sarcoplasmic reticulum Ca^{2+} ATPase, T1DM: type 1 diabetes mellitus, T2DM: type 2 diabetes mellitus. From Huynh et al., 2014 [41]

4.2.1.1 Polyol pathway

Two major enzymes are involved in the polyol pathway, namely aldose reductase and sorbitol dehydrogenase (Figure 5). Under euglycemia, aldose reductase converts reactive aldehydes into alcohols, thus protecting the cell from toxic effects of aldehydes [42]. Although the affinity of this enzyme for glucose is very low in normal conditions, in hyperglycemic conditions aldose reductase converts high amounts of glucose into sorbitol. In the next step, sorbitol is converted to fructose by sorbitol dehydrogenase with the production of NADH, potentially leading to increased ROS via NADH oxidase as shown in Figure 5 [43, 44]. Furthermore, fructose-3-phosphokinase can directly phosphorylate fructose resulting in the formation of a potent glycating agent, fructose-3-phosphate. Fructose-3-phosphate can subsequently result in the formation of 3-deoxyglucosone, a key intermediate known to accelerate the formation of AGEs [45].

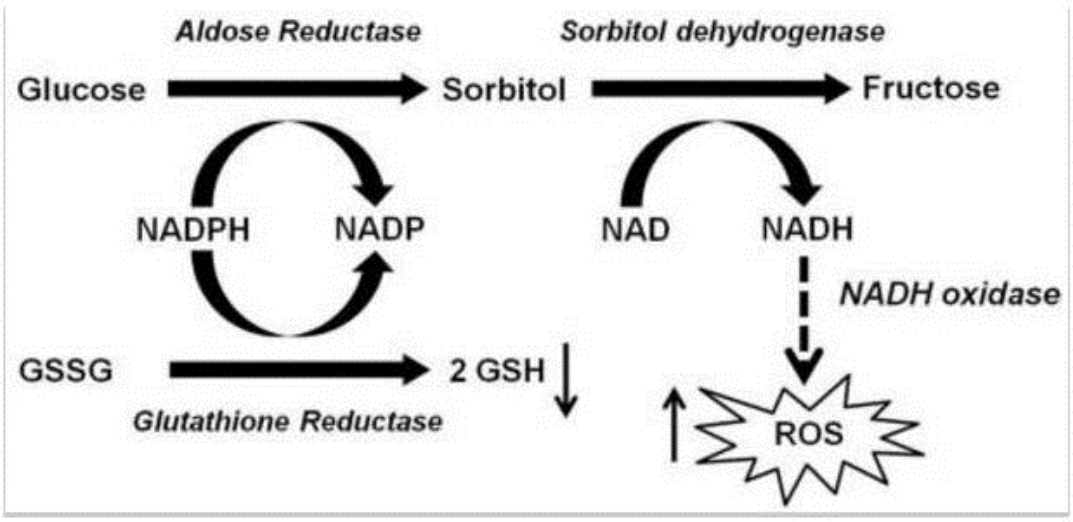

Figure 5. Role of aldose reductase in hyperglycemia-induced ROS formation. Under hyperglycemia, aldose reductase converts glucose into sorbitol at the expense of NADPH. In the next step, sorbitol is converted into fructose by sorbitol dehydrogenase resulting in the production of NADH, potentially leading to increased ROS via NADH oxidase. NADPH: nicotinamide adenine dinucleotide phosphate, ROS: reactive oxygen species. From Tang et al, 2012 [44]

A recent study demonstrated that inhibition of aldose reductase with tephrosia purpurea prevented the development of diabetic cataract in STZ-induced T1D rats [46]. Moroever, overexpression of human-aldose reductase leads to an increase in atherosclerosis in mice [47], suggesting a pathological role of this pathway in hyperglycemic conditions. Aldose reductase inhibitors have been used clinically for several years to prevent diabetic neuropathy; nevertheless, they have not been successful in preventing the occurrence of other diabetic complications.

4.2.1.2 Formation of advanced glycation end products

Glycation refers to the covalent bonding between proteins/lipids and sugars such as glucose. Glycation causes molecular rearrangements of proteins or lipids that lead to the generation of AGEs [48]. Several mechanisms through which AGEs are known to contribute to the pathogenesis of diabetic cardiomyopathy include formation of cross-links between key molecules in the extra-cellular matrix (ECM), permanently altering cellular structure and binding of AGEs to receptor for advance glycation end products (RAGE) [49]. In presence of high glucose, RAGE activation can directly induce NADPH oxidase (Nox) leading to increased ROS production [50]. Considering the detrimental effects of AGEs, several studies have tried to diminish their effects either by directly inhibiting AGEs or by preventing the interaction of AGEs with their receptors RAGE [51, 52]. Clinical trials employing these inhibitors have been unsuccessful so far and further investigation is necessary in order to better understand the formation and function of these products.

4.2.1.3 Activation of protein kinase C

Glucose regulates intracellular levels of diacylglycerol, which is known to activate several PKC isoforms [43]. Besides diacylglycerol, polyol pathway, H_2O_2 and AGEs formation are also known to activate these kinases [53, 54]. PKC phosphorylates protein serine and threonine residues and is involved in receptor desensitization, modulation of

membrane structure events, transcription regulation, immune response and cell growth regulation [55]. Multiple studies have shown that PKCβ-mediated $p66^{Shc}$ phosphorylation is required for its mitochondrial translocation, hydrogen peroxide (H_2O_2) formation and cell death [56, 57]. Besides translocation of $p66^{Shc}$, PKCβ is also involved in the activation of Nox2 leading to an increase in ROS formation in cardiomyocytes exposed to high glucose [58]. These studies indicate towards the important role of PKC-mediated phosphorylation in pathophysiology of diabetic cardiomyopathy.

4.2.1.4 Glucose auto-oxidation

Hyperglycemia induces the activity of glutamine-fructose-6-phosphate amidotransferase (GFAD) in hexosamines synthesis pathway. GFAD activity has been associated with increased transcription of transforming growth factor-β1 (TGF-β1), a cytokine known to play a role the development of cardiac fibrosis in hyperglycemic conditions [59]. The exact mechanism of hexosamine pathway- or glucose auto-oxidation-induced ROS production is not very well known. However, it is proposed that this pathway might be involved in the activation of PKC and thereby induce cellular changes as described above (Figure 4).

4.2.1.5 Activation of the 12/15-Lipoxygenases pathway

Activation of 12/15 LO pathway is associated with ROS production in pathological conditions and hyperglycemia has been shown to increase the activity of these enzymes [60]. 12/15 LO inserts the molecular oxygen at 12/15 carbon of polyunsaturated acids, such as arachidonic acid and linoleic acid, leading to the formation of oxidized lipids [61]. Studies have shown that LO and its products mediate growth factor effects in several cells types, including fibroblasts and mesangial cells [60, 61]. 15-(S)-hydroxyeicosatetraeonic acid (15-S-HETE), a metabolized product of arachidonic acid, was found to be elevated in the urine of diabetic patients [62]. It has also been shown that incubation of endothelial cells with 15-(S)-HETE led to an increase in H_2O_2 production via xanthine oxidase (XO) in a dose dependent manner [63]. This study further illustrated that genetic ablation of 12/15 LO gene completely blocks XO activity and prevents endothelial dysfunction in mice kept on high fat diet [63]. Even though LO inhibitor masoprocol improves insulin sensitivity in a rat model of type 2 diabetes [64], so far no clinical trials have been conducted.

4.3 ROS: A COMMON DENOMINATOR OF HYPERGLYCEMIA-INDUCED CHANGES

Although several potential mechanisms underlying diabetic cardiomyopathy have been addressed in the past decade, oxidative stress is widely considered as one of the major causes for the pathogenesis of the disease [65-67]. Current consensus is that hyperglycemia- and hyperlipidemia-induced ROS formation is detrimental for cardiac function and leads to cardiac damage in both T1D and T2D [68]. Indeed, increased ROS production is well documented in multiple tissues in both animal and human diabetic subjects [39, 69]. Thus, it becomes important to understand the sources of ROS and their mechanism inside the cell.

There are several sources of ROS in human tissue, including, Nox, XO, uncoupled nitric oxide synthase (NOS), arachidonic acid and mitochondria, but they vary in their pathological role and their importance depends on the disease and the organ.

4.3.1 NADPH oxidase

Nox is a family of membrane-bound enzyme complex composed of plasma membrane spanning cytochrome b558 (p22phox, gp91phox) and cytosolic components (rac, p47phox, p67phox, p40phox) as shown in Figure 6 [70]. It becomes activated following exposure to foreign microorganisms and promotes translocation of its cytosolic components to the plasma membrane to form an active NADPH complex that allows transfer of electrons to molecular oxygen to generate superoxide [70]. The reaction catalyzed by this enzyme is following:

$$NADPH + 2O_2 \rightarrow NADP + 2O_2^- + H^+$$

Nox specifically generate ROS as their primary function and have emerged as the major cellular ROS sources involved in several pathological conditions (Figure 6) [71]. Up to date, seven members of Nox family have been identified, namely Nox1–5, dual oxidase 1 (Duox 1) and Duox 2 [72]. Among these, two Nox isoforms exist in the heart, Nox2 and Nox4. Although Nox2 is located in the cell membrane, Nox4 is localized in perinuclear ER and/or mitochondria [73, 74].

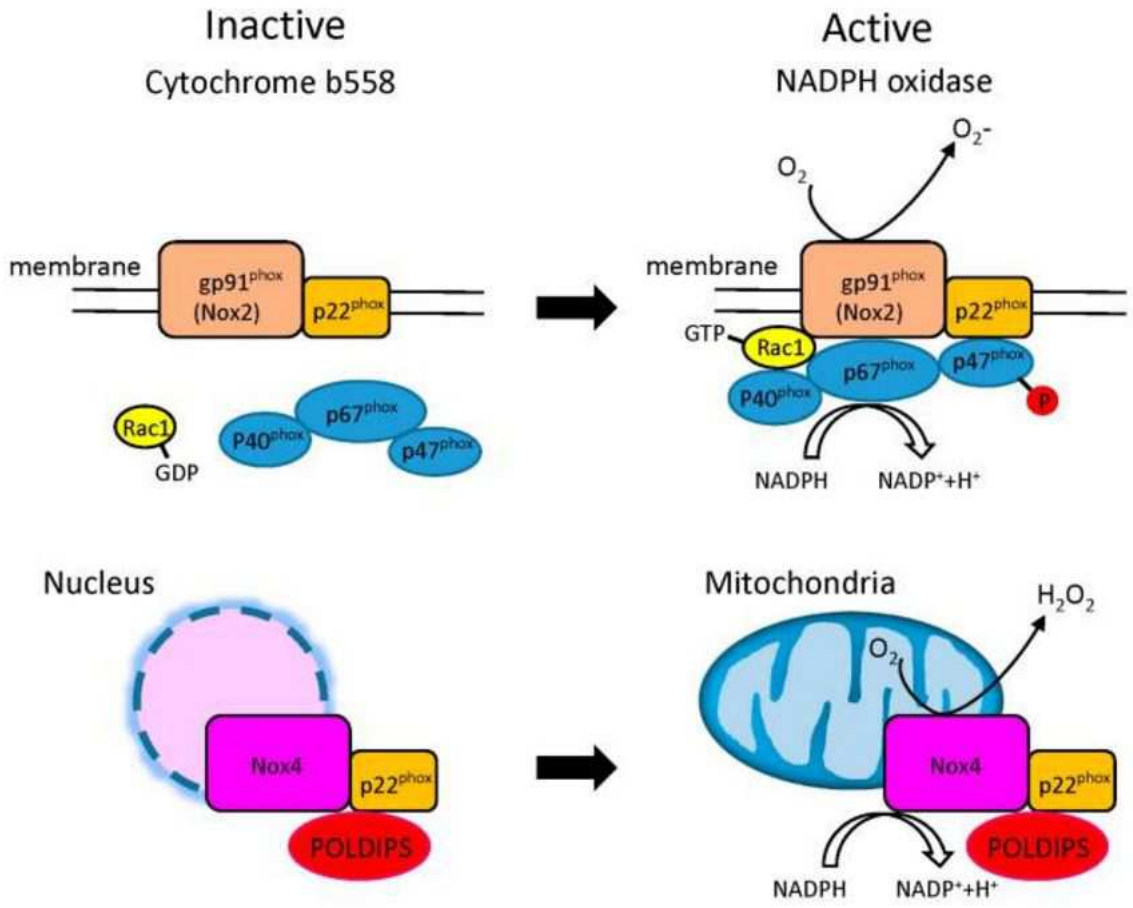

Figure 6. Nox in the heart. Nox is a membrane-bound enzyme complex. It has two subunits: cytochrome b558, composed of gp91phox and p22phox, and multidomain regulatory subunits, composed of p40phox, p47phox and p67phox. When the enzyme is inactive, multidomain regulatory subunits exist in the cytosol as a complex whereas upon stimulation, p47phox undergoes phosphorylation, and the entire multidomain regulatory complex subsequently translocates to the membrane and associates with cytochrome b558 to form the active oxidase. The active complex uses NADPH as a substrate and transfers electron to oxygen leading to the production of superoxide. Nox: Nicotinamide adenine dinucleotide phosphate oxidases. From Kayama et al., 2015 [72]

Several studies have reported the contribution of Nox to hyperglycemia-induced ROS production [75, 76]. It is well documented that the activity of Nox is increased in cardiomyocytes exposed to high glucose and in the heart of diabetic mice [75, 77]. Pathways reported to link glucose-induced ROS production via Nox include SGLT1, PKCβ and calcium/calmodulin dependent kinase II (CaMKII) [58]. A recent study identified that glucose transport through SGLT1 is responsible for Nox2 activation and subsequent increased ROS production in cardiac myocytes exposed to high glucose [78]. This study further demonstrated that oxidative pentose phosphate pathway is required to provide Nox2 with the substrate NADPH and to produce ROS [78]. PKC is involved in high glucose-induced

activation of Nox2 through a positive feedback mechanism involving the RhoA/Rho kinase pathway [58]. Indeed, PKCβ inhibition by LY333531 in cardiomyocytes treated with high glucose for 12 h prevented Nox2 dependent ROS production [58]. However, how PKCβ is activated by high glucose levels was not addressed in these studies and thus warrants further investigation. Cellular influx of Ca^{2+} led to increased CaMKII phosphorylation along with upregulation of Nox components, p47phox and p67phox, and increased ROS formation in STZ model of T1D and neonatal cardiomyocytes exposed to high glucose [79]. Interestingly, CaMKII inhibitor attenuated these events indicating the involvement of this kinase in Nox-induced ROS formation. However, although the role of Nox is confirmed in cardiovascular complications occurring in diabetes so far no clinical trials have been conducted with the inhibitors of these enzymes.

4.3.2 Xanthine oxidase

XO is a cytoplasmic enzyme that catalyzes the oxidation of hypoxanthine to xanthine and further converts xanthine to uric acid [80]. It uses O_2 as electron acceptor during this process and thus produces superoxide and H_2O_2 [80]. Hypoxanthine and XO have been shown to induce cell damage under ischemia-reperfusion conditions by reacting with O_2 and producing large amounts of superoxide and H_2O_2. Moreover, inhibition of XO by allopurinol prevented cardiac damage in pacing-induced heart failure in dogs [81]. Rajesh et al. documented the role of XO in the development of fibrosis and oxidative stress in STZ-induced T1D mice [82]. Although XO inhibition has been proven beneficial in animal studies, it cannot be used to treat cardiovascular complications in patients, since human heart does not contain detectable amount of these enzymes [83, 84].

4.3.3 Mitochondrial sources of ROS

Mitochondrial ROS formation and dysfunction have been implicated in the pathogenesis of diabetes and its complications [37, 39, 58]. Indeed, cardiac mitochondria from diabetic patients were reported to be dysfunctional, displaying increased mitochondrial H_2O_2 emission, impaired mitochondrial respiratory capacity and increased levels of hydroxynonenal- (HNE) modified proteins [85]. It is proposed that a combination of several

mechanisms leads to mitochondrial dysfunction in diabetic hearts, including fatty acid-induced mitochondrial uncoupling, increased ROS formation, mitochondrial proteome remodeling, impaired mitochondrial calcium handling and altered mitochondrial biogenesis. These changes might lead to compromised cardiac ATP generation and ultimately to cardiac dysfunction [37, 39]. Altered mitochondrial function is depicted to oppose insulin signaling in two ways: first, by interfering with oxidation of fatty acyl-CoA and consequent accumulation of intracellular lipid and diacylglycerol, and second, through generation of ROS. Both processes lead to IRS-1 serine phosphorylation and interference with insulin signal transduction. Reduction in mitochondrial ROS formation either by overexpressing manganese superoxide dismutase (Mn-SOD) or by AICAR (5-aminoimidazole-4-carboxamide ribonucleoside), prevented mitochondrial damage and many hyperglycemia-induced events, both in vitro and in vivo [86, 87]. Electron transport chain (ETC), $p66^{Shc}$ and monoamine oxidase (MAO) are the major sources of ROS formation in mitochondria.

4.3.3.1 Electron transport chain

ETC is by far the major site of ATP production in mitochondria inside any given cell, and especially in cardiomyocytes (more than 90%). At the inner mitochondrial membrane (IMM), complexes of the ETC transfer electrons from NADH and $FADH_2$ (Flavin adenine dinucleotide) to oxygen (O_2), which is reduced to water (H_2O). Transfer of electrons powers the movement of protons (H^+) into the intermembrane space [88], generating an electrochemical proton gradient that drives the synthesis of ATP by the ATP synthase (Figure 7) [88].

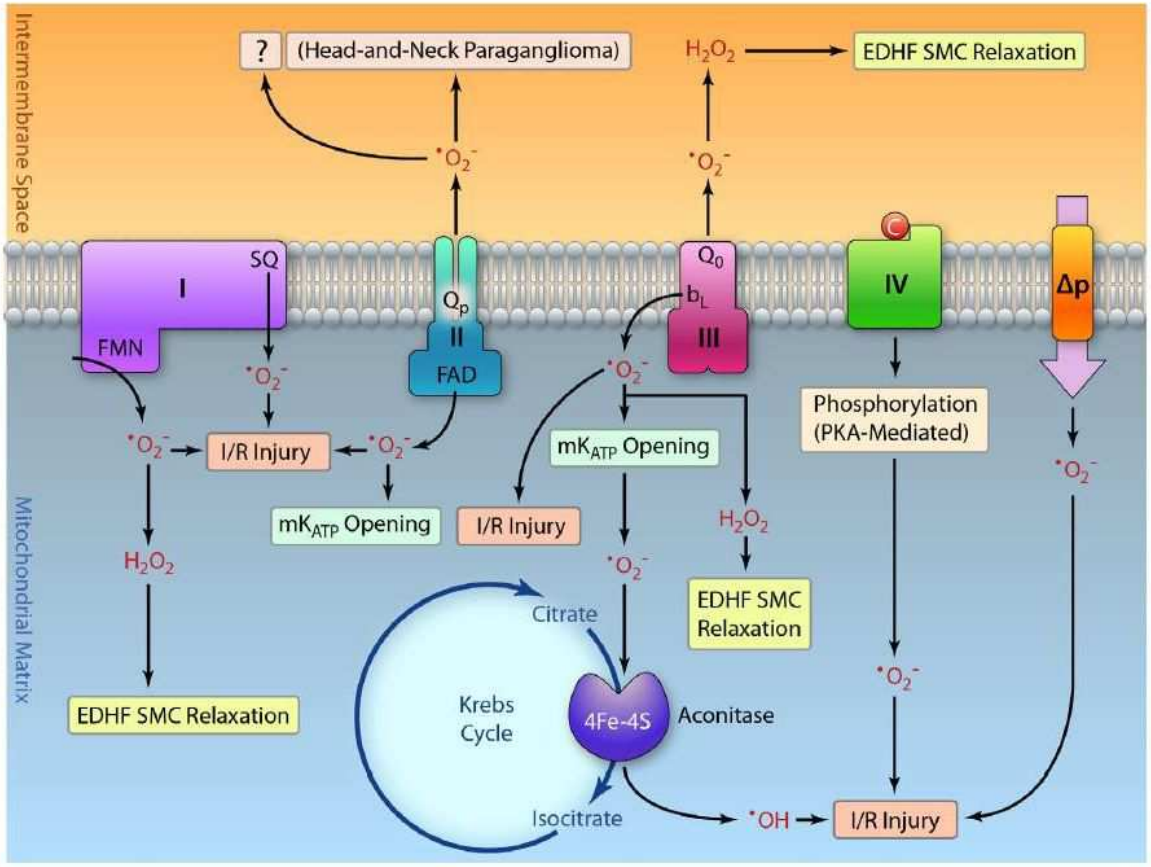

Figure 7. Sites of superoxide production in the ETC. This scheme shows the proposed physiological (highlighted with light green/yellow boxes) and pathophysiological (highlighted with pink boxes) roles of superoxide generation by each respiratory electron transport complex and the proton motive force (Δp). Superoxide generation by complexes I, III, and flavoprotein of complex II mediates I/R injury and increases the pro-oxidant activity of aconitase, thus further augmenting I/R injury. PKA-mediated phosphorylation of complex IV under ischemic conditions predisposes complex IV to generate superoxide and augment I/R injury. ETC: electron transport chain, I/R: ischemia/reperfusion injury, PKA: protein kinase A. From Chen et al., 2014 [89]

A minor fraction of electron (about 0.1%) can leak from the ETC and cause the partial reduction of O_2 into superoxide. This process occurs at the level of first three complexes where flavins or quinones are able to act as single electron donors, especially under conditions that decrease the flow of electrons toward complex IV, where O_2 is fully reduced to H_2O [90, 91]. Notably, ROS formation can also result from reverse electron flow. A recent study supported this concept by demonstrating that succinate accumulated during ischemia in vivo is oxidized during reperfusion, resulting in large ROS formation that is likely attributable to the reverse electron flow through complex I [92]. Superoxide that does not cross IMM is rapidly dismutated into the freely permeable H_2O_2 by Mn-SOD [93]. It has been

shown that Mn-SOD deficient mice develop ROS toxicity and dilated cardiomyopathy [58]. Moreover, increased catalase expression or inhibition of ETC complexes I and II with rotenone and thenoyltrifluoroacetone, respectively, attenuate ROS formation in cardiomyocytes from animals with T1D and T2D [94, 95]. These studies underline the importance of ETC in this pathology and mitochondria as their source and target.

Hyperglycemia-induced ROS formation is not observed in rho zero (ρ0) endothelial cells in which mitochondrial DNA is depleted and ETC is not functional [96]. A recent study demonstrated that hyperglycemia alters the function of respiratory chain in mitochondria via dysregulation of O-GlcNAcylation [97]. O-GlcNAc transferase (OGT) enzyme is located in the IMM and interacts with complex IV of the respiratory chain in normal conditions. In STZ-treated rats this enzyme is mislocalized to mitochondrial matrix and the interaction of OGT and complex IV is impaired leading to the loss of complex IV activity and reduced mitochondrial membrane potential [97]. Collectively, these studies show that mitochondria are important sites for ROS generation in hyperglycemic conditions and can further amplify this ROS formation by activating other sources of ROS inside the cell.

Although ETC is considered as an important source of ROS formation, Nox and MAO are able to generate 10-fold higher levels of ROS in human atrial myocardium [98]. In addition to this, it is not possible to inhibit the respiratory chain in humans without jeopardizing a wide array of vital functions. Thus, inhibition of the ETC complexes cannot be considered as potential therapeutic strategy for the treatment of this multifactorial disease.

4.3.3.2 $p66^{Shc}$

$p66^{Shc}$ is another important source of ROS in mitochondria. $p66^{Shc}$ is a ubiquitously expressed cytosolic adaptor protein [99, 100] and, along with $p46^{Shc}$ and $p52^{Shc}$, is encoded by the *ShcA* gene. $p46^{Shc}$ and $p52^{Shc}$ are ubiquitous isoforms, derived from the same mRNA through alternative start sites [99, 101]. In contrast, $p66^{Shc}$ expression is restricted to certain cell types and stimulatory conditions through epigenetic modifications of its distinct promoter. Cells and mice lacking $p66^{Shc}$ show reduction in markers of oxidative stress [101]. Under stress conditions, this enzyme translocates to mitochondria and catalyzes the electron transfer from cytochrome c to oxygen, resulting in the formation of H_2O_2 [99, 100].

$p66^{Shc}$ is readily detected in neonatal cardiomyocytes, but it is barely detectable in the adult ventricle [99]. However, its expression is increased in a dog model of dilated cardiomyopathy [65]. Moreover, genetic ablation of $p66^{Shc}$ resulted in reduced hypertrophy and apoptosis induced by angiotensin II in vivo [99, 101]. Besides heart failure, $p66^{Shc}$ - induced oxidative stress is also believed to exacerbate ischemia/reperfusion injury [100, 101]. Indeed, lack of this enzyme led to a significant decrease in oxidative stress in both ischemic muscles and isolated endothelial cells subjected to simulated ischemia [99].

As described above, $p66^{Shc}$ can be phosphorylated at Ser-36 residue by PKCβ, and this is required for its translocation to mitochondria. Importantly, hyperglycemia can directly activate PKC thus leading to increased ROS formation in diabetic conditions [102]. Moreover, lack of $p66^{Shc}$ was shown to protect against diabetic cardiomyopathy by preventing the senescence of cardiac progenitor cells, a process that hampers cardiac and vascular cell turnover [103].

Genetic ablation of $p66^{Shc}$ has been proven protective in many pathologies, including cardiovascular complications. Unfortunately, there are no drugs available that can inhibit the ROS forming activity of $p66^{Shc}$.

4.4 MONOAMINE OXIDASES

4.4.1 Structural properties

MAOs are flavoenzymes located at the outer mitochondrial membrane (OMM) and catalyze the oxidative deamination of catecholamines and biogenic amines resulting in the formation of H_2O_2, aldehydes and ammonia [90]. These flavoenzymes exist in two isoforms, MAO-A and MAO-B (Figure 8) and are distinguished by different substrate specificity and their sensitivity to inhibitors. The sequence homology of the two isoforms is 70% and both the sequences contain the penta-peptide Ser-Gly-Gly-Cys-Tyr, in which the obligatory cofactor flavin adenine dinucleotide (FAD) is covalently bound to cysteine residue, namely Cys406 in MAO-A and Cys397 in MAO-B [90]. Human MAO-A (hMAO-A) is known to exist in monomeric form whereas rat MAO-A (rMAO-A) and human MAO-B (hMAO-B) exist as dimers [104]. hMAO-A contains a single hydrophobic cavity of ≈550 Å at its active site, which is smaller than hMAO-B (≈700 Å3) but larger than that of rat MAO-A (≈450 Å3) [104]. This study also proposed that the mutation Glu-151→Lys is responsible for hMAO-A transition from dimeric to monomeric form. Genes encoding for MAO-A and MAO-B are located side-by-side on the short arm of X-chromosome and have 92% similarity in their sequence. In both the genes, exon 12 encodes for the covalent FAD binding site and is the most conserved exon, showing 94% amino acid identity between MAO-A and B [105].

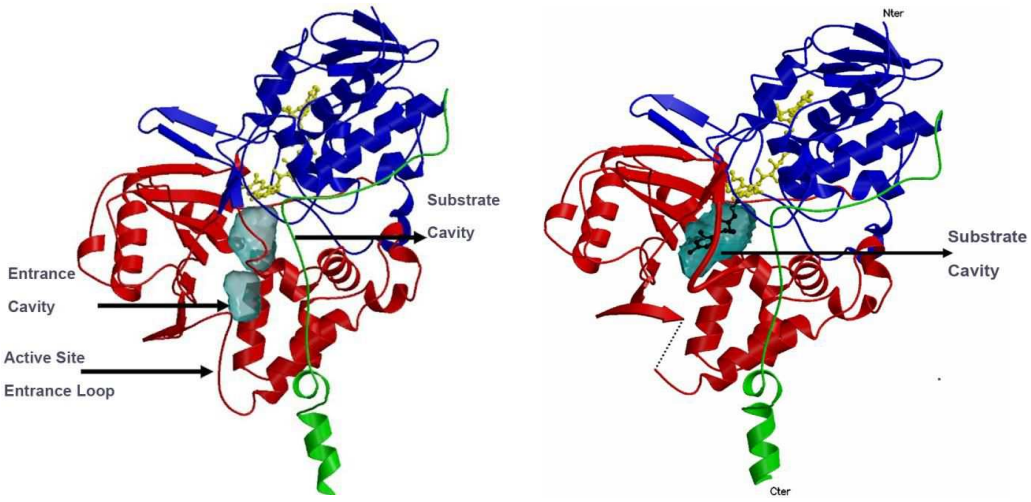

Figure 8. Ribbon structures of two isoforms of MAO. The covalent flavin moiety is shown in a ball and stick model in yellow. The flavin binding domain is in blue, the substrate domain in red and the membrane binding domain in green. MAO: monoamine oxidase; From Edmondson et al., 2004 [105].

4.4.2 Physiological roles

MAO catalyzes the oxidative deamination of monoamines according to the following reaction:

$$RCH_2NR'R'' + O_2 + H_2O \rightarrow RCHO + NR'R'' + H_2O_2$$

This reaction is known to take place in two steps. In the first step, the cofactor FAD is reduced to yield an aldehyde intermediate and ammonia, while in the second step the oxidized form of the prosthetic group is restored with the concomitant production of H_2O_2 [90]:

$$RCH_2NH_2 + MAO \rightarrow RCHO + NH_3 + MAO\text{-reduced}$$

$$MAO\text{-reduced} + O_2 \rightarrow MAO + H_2O_2$$

Aldehyde dehydrogenase (ALDH) immediately metabolizes the reactive aldehyde into the corresponding acid.

The main physiological role of MAO is the degradation of endogenous monoamine neurotransmitters and dietary amines, such as tyramine, that, if not properly catabolized, may cause hypertensive crises [106]. MAO-A preferentially catalyzes the oxidative deamination of norepinephrine and serotonin (5-HT) whereas MAO-B has major affinity for phenylethylamine and benzylamine [90]. Thus, MAOs are important to control the turnover of these amines [90]. Moreover, in peripheral tissues, MAO prevents the entry of biogenic amines in the blood by catabolizing them [107]. Likewise, it has been shown that MAO also acts as a metabolic barrier in the microvessels and blood-brain barrier by preventing the entrance of false and potentially toxic neurotransmitters [107].

Shih et al. have shown that MAO-A and MAO-B knockout (KO) mice display differences in neurotransmitter metabolism and behavior [108]. They observed that MAO-A KO mice had elevated levels of serotonin, norepinephrine and dopamine in the brain and manifest aggressive behaviour. On the other hand, no aggression was observed in MAO-B KO mice that displayed only increased levels of phenylethylamine. Both MAO-A and MAO-B KO mice show increased reactivity to stress. It has been also demonstrated that MAO is important during development [108]. Studies in MAO-A KO mice also confirmed that

maintenance of serotonin levels is important for the normal development of thalamocortical axons and the aggregation of neurons to form barrels.

4.4.3 Tissue distribution and localization

It is known that both MAO-A and MAO-B are tightly associated with the OMM However, a small portion of these isoforms is also associated with microsomal fractions [109]. MAO-A is expressed before MAO-B during development, but levels of the latter are known to increase remarkably in the brain after birth [104]. MAO is present in most mammalian tissues but the proportion of two isoforms varies from tissue to tissue [104]. The distribution of MAO in various tissues of different species has been investigated by use of specific inhibitors, immunohistochemistry, enzyme autoradiography and in situ hybridization [109]. In the brain, MAO-A has been prevalently found in noradrenergic neurons whereas MAO-B has been detected in serotoninergic and histaminergic neurons and in glial cells [90]. Regarding peripheral tissues, mainly MAO-B has been found in liver, platelets and kidney while MAO-A was present in placenta, liver, intestine and thyroid gland. Human heart contains predominantly MAO-A, but MAO-B is also present [90]. In mouse cardiomyocytes, MAO-B is the predominant isoform while, in contrast, rat cardiomyocytes express more MAO-A [90].

4.4.4 Monoamine oxidases inhibitors as therapeutic agents

MAOs catalyze the oxidative deamination and the byproducts of this reaction include several chemical species with neurotoxic potential, such as H_2O_2, ammonia and aldehydes [110]. In the past years, it has been well documented that these flavoenzymes contribute to mitochondrial dysfunction and neurodegenerative diseases in both patients and animal models [111]. Moreover, MAOs are also involved in numerous other pathologies, in particular neuronal and psychiatric disorders [108, 111]. Development of MAO inhibitors started receiving attention with the serendipitous finding of antidepressant effects in patients treated with iproniazid, a hydrazine-based anti-tubercular agent structurally similar to isoniazid [104]. Up to date several MAO inhibitors have been developed and can be classified in three groups as stated below:

- Irreversible and non-selective inhibitors, such as phenelzine, pargyline and tranylcypromine;
- Irreversible and selective inhibitors, such as selegiline for MAO-B and clorgyline for MAO-A;
- Reversible and selective MAO inhibitors, such as moclobemide for MAO-A and safinamide for MAO-B.

MAO inhibitors have been used for decades for the treatment of depression. The antidepressant properties result from selective MAO-A inhibition in the central nervous system, which leads to increased brain levels of dopamine, noradrenalin and serotonin [112]. Some of the non-selective irreversible inhibitors, such as phenelzine and tranylcypromine, are still in clinical use along with the reversible MAO inhibitors moclobemide, befloxatone, toloxatone and safinamide [104]. As levels of MAO-B are increased in patients with Parkinson's disease, MAO-B inhibitor selegiline has been used as a dopamine sparing agent [111, 113]. Some side-effects of these drugs include liver toxicity, hypertensive crises and haemorrhage [90]. Hydrazine-derived inhibitors were highly associated with liver toxicity, but this side-effect was avoided with the development of non-hydrazine compounds [104]. Irreversible MAO-A inhibitors may cause "cheese effect" which even led to death in some cases [104, 106]. This side-effect occurs when tyramine and other sympathomimetic amines ingested with food are not degraded in the intestines. They are therefore able to enter the circulation and potentiate sympathetic cardiovascular activity by triggering the release of noradrenaline [113]. Although this side-effect represents a major drawback, this problem was resolved by using reversible MAO-A inhibitors such as brofaromine, caroxazone, moclobemide, toloxatone and minaprine. In addition to these, safinamide, a reversible MAO-B inhibitor, was recently licensed by EMA (Emergency medical assistant licensing board) for the treatment of Parkinson's disease in combination with L-DOPA or with other anti-Parkinson drugs in mid-to advanced-stage fluctuating patients [114].

4.4.5 Monoamine oxidases in cardiovascular diseases

MAO has been extensively studied in the brain but it is only recent that the role of these flavoenzymes is emerging also in relation to cardiac pathophysiology. Parini's group was the first to demonstrate that MAO-A is an important source of ROS in the myocardium [115].

They showed that MAO-A induced ROS formation is able to trigger signaling pathways that are receptor-independent and lead to cell proliferation and hypertrophy or apoptosis. Moreover, another study from the same group demonstrated that incubation of cardiomyocytes with serotonin led to an increase in ROS production and hypertrophy that involved the activation of extracellular signal regulated kinase (ERK) 1/2 in a MAO-A dependent manner [115, 116]. It was further demonstrated that hypertrophy induced by serotonin requires both MAO-A activity and receptor-mediated effects [115]. Indeed, serotonin receptor-mediated effect is required for the phosphorylation of ERK1/2 whereas MAO-generated H_2O_2 is necessary for the translocation of ERK into nucleus [115]. Kaludercic et al. provided an important evidence of the contribution of MAO-A in maladaptive remodeling and myocardial dysfunction in hearts subjected to hemodynamic stress [117]. They further showed that triggering MAO-A activity leads to increased ROS formation, oxidative stress, mitochondrial dysfunction, caspase activation and apoptosis in cardiomyocytes (Figure 9). In this study, clorgyline was used as a MAO inhibitor and no side-effects were observed in control mice. Moreover, the effect of genetic deletion of MAO-A in cardiovascular setting was further characterized using mice expressing a dominant-negative MAO-A (MAO^{neo}). After 9 weeks of transverse aortic constriction (TAC) wild type (WT) hearts displayed greater chamber dilation and impairment in LV function accompanied by increased cardiac fibrosis whereas MAO^{neo} mice showed a complete protection against TAC-induced cardiac remodeling. In contrast, another study showed that MAO-A KO mice performed worse after aortic banding [118]. This discrepancy could be due to different genetic models used in these studies or due to differences in the severity of the aortic banding used to induce hypertrophy and heart failure.

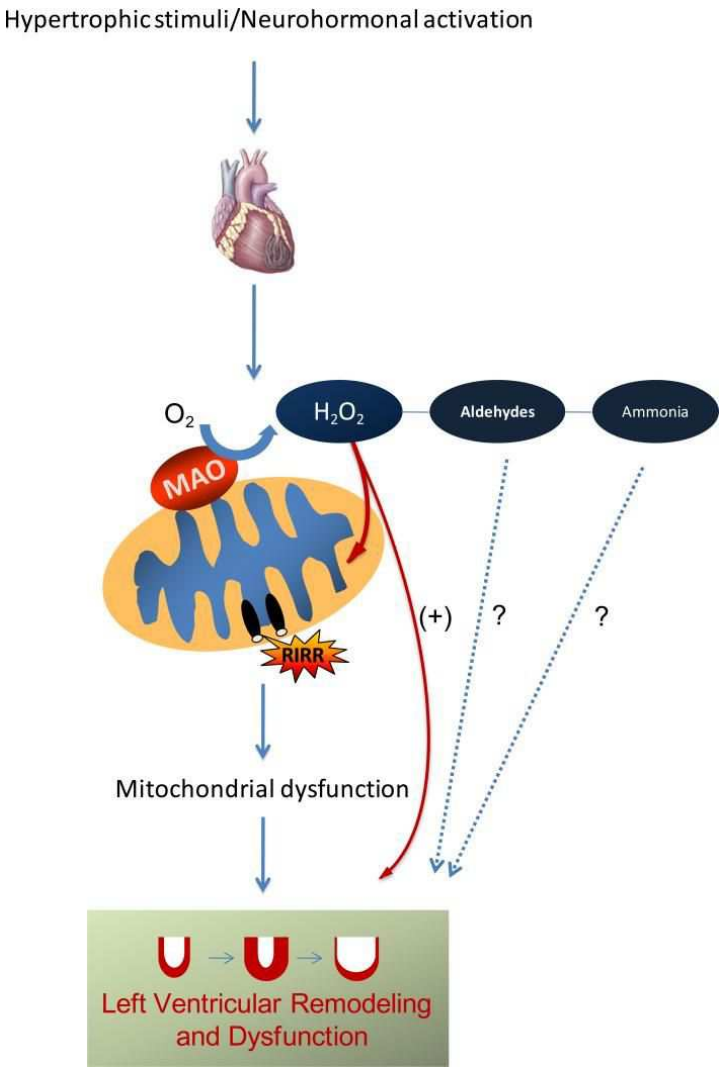

Figure 9. MAO-induced ROS formation and LV dysfunction in the heart. Stress stimuli such as pressure-overload can trigger hyperadrenergic activation leading to increased availability of catecholamines for MAO-dependent degradation. Consequently, increased H_2O_2 formation can directly influence LV remodeling and myocardial function, but it may also target mitochondria resulting in permeability transition pore opening and ROS induced ROS release. Moreover, other products of these flavoenzymes, such as aldehydes and ammonia, may also participate and exacerbate these processes. LV: left ventricle, ROS: reactive oxygen species, MAO: monoamine oxidase. From Kaludercic et al., 2011 [110]

A genetic expression profile study reported that MAO-A expression is increased in pathological cardiac hypertrophy and heart failure in rats, but not in physiological hypertrophy induced by exercise [119]. The role of MAO-B has also been documented in pressure overload induced heart failure [120]. In these mice, MAO-$B^{-/-}$ mice displayed reduced cardiac oxidative stress, LV remodeling and apoptosis. Furthermore, absence of MAO-B activity in those hearts completely prevented LV dilation/pump failure [120]. MAO-

dependent aldehyde production is also shown to be detrimental for mitochondrial function suggesting that these flavoenzymes not only act as ROS sources but are also producing toxic aldehydes that are injurious for heart [120-122]. On the other hand, catecholamine cycling was also improved in mice lacking MAO-A or MAO-B activity. Indeed, both norepinephrine and dopamine degradation were increased in failing hearts due to MAO activation, and its inhibition led to improved neuronal pools and availability of these catecholamines [117, 120].

Studies employing genetically modified mice show that MAO-$A^{-/-}$ and MAO-$B^{-/-}$ display a slight reduction in contractility/relaxation, although fractional shortening and ejection fraction remain unchanged when compared to WT mice [117, 120]. In contrast, another study demonstrated that MAO-$A^{-/-}$ mice display cardiomyocyte hypertrophy and LV dilation at baseline, although LV dysfunction was absent and no hemodynamic alterations were observed [118]. Since MAO deletion in these mice is global and constitutive, it is likely that changes in function and morphology at baseline are due to excessive catecholamine build-up from birth. This issue could be better evaluated using conditional cardiomyocyte-specific MAO-$A^{-/-}$ or -$B^{-/-}$ mice. Notably, pharmacological MAO inhibition does not have any effects on basal cardiac structure or function.

Several studies have also investigated the role of MAO in ischemia/reperfusion (I/R) injury [123, 124]. MAO inhibition with both clorgyline and pargyline remarkably reduced infarct size in an in vivo rat model of I/R injury [123]. Another independent study also showed that pargyline completely prevented I/R induced injury in isolated Langendorff perfused mouse hearts [101]. It has been also demonstrated that MAO-A generated ROS in I/R is responsible for sphingosine kinase inhibition, ceramide accumulation and S1P (sphingosine-1-phosphate) degradation in cardiac myocytes thereby leading to mitochondria-mediated apoptosis [125].

The significant role of MAO in generating ROS formation and cardiac dysfunction is also supported by in vitro and in vivo models of MAO overexpression [126]. Cardiomyocyte specific overexpression of MAO-A in mice led to dramatic loss of cardiomyocytes (around 50%), increased fibrosis and ventricular failure [126]. Moreover, these hearts displayed p53 accumulation and reduced levels of PGC-1α (peroxisome proliferator-activated receptor-γ coactivator-1α), a master regulator of mitochondrial biogenesis. These changes were accompanied by excessive H_2O_2 formation, reduced ATP levels and mitochondrial

dysfunction [126]. Recent work has linked these flavoenzymes with lysosomal dysfunction both in vitro and in vivo [127]. MAO-A dependent ROS generation blocked autophagic flux with accumulation of LC3II, p62, and ubiquitylated proteins, leading to mitochondrial fission and cardiomyocyte necrosis. These effects are likely due to MAO-A induced inhibition of nuclear translocation of TFEB (transcription factor-EB), a master regulator of autophagy and lysosome biogenesis [127].

The involvement and the pivotal role of MAO in cardiovascular injury highlighted by these studies prompt the question whether MAOs could play a role in the oxidative stress and cardiac dysfunction triggered by hyperglycemia. Moreover, the fact that these enzymes can be targeted pharmacologically makes it tempting to hypothesize that their inhibition might represent an attractive therapy for the treatment of diabetic cardiomyopathy. This concept is supported by recent work showing the protective efficacy of MAO inhibition on diabetes-induced cardiac dysfunction [128]. However, the mechanisms linking MAO activity with mitochondrial dysfunction, ROS formation, inflammation and adverse remodeling are still far from being elucidated. In addition, it remains an open question whether MAO-dependent ROS generation might affect the crucial cross-talk between mitochondria and ER that occurs in diabetic conditions and leads to the impairment in ER homeostasis.

4.5 ENDOPLASMIC RETICULUM STRESS

ER is a network of tubules in the cytoplasm essential for the synthesis, folding and processing of secretory and transmembrane proteins. In order to maintain ER homeostasis, a balance between ER protein load and folding capacity of this organelle must be achieved. However, under several physiological and pathological conditions this balance is disrupted, resulting in the accumulation of mis/unfolded proteins, a condition known as ER stress. Under these conditions, ER activates a signaling network to maintain its homeostasis known as unfolded protein response (UPR). When the UPR is unable to re-establish the balance between protein load and folding capacity, it causes cell death and dysfunction [129]. In the past decade, ER stress has been associated with several cardiovascular complications and neurodegeneration [130].

4.5.1 Unfolded protein response

The UPR maintains ER homeostasis with the following three distinct functions: (i) attenuation of protein translation to reduce ER protein load, (ii) upregulation of molecular chaperones to increase the folding capacity of ER, and (iii) activation of ER-associated protein degradation (ERAD) pathway to remove the accumulated misfolded proteins and prevents them from forming toxic protein aggregates [129]. The UPR activates signaling pathways through three major transmembrane proteins: protein kinase R-like ER kinase (PERK), the inositol-requiring kinase-1 (IRE-1) and the activating transcription factor 6 (ATF6) (Figure 10) [129]. In normal conditions, ER chaperone binding immunoglobulin protein (BiP), also known as 78 kDa glucose-regulated protein (GRP78), is bound to the ER luminal domain of PERK, IRE1 and ATF6 thereby keeping them inactive [131]. However, accumulation of misfolded proteins causes BiP/GRP78 to dissociate from these three ER sensors and translocate to misfolded protein, leading to the activation of all three UPR branches.

4.5.1.1 Protein kinase R-like ER kinase

When GRP78 dissociates from PERK, it allows this transmembrane protein to dimerize facilitating its trans-autophosphorylation. PERK is then activated and phosphorylates the eukaryotic translation initiation factor 2α (eIF2α) on serine 51 (Figure 10) [132]. This phosphorylation event downregulates cap- or eIF2α- dependent translation, thus attenuating global mRNA translation [133]. This helps ER to reduce its protein load and favors cell survival. When general translation is inhibited, PERK/eIF2α stimulates translation of specific proteins, including activating-transcription factor 4 (ATF4), C/EBP homologous protein (CHOP) and growth arrest and DNA damage 34 (GADD34) [129]. It has been also demonstrated that PERK can phosphorylate nuclear factor (erythroid-derived 2)-like-2 factor (Nrf2), causing it to translocate to the nucleus and activate the expression of anti-oxidant genes in response to oxidative stress [134]. Therefore, this UPR signaling pathway acts to preserve redox balance during ER stress through activation of ATF4 and Nrf2.

4.5.1.2 Inositol-requiring kinase-1

The IRE1 exists in two isoforms, namely IRE1α and IRE1β, but UPR is mainly governed by the IRE1α isoform. This enzyme functions as both kinase and endoribonuclease [130, 135]. Like PERK, IRE1α also dimerizes and undergoes trans-autophosphorylation, which activates its endoribonuclease activity. Upon activation, IRE1α endoribonuclease splices 26-nucleotide intron from X-box-binding protein 1 (XBP1) mRNA, yielding an activated spliced form of this protein (Figure 10). The spliced XBP1 translocates to the nucleus and binds to the promoter region of ERSEs (ER stress response elements) activating the transcription of several ER chaperones and proteins involved in the ERAD machinery [136]. IRE1α branch is also known to recruit the ASK1 (apoptosis signal-regulating kinase 1), caspase-12 and TRAF2 (tumor necrosis factor receptor-associated factor 2) and thus activates JNK (jun N terminal kinase) pathway [137]. Therefore, this branch of UPR regulates chaperone induction and ERAD pathway.

4.5.1.3 Activating transcription factor 6

In mammals, ATF6 protein exists in two isoforms, namely ATF6α and ATF6β. This transcription factor has golgi localization sequence [138]. In normal conditions, ATF6 is

resident in the ER via an interaction with GRP78, but under ER stress conditions this interaction is disrupted causing ATF6 to translocate to golgi (Figure 10) [138]. Once there, ATP6 is cleaved, first by site 1 protease and then in the intramembrane region by S2P, yielding a 50 kDa ATF6 protein which then translocates to the nucleus [135]. ATF6 acts a transcriptional activator of genes involved in ERAD, lipid biosynthesis, protein folding and ER expansion [138].

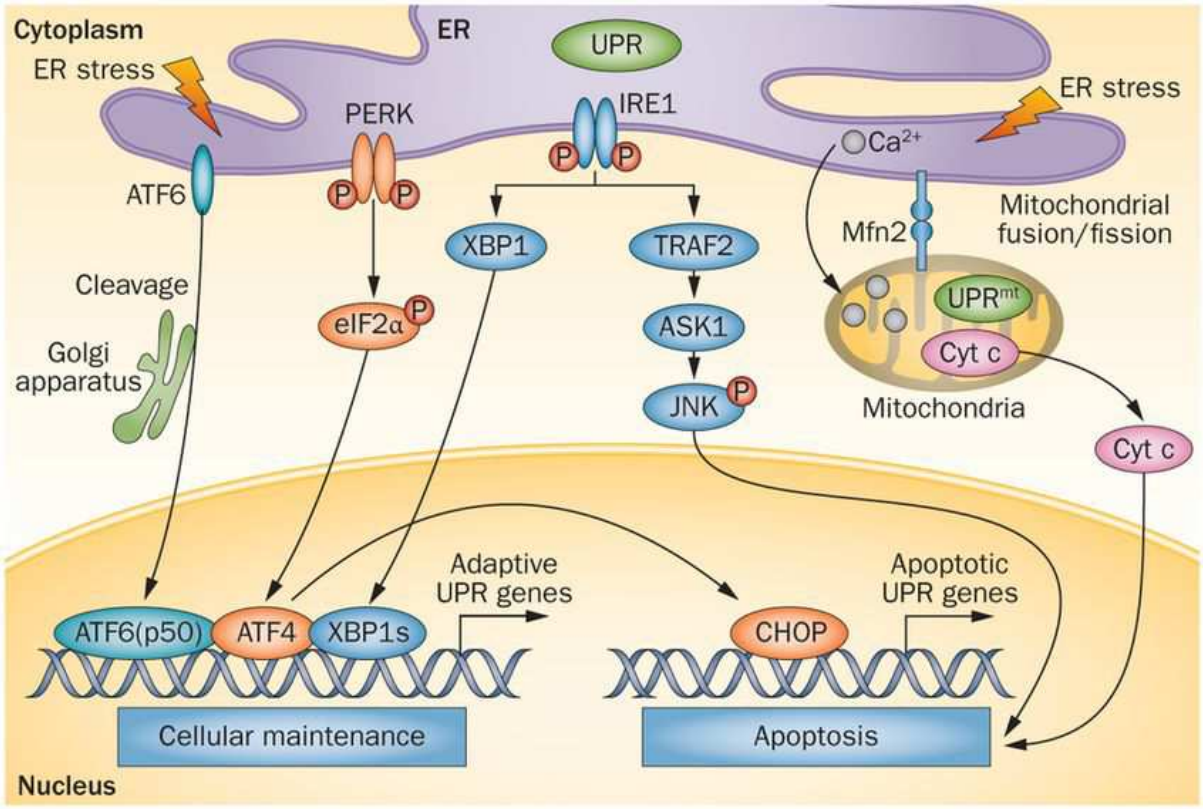

Figure 10. UPR pathway in the ER. ER stress activates three branches of UPR, namely ATF6, PERK and IRE1α. ATF6 translocates to golgi upon activation, where it is cleaved by proteases and yields a 50 kDa fragment, which then translocates to the nucleus and activates several ER stress genes. PERK and IRE1α undergo trans-autophosphorylation and activate the downstream eIF2α and XBP1 pathways, respectively. This leads to the inhibition of global translation but activates specific genes including ATF4 and CHOP to maintain the ER homeostasis. UPR: unfolded protein response, ER: endoplasmic reticulum, ATF6: activation transcription factor 6, PERK: protein kinase R-like ER kinase, IRE1α: inositol-requiring kinase-1α, eIF2α: eukaryotic translation initiation factor 2α. From Inagi et al., 2014 [132]

4.5.2 Contribution of the unfolded protein response to diabetic cardiomyopathy

Diabetic cardiomyopathy is associated with alterations in both intracellular Ca^{2+} homeostasis and metabolism, which together with increased protein synthesis can induce ER stress and consequently trigger the UPR. Several studies reported the upregulation of BiP/GRP78, accompanied with the activation of PERK and IRE1α pathway in both T1D and T2D animal models. Moreover, Dally et al. showed that upregulation of XBP1 and GRP78 along with sarco/ER Ca^{2+} ATPase (SERCA) occurs in hearts from patients with diverse cardiomyopathies [139]. ER stress is also associated with the activation of caspase-12 in STZ-induced model of T1D, leading to myocardial apoptosis and thus contributing to the pathogenesis of diabetic cardiomyopathy [140]. Several studies indicate that ER stress is both a trigger and a consequence of autophagy in diabetes. Under conditions leading to ER stress, Ca^{2+} release from ER can inhibit the activity of mammalian target of rapamycin complex 1 (mTORC1) via activation and phosphorylation of AMPK [141]. Inhibition of mTORC1 is proposed to facilitate autophagy [142]. On the other hand, it has been demonstrated that restoration of autophagy alleviates obesity-induced ER stress [143, 144]. Chemical chaperones, such as 4-phenyl butyric acid and tauroursodeoxycholic acid (TUDCA), have been shown to reduce ER stress in T2D mice [145]. These chaperones also prevented apoptosis in cardiomyoblasts treated with high glucose [143]. Moreover, inhibition of IRE1α activity in STZ-induced T1D blocked ER stress and CHOP-mediated apoptosis thereby preventing cardiac damage [146]. Collectively, all these studies demonstrate the important role of ER stress in the development and progression of diabetic cardiomyopathy.

Although several studies have been conducted in order to understand the role of ER stress in diabetic cardiomyopathy, it still remains to be elucidated how the cell decides between survival and death following UPR activation. It also remains to be elucidated to what extent these UPR pathways are involved in the pathophysiology of diabetic cardiomyopathy. A better understanding of these questions might provide us with new targets for drug discovery and therapeutic intervention.

4.6 FIBROSIS

Fibroblasts constitute the most numerous cell population in the myocardium and are found in all vertebrate organisms. They are responsible for the synthesis of a variety of extracellular matrix (ECM) components, including multiple collagen isoforms, as well as fibronectin, and thus play a prominent role in defining cardiac structure and function [147]. Fibroblasts are responsible for the development of fibrosis in the heart as well as in other organs [148]. Upon injury, cardiac fibroblasts within the connective tissue convert to their activated form, often known as myofibroblasts, and secrete elevated levels of ECM proteins to promote a pro-fibrotic environment ultimately leading to distorted organ architecture and function [149]. Fibrosis is associated with the majority of cardiovascular diseases in experimental animal models and humans [150]. Increased ECM synthesis and decreased degradation result in increased mechanical stiffness and diastolic dysfunction in the heart. In addition to this, increased ECM deposition between the layers of cardiac myocytes also disturbs their electrical signaling resulting in impaired cardiac contraction.

Fibrosis may occur in two forms, reactive interstitial fibrosis or replacement fibrosis [151]. Reactive interstitial fibrosis progresses without cardiomyocyte loss in pressure overloaded hearts, in order to preserve the pressure generating capacity of the heart [152]. However, it is believed that reactive interstitial fibrosis later develops into a state of replacement fibrosis causing cardiomyocyte hypertrophy and death [152]. Indeed, cardiomyocyte apoptosis and replacement fibrosis have been documented in animal models of acute myocardial infarction [152].

In vitro, high glucose stimulates fibroblast proliferation, promotes myofibroblast transdifferentiation and activates transcription and secretion of ECM proteins [153, 154]. It is demonstrated that high glucose can enhance the synthesis of collagen III, both at mRNA and protein levels, in human skin fibroblasts and increase the cell proliferation in human cardiac myofibroblasts [153, 155]. Moreover, high glucose treatment increas the deposition of type I collagen in adult rat cardiac fibroblasts [156]. It has been proposed that high glucose might induce fibrosis via activation of angiotensin II, TGF-β signaling and ROS generation pathways [157]. However, it appears that hyperglycemia *per se* is not responsible for diabetes-associated cardiac fibrosis, but rather it is the inflammation and ROS formation that

lead to fibrosis [154]. In this regard, it has been demonstrated that renal fibrosis persisted despite tight glycemic control in STZ-induced T1D mice [158].

Inflammation and fibrosis are tightly linked in diabetic cardiomyopathy. In particular, pro-inflammatory cytokine tumor necrosis factor α (TNFα) and growth factor TGF-β have been shown to modulate fibroblast phenotype and trigger fibrosis [159]. Incubation of fibroblasts with TNFα resulted in cell proliferation and increased collagen synthesis whereas TGF-β induced differentiation of cardiac fibroblasts into myofibroblasts [159, 160]. TGF-β is upregulated in both T1D and T2D hearts and may mediate pro-fibrotic effects via Smad-dependent and Smad-independent pathways [154]. In addition to cytokines and growth factors, infiltration of inflammatory monocytes/macrophages and mast cell degranulation are also known to contribute to the development of cardiac fibrosis [161]. Abolishing macrophage accumulation prevented cardiac fibrosis and ameliorated diastolic dysfunction in hypertensive rats [161]. Cardiac mast cells may induce cardiac hypertrophy and fibrosis by synthesizing and secreting pro-fibrotic and pro-inflammatory factors [161, 162]. In fact, administration of mast cell-stabilizing agent tranilast to pressure overloaded mice reduced fibrosis and prevented cardiac damage [162]. Interestingly, oxidative stress has been shown to induce mast cell degranulation [163-165]. These studies suggest that targeting ROS producing enzymes, inflammation and/or pro-inflammatory cells might be a new strategy to prevent myocardial fibrosis.

Besides inflammation, oxidative stress, AGE/RAGE formation, adipokines and recently identified miroRNA-133 are also associated with cardiac fibrosis [154]. Using pharmacological interventions, several studies have demonstrated the role and contribution of oxidative stress in diabetes-associated cardiac fibrosis [154, 166, 167]. In T1D and T2D mice, inhibition of oxidative stress with dehydroepiandrosterone, a steroid that possesses multi-targeted antioxidant properties, reduced interstitial fibrosis, cardiomyocyte hypertrophy and improved diastolic function [154, 168].

AGE/RAGE signaling is known to activate inflammatory genes, crosslink collagens and laminins in the extracellular matrix, and stimulate fibroblast proliferation that may increase diastolic stiffness and cause diastolic dysfunction [169]. Indeed, inhibition of RAGE activity prevented fibrosis and development of cardiac dysfunction in db/db T2D mice [154].

Adipokines leptin and adiponectin have also been associated with cardiac fibrosis [154]. Leptin is known to induce matrix metalloproteinases in fibroblasts. Its role in cardiomyocytes remains controversial since it can exert both hypertrophic and anti-hypertrophic actions [154, 170, 171]. Adiponectin is an anti-inflammatory agent that exerts anti-fibrotic effects in angiotensin II-induced cardiac remodeling and reduced cardiac hypertrophy via AMPK signaling in T2D mice [154].

Several mechanisms by which fibrosis can lead to heart failure have been proposed, including reduced ventricular compliance causing HFpEF, atrial fibrillation, increased risk of ventricular arrhythmias, diabetes-related perturbation of the reparative response following infarction, adverse remodeling and development of post-infarction heart failure [154]. Thus, preventing cardiac fibrosis might reduce mortality and morbidity in patients with diabetic cardiomyopathy. It appears that novel therapies targeting ROS formation, AGE-mediated crosslinking and TGF-β system hold significant promise.

4.7 INFLAMMATION

Emerging evidence indicates that inflammation is a crucial process in adverse myocardial remodeling [172]. A number of clinical and animal studies reported that activation of several inflammatory pathways occurs in cardiovascular complications [172]. Inflammation involves the secretion of cytokines, such as chemokines, interferons, ILs, TNFs and recruitment of innate immune cells, such as neutrophils, mast cells and monocyte/macrophages [173]. Prolonged exposure of heart to these inflammatory agents can exacerbate myocardial remodeling and lead to myocardial damage [173]. Notably, in addition to local adverse effects it has been demonstrated that cardiac injury-induced inflammation in the heart results in the release of TNFα, IL-1β, IL-18 and growth factor TGF-β into the circulation [173]. In agreement with this, a recent study reported elevation of these cytokines in the serum of diabetic patients suggesting that they might be used as biomarkers to diagnose early stage diabetic cardiomyopathy. Early diagnosis of diabetic cardiomyopathy would allow for the timely start of treatment, thus attenuating disease progression prior to the onset of irreversible complications [174].

Cytokines can lead to contractile dysfunction and cell death by various mechanisms. For instance, cytokines can trigger peroxynitrite formation via iNOS activation [66]. Upon stimulation, iNOS produces large amounts of NO that can react with superoxide to form peroxynitrite, a species known to cause myocardial contractile failure. Rat hearts perfused with cocktail of cytokines, including IL-1β, interferon-γ and TNF-α, resulted in an enhanced activity of Nox and iNOS accompanied by increased NO content, superoxide production and markers of peroxynitrite formation [175]. The peroxynitrite decomposition catalyst FeTPPS (5,10,15,20-tetrakis-[4-sulfonatophenyl]-porphyrinato-iron[III]), inhibited the decline in myocardial function and decreased perfusate nitrotyrosine levels indicating that cytokine-induced myocardial contractile failure is mediated by peroxynitrite [175].

Another cytokine-mediated mechanism involves the regulation of SERCA expression and activity by oxidation/nitration leading to impaired ER function [66]. It is also known that cytokines can increase the synthesis of ECM in the heart leading to fibrosis and ultimately cardiac dysfunction as discussed above. Indeed, TNFα inhibition with a monoclonal antibody prevented intra-myocardial inflammation, fibrosis and cardiac damage in STZ-induced T1D

rats [176]. Importantly, clinical studies demonstrated that recombinant human IL-1 receptor antagonist Anakinra improved glycaemia and β-cell secretory function and reduced markers of systemic inflammation in patients with T1D and T2D, suggesting that antagonizing the IL-1 system may prevent or delay the onset of diabetes [177, 178].

Expression of pro-inflammatory cytokines is under the control of nuclear factor kappa-light-chain-enhancer of activated B cells (NF-κB), a transcription factor activated in myocarditis, congestive heart failure and cardiac hypertrophy [179]. Several stimuli may induce the activation of this transcription factor including pro-inflammatory cytokines themselves, elevated free fatty acid levels in plasma, hyperglycemia, ROS, angiotensin II, endothelin-1, toll-like receptors and hyperglycemia-induced AGE formation [66]. It has been demonstrated that high glucose can promote NF-κB activity in cultured neonatal rat cardiomyocytes through diacylglycerol-PKC signal transduction pathway [102]. In normal conditions, NF-κB resides in the cytoplasm as an inactive heterodimer bound to the inhibitory protein IκB [179]. Several stress stimuli induce IκB phosphorylation leading to its ubiquitination and proteasome-mediated degradation that releases the NF-κB heterodimer, which can then translocate to the nucleus [179]. NF-kB transcription factors bind to 9-10 base pair DNA sites (called kB sites) as dimers and induce cytokine gene expression in the nucleus. Resveratrol inhibits NF-κB activity by upregulating SIRT1-mediated deacetylation of lysine 310, thus preventing metabolic dysregulation and inflammatory processes in several murine models [180]. While the expression of pro-IL-1β and pro-IL-18 is mediated by NF-κB, their processing to the mature form is mediated by active caspase-1. This caspase is a part of inflammasome complex, nucleotide-binding oligomerization domain-like receptors with pyrin domain (NLRP3) [173]. Inflammasome is a multiprotein complex necessary for caspase-1 activation and amplification of the inflammatory response. Indeed, NLRP3 gene silencing therapy ameliorated inflammation, cardiac fibrosis and improved cardiac function in high fat diet-induced T2D rats [181]. Recently, it has been proposed that inflammasome activation depends on cell-to-cell communication in the heart, including cardiomyocytes, fibroblast and innate immune cells [173].

Mitochondrial ROS formation has been identified as an important NLRP3 inflammasome activator in cardiac diseases [182]. The saturated fatty acid palmitate leads to the activation of the NLRP3 inflammasome and release of active IL-1β in a mitochondrial ROS-dependent manner [183]. Fibroblasts have been shown to secrete IL-1β in response to

ATP and mitochondrial DNA released from neighboring cells such as cardiomyocytes [173, 181, 184]. In addition to fibroblasts, injured cardiomyocytes also secrete IL-1β and release damage-associated molecular pattern molecules, DNA fragments and heat-shock proteins which mandate surrounding healthy cardiomyocytes to produce inflammatory factors such as IL-1β, IL-18, IL-6, monocyte chemoattractant protein-1 and TNFα [181]. These factors in turn activate versatile signaling networks within surviving cardiomyocytes and trigger the activation and recruitment of immune cells including macrophages, leukocytes and mast cells further exacerbating inflammatory response [181]. Collectively, these studies indicate that cross-talk between different cardiac cell populations, including cardiomyocytes, fibroblasts and immune cells, plays a very important role in triggering myocardial inflammation, which then contributes to reduced contractile function and heart failure in various diseases including diabetic cardiomyopathy.

In summary, diabetic cardiomyopathy is a very complex disease associated with structural, functional and metabolic changes in the heart. It is proposed that, not one single mechanism, but rather the combination of several mechanisms contributes to the pathogenesis of this epidemic disease [37, 39, 66, 185]. From preclinical and animal studies it has become clear that oxidative stress and inflammation are central components in triggering and driving the pathological processes associated with diabetic cardiomyopathy [39, 66]. Mitochondria play a critical role in inducing oxidative stress and triggering inflammation via inflammasome pathway [39, 181, 186]. This notion is more relevant for the heart since cardiomyocytes have higher mitochondrial content relative to other cell types, thus making cardiac tissue more susceptible to mitochondria-induced damage compared to other organs. This suggests that therapeutic interventions targeting mitochondria or preventing mitochondria-induced damage may be required to treat patients with diabetes-associated cardiovascular complications.

5. AIMS AND HYPOTHESES

The aim of this study was to investigate the role of MAOs in oxidative stress, mitochondrial dysfunction and cardiac damage in T1D. Diabetes-induced derangements and protective mechanisms were investigated in the following experimental models: (i) mimicking the diabetic conditions with high glucose (HG) and/or pro-inflammatory cytokine IL-1β in primary cardiomyocytes in vitro and (ii) using STZ-induced T1D mice in vivo.

The working hypothesis was that mitochondrial ROS formation plays a central role in diabetic cardiomyopathy. Based upon previous work from our laboratory demonstrating the involvement of MAO in cardiac pathology, we investigated whether MAOs contribute to increased ROS formation and mitochondrial dysfunction in cultured primary cardiomyocytes treated with HG and/or IL-1β, a pro-inflammatory cytokine found to be elevated in diabetic patients. MAO involvement and contribution were evaluated through a classical pharmacological approach, using pargyline as an inhibitor for both MAO-A and MAO-B. We further assessed whether MAO activity is involved in the interplay between mitochondria and ER and whether MAO-generated ROS contribute to impaired ER homeostasis and activation of UPR in this setting.

Next, we aimed to assess the efficacy of MAO inhibitor pargyline in preventing structural and functional changes in T1D hearts in vivo. We hypothesized that MAOs contribute to the oxidative stress and diastolic dysfunction occurring in T1D hearts. Diabetic cardiomyopathy is associated with cardiac inflammation, mitochondrial ROS formation, oxidative stress and fibrosis in, but the exact source of ROS linking these events in the heart has not been identified yet. To this aim, we investigated whether MAO activity might be involved in the formation of the vicious cycle between mitochondrial ROS and pro-inflammatory response ultimately leading to fibrosis and LV dysfunction.

6. MATERIALS AND METHODS

6.1 Primary cardiomyocytes isolation and culture

6.1.1 Isolation and culture of neonatal rat ventricular myocytes

Neonatal rat ventricular myocytes (NRVMs) were isolated from 1-3 days old Wistar rats as previously described [120]. Briefly, hearts were excised, cut into smaller pieces and left for overnight digestion with 2.5% trypsin 10X (Thermo Fisher Scientific) at 4°C in Hank's balanced salt solution (HBSS, Sigma). Next day, tissues were incubated with 0.75 mg/ml collagenase type II (Thermo Fisher Scientific) in HBSS for 10 min (at 2 min intervals) at 37°C and cells dissociated by pipetting. Following centrifugation at 1000 rpm for 7 min, cells were resuspended in minimum essential media (MEM, Invitrogen) and pre-plated for an hour to let cardiac fibroblasts attach to the plastic surface. Plates/coverslips were coated with a solution of 0.1% porcine gelatin (Sigma) and incubated at 37°C for 1 h. The non-adherent myocytes were plated in gelatin coated plates at the density of $1x10^5$ cells/ml in MEM supplemented with 10% FBS, 1% penicillin/streptomycin, non-essential amino acids, 1 mM BrdU. Cells were maintained at 37°C in presence of 5% CO_2. The medium was changed to MEM supplemented with 1% FBS after 24 h of plating.

6.1.2 Isolation and culture of adult mouse ventricular cardiomyocytes

Adult mouse ventricular myocytes were isolated from the hearts of 12 week old C57Bl6/J mice as described previously [120]. In brief, mice were injected intraperitoneally (i.p.) with 1,000U heparin 30 min before the isolation procedure to prevent coagulation of blood in the arteries. Hearts were quickly excised and the aorta cannulated. Hearts were then perfused with perfusion buffer (PB, in mM: NaCl 120, KCl 14.75, KH_2PO_4 0.6, Na_2HPO_4 0.3, $MgSO_4$ 1.2, HEPES 10, $NaHCO_3$ 4.6, taurine 30, BDM 10, glucose 5.5, pH 7.4) for 2 min to remove the blood. Next, hearts were perfused with PB containing 1.2 mg/ml collagenase type II (Worthington) and 0.05 mg/ml protease type XIV (Sigma) for 3 min at 2 ml/min and then for 8 min at1.5 ml/min. After perfusion hearts were placed into 5 ml of PB added with 10% FBS and 12.5 μM $CaCl_2$, cut into smaller pieces and cardiomyocytes

dissociated by gentle pipetting. The suspension was filtered through 100 μm mesh, centrifuged at 500 g for 1 min and resuspended in PB containing increasing Ca^{2+} concentration. Ca^{2+} concentration was gradually increased from 0.25 mM to 1 mM to avoid Ca^{2+} overload and hypercontracture. After each step cardiomyocytes were allowed to sediment by gravity. Cells were plated at a non-confluent density of 25,000 rod-shaped myocytes/ml on glass coverslips pre-coated with laminin (20 μg/ml) in MEM with Hank's salts supplemented with 10 mM $NaHCO_3$, 5% FBS, 1% penicillin/streptomycin, 10 μM blebbistatin and kept at 37°C in presence of 2% CO_2. After 1h media was changed to MEM with Hank's salts supplemented with 10 mM $NaHCO_3$, 0.2% BSA, 10 μM blebbistatin, 1% insulin-transferrin-selenium (ITS, Thermo Scientific), 2 mM L-glutamine, 2 mM L-carnitine, 5 mM creatine and 5 mM taurine.

6.2 Treatment of primary cardiomyocytes

NRVMs and adult cardiomyocytes were treated in culture media with following additions: normal glucose (NG, 5 mM), high glucose (HG, 25 mM) or high mannitol (HM 25 mM, osmotic control) in presence or absence of IL-1β 25 ng/ml (Sigma). To inhibit MAO activity cells were pre-treated with 100 μM pargyline (Sigma) for 30 min. ROS formation and mitochondrial membrane potential were measured after 48 h in NRVMs and after 3 h of treatment in adult cardiomyocytes. ER stress was assessed after 48 h of incubation.

To induce ER stress, NRVMs were incubated overnight with tunicamycin (1 μg/ml) or thapsigargin (1 μM) in presence or absence of ER stress inhibitor TUDCA (100 μM, Sigma). To assess the effect of MAO inhibition on ER stress, cells were pre-treated with 100 μM pargyline in presence of ER stress-inducers. After overnight incubation, samples were collected to assess ER stress markers gene expression or cells were loaded with MTR to measure ROS formation in these conditions.

6.3 Measurement of mitochondrial ROS formation

6.3.1 Assessment of ROS formation with MitoTracker Red

To measure mitochondrial ROS formation, cells were loaded with 25 nM (NRVMs) or 250 nM (adult cardiomyocytes) MitoTracker Red CM-H_2XRos (MTR, Thermo Fisher Scientific, excitation/emission 579/599 nm), a reduced dye that fluoresces upon oxidation and accumulates inside the mitochondria depending on the mitochondrial membrane potential ($\Delta\Psi m$). After 30 min incubation at 37°C cells were washed and images were captured using fluorescence microscope (Leica TCS SP5). Fluorescence intensity was quantified using Java-based image processing program ImageJ (NIH). For NRVMs, results were normalized to the control values (NG vehicle) and expressed as % vs control. For the adult cardiomyocytes, background signal was subtracted from all analyzed regions of interest and results were expressed as arbitrary fluorescence units (AU).

6.3.2 Transfection of neonatal rat cardiomyocytes and assessment of ROS formation with HyPer

Alternatively, ROS formation in NRVMs was measured using genetically encoded H_2O_2 probe HyPer (Evrogen) targeted either to mitochondria or cytosol. HyPer is a ratiometric dye with two excitation peaks (maxima at 420 nm and 500 nm), and one emission peak (maximum at 516 nm). Upon exposure to H_2O_2, the excitation peak at 420 nm decreases proportionally to the increase in the peak at 500 nm, allowing for ratiometric measurement of H_2O_2. NRVMs were plated in six-well plates at a density of $3x10^5$ cells/well and transfected with calcium phosphate method. For each transfection, 2 µg of plasmid (mito-HyPer or cyto-HyPer) were rapidly mixed with ice cold 250 mM $CaCl_2$ in HBSS (274 mM NaCl, 10 mM KCl and 1.4 mM Na_2HPO_4) and left for 4 min to precipitate. The mixture was added to the cells and after 4 h of incubation, cells were washed with PBS and new MEM media was added. Transfected cells were used for experiments after 48 h.

6.4 Assessment of mitochondrial membrane potential

To measure the ΔΨm, cells were pre-incubated with 25 nM tetramethylrhodamine (TMRM, Thermo Fisher Scientific) in presence of 1.6 µM cyclosporin H. TMRM (excitation 535 nm and emission 600 nm) is a lyophilic rhodamine dye that accumulates into the mitochondria of live cells depending on their ΔΨm. After incubation, cells were analyzed under Leica fluorescence microscope and images were captured before and after the addition of 2.5 µM FCCP (Sigma), a protonophore (H^+ ionophore) and uncoupler of oxidative phosphorylation, to completely abolish ΔΨm . TMRM fluorescence intensity was analyzed using ImageJ and results are expressed ΔF according to the following formula: $\Delta F = F_0/F_{FCCP}$, where F_0= TMRM fluorescence intensity at baseline and F_{FCCP}= fluorescence intensity after addition of FCCP. For kinetics experiments, TMRM fluorescence intensity was monitored following addition of oligomycin (5 µM) or FCCP (2.5 µM). TMRM fluorescence intensity was quantified as described above and data were expressed as % vs the initial value.

6.5 cDNA synthesis and Real time-PCR

Total RNA was extracted from NRVMs using TRIzol reagent (Invitrogen), a monophasic solution of phenol and guanidine isothiocyanate, according to the manufacturer instructions. Reverse transcription reactions were performed using 5 µg of total RNA. After addition of dNTP and random hexamer primers to prime the first strand for cDNA synthesis, RNA was denatured at 65°C for 5 min and then placed on ice. Superscript III (Invitrogen) was added to the mixture which was further incubated at 52°C for 50 min and 70°C for 15 min to synthesize cDNA.

Each PCR reaction was performed in a 20 µl volume combining 10 ng of cDNA, 0.25 µM of forward and reverse primers and 10 µl of SYBR green 2X PCR master mix (Invitrogen). RotorGene 3000 (Qiagen) thermal cycler was used to carry out the real-time PCR reaction. The sequences of forward and reverse primers used to detect the expression of each gene are listed in Table 2.

Target gene	Primer sequence

ATF4	F-5'AATGGATGACCTGGAAACCA3' R-5'TCTTGGACTAGAGGGGCAAA3'
CHOP	F-5'AGAGTGGTCAGTGCGCAGC3' R-5'CTCATTCTCCTGCTCCTTCTCC3'
total-XBP1	F-5'TGGCCGGGTCTGCTGAGTCCG3' R-5'ATCCATGGGAAGAGTTCTGG3'
spliced-XBP1	F-5'CTGAGTCCGAATCAGGTGCAG3' R-5'ATCCATGGGAAGATGTTCTGG3'
unspliced-XBP1	F-5'CAGCACTCAGACTACGTGCG3' R-5'ATCCATGGGAAGATGTTCTGG3'
α-tubulin	F-5'CAACACCTTCTTCAGTGAGACAGG3' R-5'TCAATGATCTCCTTGCCAATGGT3'

Table 2. Sequences of primers used for real-time PCR

6.6 Determination of cell viability

Resazurin based in vitro toxicology kit (Sigma) was used for determination of cell viability. Resazurin is a redox indicator dye that can be added directly to cells in culture. Cells convert the dark blue oxidized form of the dye (resazurin) to a red reduced form (resorufin). This system is specific for viable cells since non-viable cells rapidly lose metabolic capacity and are no longer able to reduce resazurin. Fluorescence intensity was recorded with a fluorimeter using 544 nm excitation and 590 nm emission wavelengths to assess resorufin formation. This value was normalized to the one obtained from control cells treated in the same conditions. Cells were plated in 12 well plates at a density of $2x10^5$ cells/well, and treated with tunicamycin (1μg/ml) or thapsigargin (1μM) in presence or absence of pargyline (100 μM). After 24 h of treatment, culture medium was aspirated and

another 1 ml of culture medium containing 10% resazurin was added. Fluorescence intensity of the supernatant was recorded at the beginning and after 2 h of incubation with resazurin.

6.7 Animal model of type 1 diabetes

All the animal studies were performed using male C57BL6/J mice (6-7 weeks of age and at least 20 g in weight; Charles River Laboratories, UK). T1D was induced with STZ (50 mg/kg/day in citrate buffer pH 4.5) administered intraperitoneally for five consecutive days. Mice were then randomized to receive either vehicle or MAO inhibitor pargyline (50 mg/kg/day) for 12 weeks. Blood glucose levels were measured twice a month using glucose meter (OneTouch Ultra 2) and mice with blood glucose levels ≥17 mM were considered diabetic.

6.8 Assessment of pressure-volume relationships

Cardiac function was assessed using MRI-calibrated PV loops in vivo. MRI scan was performed as previously described [30, 31] and volumes obtained at end systole and end diastole were later used to calibrate hemodynamic data. To acquire PV catheter data, mice were quickly anaesthetized using an isoflurane chamber followed by a 70 mg/kg intraperitoneal injection of pentobarbital. We monitored the adequacy of anesthesia using corneal and withdrawal reflexes. Temperature was maintained at 37°C with a thermostatically controlled heating control unit (Harvard apparatus, Holliston, MA). After endotracheal intubation for mechanical ventilation (ventilation frequency 110 breaths per minute with a tidal volume of 1.2 ml/min; Harvard apparatus, Holliston, MA), mice underwent closed-chest catheterization of the left ventricle via the carotid artery. After a stabilization period of 15 min, pressure and volume data was acquired using a Transonic ADV 500 system (iWorx 125 Systems Inc., NH). Under these conditions, mean heart rate across all groups was 359.6±9.6 (SE). PV-loop analysis was performed by a single investigator blinded to subject identity. Before PV loop analysis, volumes were smoothed (smoothing kernel of 4 ms), and calibrated using the MRI data. Here, the maximum and minimum volumes obtained with the catheter were matched to the MRI-derived LV volumes. Summary pressure values and diastolic stiffness values were derived using Labscribe 2 (iWorx 125 Systems Inc., NH).

6.9 Histology

Hearts were fixed in 10% formalin overnight, embedded in paraffin and sectioned at 10 µm thickness. Samples were analyzed for fibrosis and mast cell degranulation using Masson's Trichrome staining and toluidine blue staining, respectively [117]. Before staining, tissue sections were deparaffinized, rehydrated through 100%, 95%, 85%, 80% and 70% alcohol and washed in distilled water or PBS.

Fibrosis staining was performed on tissue sections using Masson's Trichome kit (Sigma) following manufacturer instructions. In this protocol, collagen and muscle fibers stain differentially when treated sequentially with biebrich scarlet-acid fuchsin, phosphomolybdic-phosphotungstic acid solution and aniline blue. Cytoplasm and muscle fibers stain red whereas collagen displays blue coloration as shown in Figure 11A. Photomicrographs of the sections were evaluated for interstitial collagen fractions using computer-assisted image analysis systems (Adobe Photoshop).

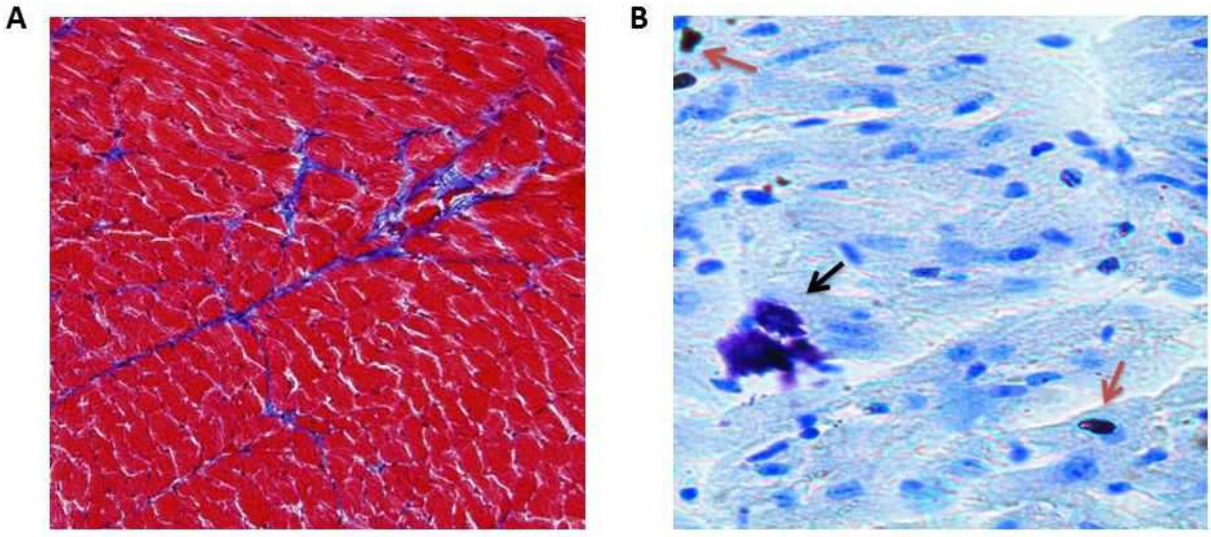

Figure 11. Masson's Trichome and toluidine blue staining. (A) Cardiac muscle fibers stained in red and collagen stained in blue following Masson's Trichome staining on paraffin embedded sections. (B) Red arrows point toward intact mast cells whereas black arrow indicate actively degranulating mast cell.

Toluidine blue stains mast cells red-purple (metachromatic staining) and the background blue (orthochromatic staining) as shown in Figure 11B. Briefly, deparaffinized

and rehydrated tissue sections were stained in toluidine blue 0.1% solution at pH 2.3 for 3 minutes. Slides were than washed in distilled water, quickly dehydrated through 95% and 100% ethanol, cleared in xylene (3 x 15 min) and mounted with Permount. Mast cell density was determined by counting the total number of mast cells per field. Mast cell degranulation was expressed as the number of degranulating mast cells normalized to total number of mast cells.

6.10 Western blot

Isolated cardiomyocytes or heart tissue were homogenized in lysis buffer (1% NP-40, 50 mM Tris HCl, 150 mM NaCl and 2 mM EDTA, pH 7.5) containing phosphatase (PhosSTOP, Roche) and protease inhibitors (cOmplete mini protease inhibitor cocktail, Roche). Homogenized samples were centrifuged at 13,000 x g for 15 min at 4°C and the pellet was discarded. Protein concentration was determined using BCA Protein Assay Kit (Pierce) following the manufacturer's protocol. To denature and solubilize the proteins, 1X NuPage sample buffer (Novex) and β-mercaptoethanol (3%) were added to the samples. Samples were boiled at 100°C for 10 minutes. Then they were loaded on the gel or aliquoted and stored at -20°C.

Proteins were separated on 4-12% gradient SDS-PAGE (NuPage) using MES running buffer (50 mM MES, 50 mM Tris Base, 0.1% SDS, 1 mM EDTA, pH 7.3) at 150 V and transferred to the nitrocellulose membrane (Bio-rad) overnight using transfer buffer (25 mM Tris, 192 mM glycine, 10% methanol, pH 8.0) at 150 mA . Once the transfer was carried out, the membrane was incubated with Red Ponceau dye (EuroClone) to stain all the proteins on the membrane. Next, membrane was destained with NaOH, washed and saturated using a blocking solution composed of 50 mM Tris-HCl, 2 mM $CaCl_2$, 85 mM NaCl, 5% BSA, pH 8.0. After 1 h of blocking at room temperature, blots were incubated at 4°C overnight with primary antibody diluted in blocking solution. Antibodies used in this study to detect proteins of interest are listed in Table 3.

Primary antibody	Manufacturer	Dilution
Anti-MAO-A	Abcam (ab126571)	1:1000
Anti-MAO-B	Sigma (AV43557)	1:1500
Anti-GRP78	Abcam (ab21685)	1:1000
Anti-phospho IRE1α	Novus (NB100-2323)	1:500
Anti-4-HNE	Abcam (ab46545)	1:1000
Anti-ATF4 (CREB-2)	Santa Cruz (SC-200)	1:1000
Anti-GADD34	Santa Cruz (SC-8327)	1:1000
Anti-GAPDH	Sigma (G8795)	1:5000
Anti-α-Tubulin	Abcam (ab4074)	1:1000
Anti-β-Actin	Sigma (A2228)	1:1000

Table 3: List of primary antibodies used in the study

Following incubation with primary antibodies, membranes were washed three times for 10 min with the washing buffer (50 mM Tris-HCl, 85mM NaCl, 0.1% Tween 20, pH 7.4). Secondary antibodies were diluted in blocking solution and incubated with the membrane for 1 hour at room temperature. Secondary antibodies used were:

Anti-mouse (Santa Cruz), dilution 1:5000

Anti-rabbit (Santa Cruz), dilution 1:5000

Secondary antibody is conjugated to reporter enzyme HRP (horseradish peroxidase). After incubation with secondary antibody, membrane was washed three times (10 min each). Protein bands were revealed using LiteAblot luminol solutions (EuroClone). Bands were detected using KODAK Image station 4000 MM PRO and analyzed using Gel-Pro software.

6.11 Statistical analysis

All values are expressed as mean ± SEM. Comparison between groups was performed by one-way or two-way ANOVA, followed by a Tukey's post hoc multiple comparison for normally distributed data and non-parametric Dunn's test for data that was not normally distributed. Comparisons between two groups were performed using non paired two-tailed Student's t-test. A value of $p<0.05$ was considered significant.

7. RESULTS

7.1 HG and IL-1β induce ROS formation in primary cardiomyocytes in a MAO-dependent manner

Hyperglycemia and inflammation are tightly associated with diabetic cardiomyopathy [37, 187, 188]. It has been shown that over-production of pro-inflammatory cytokines, such as TNF-α and IL-1β, provoke cardiomyocyte apoptosis and cardiac remodeling through activation of various cell death pathways. Moreover, patients with cardiomyopathy show elevated levels of IL-1β produced by endothelial cells and myocytes [189, 190]. Thus, to mimic diabetic conditions in vitro more realistically, NRVMs were treated with HG and pro-inflammatory cytokine IL-1β alone or in combination, and ROS levels were initially assessed with MTR after 48 h. To rule out the effect of hyperosmolarity induced by HG, identical concentrations of mannitol were added to cells cultured with NG. HG lead to a mild but significant increase in ROS formation, whereas mannitol treated NRVMs did not show any changes when compared to NG cultured cells (Figure 12). Interestingly, the combination of HG and IL-1β led to a further dramatic increase in ROS formation when compared to HG or IL-1β treatment alone, indicating a synergistic effect of these stimuli in inducing mitochondrial ROS formation. To investigate whether MAO contributes to increased ROS formation in these conditions, we pre-treated cardiomyocytes with pargyline, an irreversible inhibitor of both MAO-A and MAO-B. MAO inhibition abolished ROS formation induced by both HG alone and by combination of HG and IL-1β, suggesting that both stimuli induce ROS formation in a MAO-dependent manner.

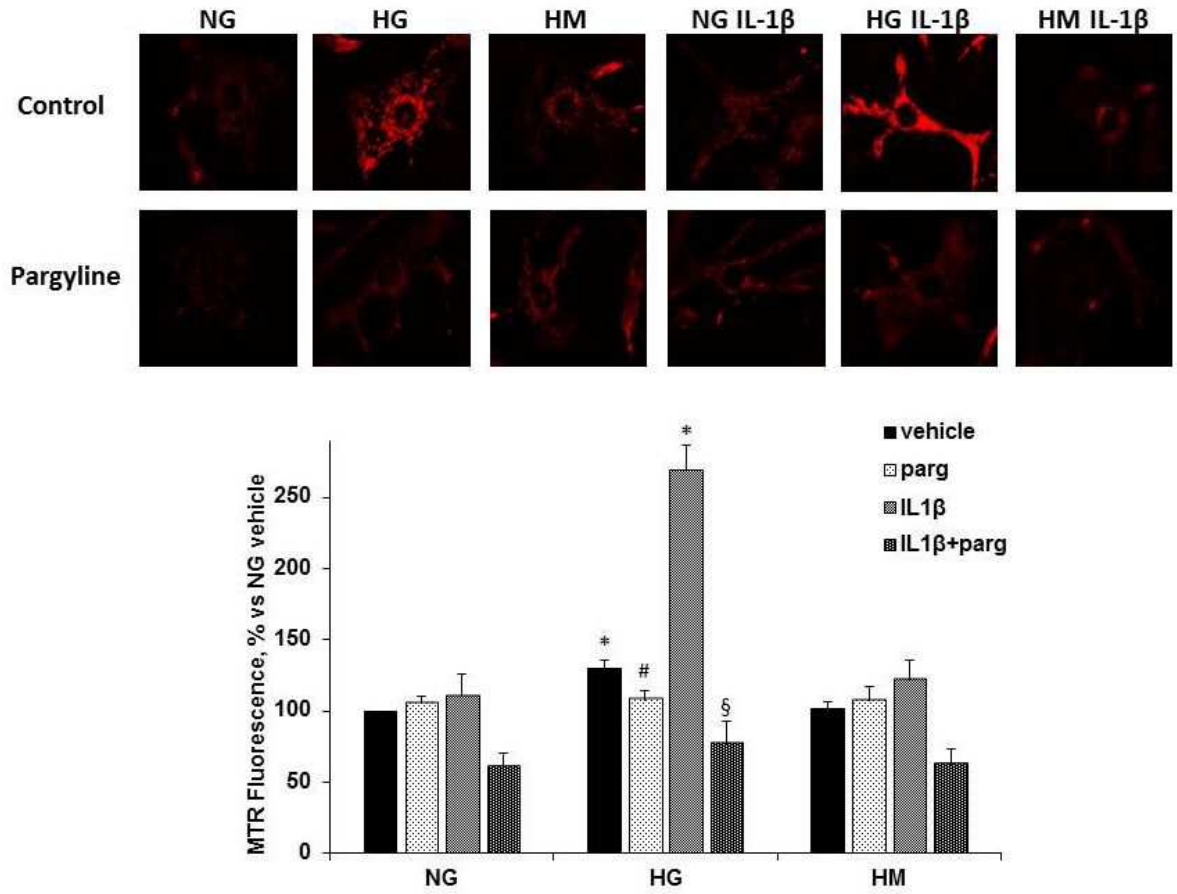

Figure 12. Effects of HG and pro-inflammatory cytokine IL-1β on ROS formation. Mitochondrial ROS formation determined by MTR in isolated NRVMs cultured with NG (5 mM), HG (25 mM) and HM (25 mM) for 48 h, in the absence or presence of IL-1β (25 ng/ml), and with or without pargyline (100 μM). *p<0.05 vs NG vehicle; #p<0.01 vs HG vehicle and §p<0.05 HG-IL1β vehicle. NG: normal glucose, HG: high glucose, HM: high mannitol, ROS: reactive oxygen species, IL-1β: interleukin-1β, MTR: MitoTracker Red CMH_2X-ROS, NRVMs: neonatal rat ventricular myocytes.

The initial evidence of MAO-reduced ROS formation was obtained by means of MTR fluorescence. However, this fluorescent probe presents some limitations. For instance, (i) its accumulation in the mitochondrial matrix is ΔΨm-dependent and might be influenced by the changes in ΔΨm induced by different treatments [191], (ii) it is not specific for single ROS species and (iii) it can get oxidized in the cytosol before entering the mitochondrial matrix. To overcome these limitations and to further confirm our results obtained with MTR, we used a genetically encoded probe HyPer to measure ROS formation in cells treated with HG and IL-1β. HyPer has several advantages over MTR; for instance, it can be targeted to different subcellular compartments, it is specifically oxidized by H_2O_2 and it is more sensitive, thus

making it a more suitable probe to assess MAO-dependent H_2O_2 formation in our experimental conditions.

Using HyPer constructs targeted either to the mitochondria or cytosol (Figure 13A), we observed that HG-treated NRVMs displayed a significant increase in both mitochondrial and cytosolic H_2O_2 formation and, similarly to results obtained with MTR, co-treatment with HG and IL-1β led to an even higher increase in H_2O_2 levels (Figure 13B). Moreover, MAO inhibitor pargyline prevented this increase in H_2O_2 formation, further confirming that HG and IL-1β induced ROS formation in a MAO dependent manner. Measurements obtained with HyPer also indicate that MAO-dependent ROS formation induced by HG and IL-1β is not only limited to mitochondria but it also occurs in the cytosol. However, it still remains to be elucidated whether ROS formation might occur with different kinetics in these compartments as reported previously for MAO-dependent ROS generation [192].

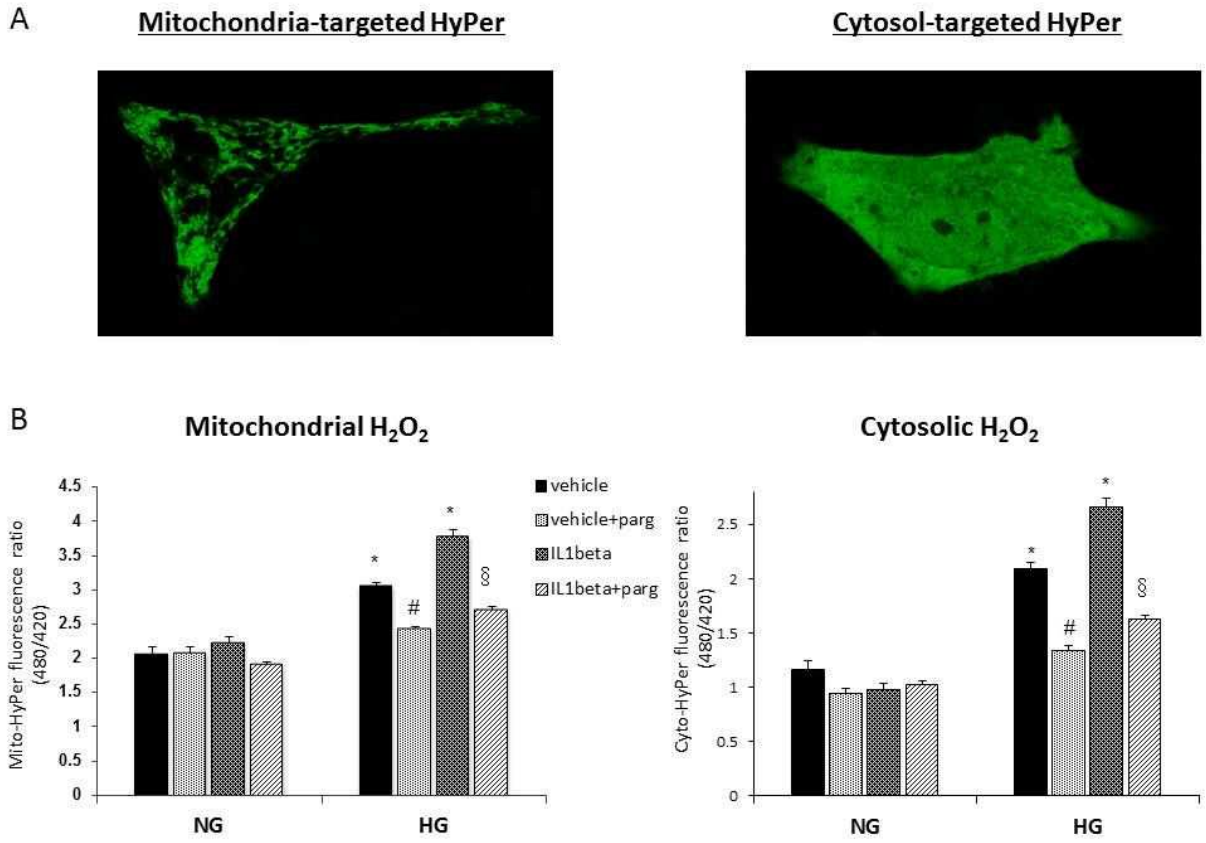

Figure 13. Compartment-specific H_2O_2 formation following HG and IL-1β treatment of NRVMs. (A) Fluorescent images of NRVMs transfected with genetically encoded H_2O_2 sensitive probe HyPer, targeted to mitochondria or to the cytosol. (B) H_2O_2 formation measured after 48 h of treatment with NG (5 mM), HG (25 mM) in presence or absence of IL-1β (25 ng/ml), with or without

pargyline (100 μM). *p<0.05 vs NG vehicle, #p<0.05 vs HG vehicle and §p<0.05 vs HG-IL1β. NG: normal glucose, HG: high glucose, IL-1β: interleukin-1β, NRVMs: neonatal rat ventricular myocytes.

We next examined whether the same effects could be observed in adult mouse cardiomyocytes. Neonatal hearts are relatively more dependent on glucose as a preferred substrate, whereas adult hearts rely on fatty acid oxidation for the generation of ATP necessary to support cardiac contraction and relaxation [193, 194]. Consequently, neonatal cells might be less susceptible to HG-induced derangements as compared to adult cardiomyocytes.

Indeed, HG showed a more prominent effect in adult cardiomyocytes leading to a ~2 fold increase in ROS formation after only 2 hours of incubation (Figure 14). However, no further increase in oxidative stress was observed with the co-treatment of HG and IL-1β. Pargyline treatment reduced ROS formation in both conditions, further confirming that MAO plays a pivotal role in HG and IL-1β induced oxidative stress. Taken together, these results indicate a crosstalk between MAO-generated oxidative stress, inflammation and mitochondria.

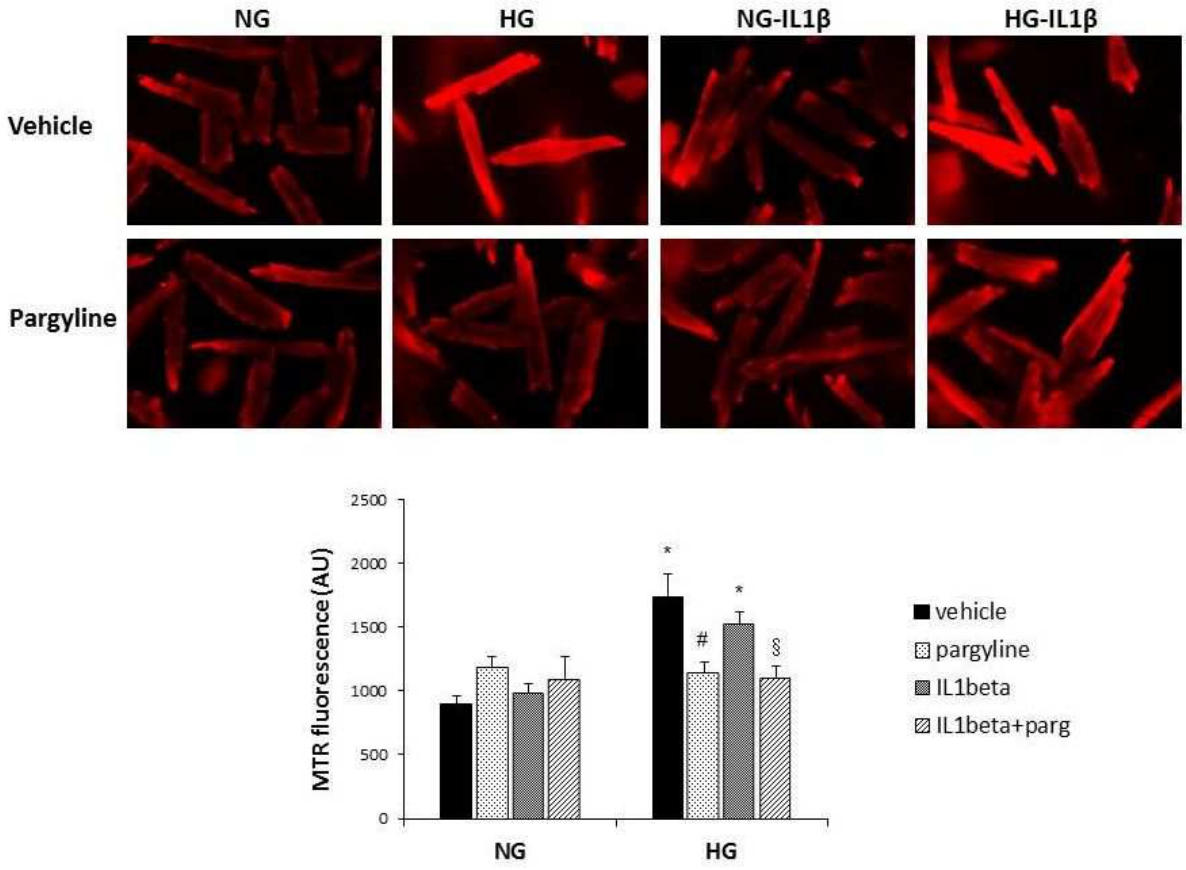

Figure 14. Mitochondrial ROS formation in isolated adult mouse cardiomyocytes following HG and IL-1β exposure. Cells were treated with NG (5 mM), HG (25 mM) in presence or absence of IL-1β (25 ng/ml), with or without pargyline (100 µM) for 2 h. Mitochondrial ROS formation was measured by MTR. *p<0.05 vs NG vehicle; #p<0.05 vs HG vehicle, §p<0.05 vs HG+IL-1β vehicle. NG: normal glucose, HG: high glucose, ROS: reactive oxygen species, IL-1β: interleukin-1β, MTR: MitoTracker Red CMH_2X-ROS

In order to elucidate whether enhanced H_2O_2 generation observed in our conditions was due to an increase in MAO protein expression, we performed Western blot to assess the abundance of MAO-A, the main isoform present in NRVMs. However, we did not observe any significant changes in MAO-A protein expression between different experimental groups (Figure 15).

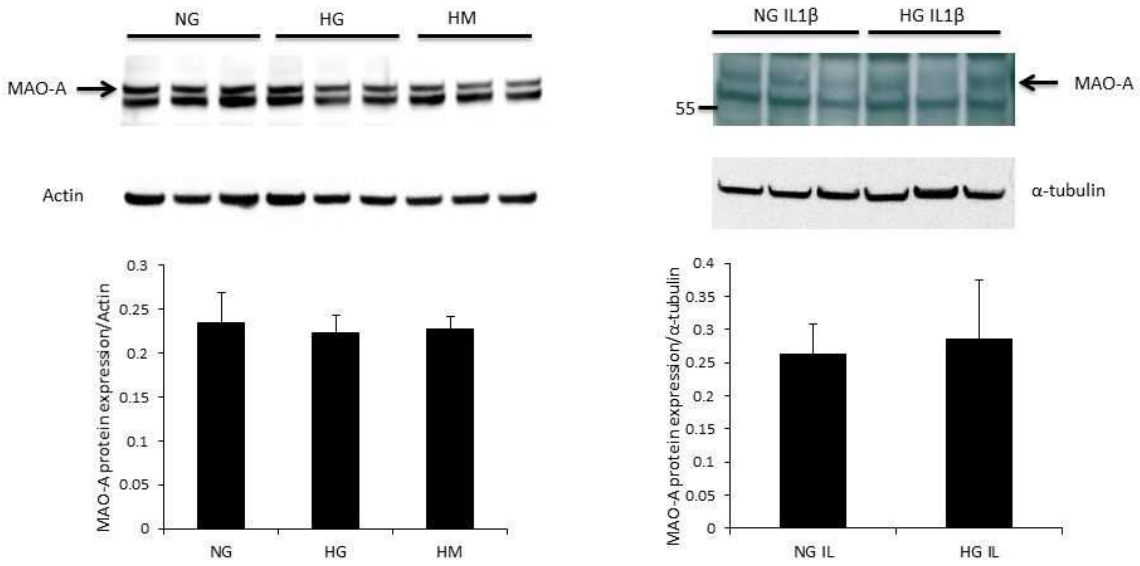

Figure 15. MAO-A protein expression in NRVMs treated with HG and/or IL-1β. Representative blots are shown for MAO-A protein expression in NRVMs treated with different conditions after 48 h. The quantification of band intensity is shown normalized to β-actin and α-tubulin, respectively. MAO: monoamine oxidase, NG: normal glucose, HG: high glucose, HM: high mannitol, IL-1β: interleukin-1β, NRVMs: neonatal rat ventricular myocytes.

7.2 Mitochondrial function in isolated cardiomyocytes exposed to HG and IL-1β

Several studies have shown that hyperglycemia induces alterations in mitochondrial function in diabetic hearts [195-197]. It has been demonstrated that cardiac mitochondria from diabetic rats display decreased respiration and increased susceptibility to undergo calcium-mediated mitochondrial permeability transition [198-200]. Emerging evidence suggests that hyperglycemia-induced oxidative stress could lead to mitochondrial dysfunction in the heart. Thus, we investigated whether also in HG- and IL-1β-treated cardiomyocytes ROS formation was accompanied by mitochondrial dysfunction and whether MAO-generated ROS might contribute to mitochondrial damage in these conditions.

To assess mitochondrial function, we measured $\Delta\Psi m$ by means of the fluorescent indicator TMRM. HG treatment in NRVMs did not show any changes in $\Delta\Psi m$ even after 48 h (Figure 16A). These results prompted us to examine whether HG is inducing latent mitochondrial dysfunction. It is well established that ATP synthase can mask the loss of $\Delta\Psi m$ by working in a reverse mode [201]. The respiratory chain generates a proton gradient across the IMM, with a higher concentration of H^+ ions in the intermembrane space and a lower concentration in the matrix. ATP synthase uses this proton gradient to synthesize ATP from adenosine di-phosphate (ADP) and phosphate (Pi). Under stress conditions, when mitochondrial respiratory chain is dysfunctional and proton gradient is impaired, ATP synthase may start working in a reverse mode hydrolyzing glycolytically synthesized ATP in order to maintain the $\Delta\Psi m$ [201]. Thus, to assess whether ATP synthase activity was compensating for the dysfunctional respiratory chain in HG-treated NRVMs, we monitored TMRM fluorescence intensity in presence of ATP synthase inhibitor oligomycin. NG- or HM-treated cells were able to maintain $\Delta\Psi m$ up to 1 hour following oligomycin administration (Figure 16B). On the other hand, TMRM fluorescence intensity started dropping immediately in HG-treated cells upon oligomycin addition. These results suggest that HG induced mitochondrial dysfunction in NRVMs, but in order to maintain $\Delta\Psi m$ these cells hydrolyze glycolytically synthesized ATP by reversing the activity of ATP synthase.

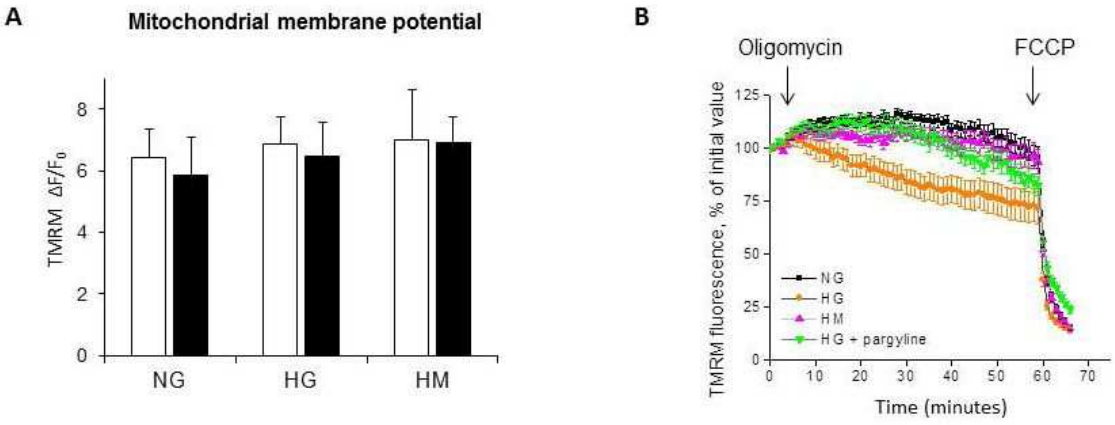

Figure 16. Mitochondrial membrane potential in NRVMs following treatment with HG and/or IL-1β. (A) Mitochondrial membrane potential determined by TMRM in NRVMs treated with NG, HG and HM after 48 h with (black) or without (white) pargyline. (B) Kinetics experiments were performed to follow changes in mitochondrial membrane potential upon addition of oligomycin and FCCP (indicated by arrows). NG: normal glucose, HG: high glucose, HM: high mannitol, NRVMs: neonatal rat ventricular myocytes, TMRM: tetramethylrhodamine, FCCP: carbonyl cyanide-4-(trifluoromethoxy) phenylhydrazone.

On the contrary, ΔΨm was remarkably reduced in adult cardiomyocytes already after 5h of HG treatment and this effect was further exacerbated when HG was combined with IL-1β (Figure 17). Noteworthy, since accumulation of MTR in mitochondria is ΔΨm dependent, loss of ΔΨm in these conditions might explain the absence of an additional increase in ROS levels (measured with MTR) in adult cardiomyocytes after HG+IL1-β treatment. Cells pre-treated with pargyline were able to maintain ΔΨm in both neonatal and adult cardiomyocytes, indicating that MAO-generated ROS trigger mitochondrial dysfunction in cardiomyocytes treated with HG and/or IL-1β.

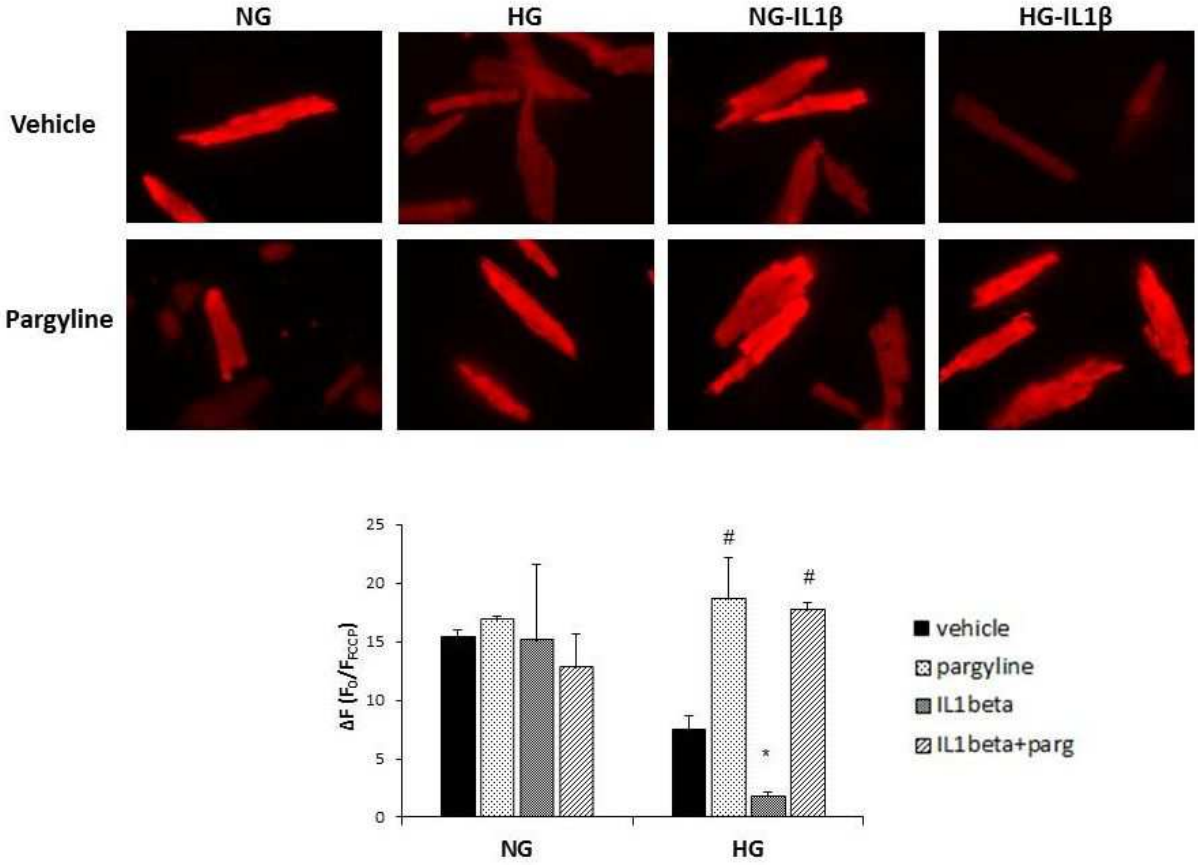

Figure 17. Mitochondrial membrane potential in adult mouse cardiac myocytes following treatment with HG and/or IL-1β. Adult cardiomyocytes were treated with NG (5 mM), HG (25 mM) in presence or absence of IL-1β (25 ng/ml), with or without pargyline (100 μM) for 5 h. Mitochondrial membrane potential was measured with the fluorescent dye TMRM. *$p<0.005$ vs NG vehicle, $^{\#}p<0.005$ vs HG+IL-1β vehicle. NG: normal glucose, HG: high glucose, IL-1β: interleukin-1β, TMRM: tetramethylrhodamine, methyl ester.

7.3 MAO-generated ROS perturb ER function in cardiomyocytes exposed to HG and pro-inflammatory stimuli

Accumulating evidence suggests that, in addition to oxidative stress and inflammation, ER stress also contributes to the development of diabetic cardiomyopathy [24, 145, 202]. Several pathological conditions can lead to the accumulation of misfolded proteins in the ER lumen leading to the activation of UPR. It was reported that hyperglycemia-induced ER stress is involved in myocardial apoptosis leading to cardiac dysfunction in diabetic rodents [203]. Although many studies have linked ER and oxidative stress in pathological conditions, molecular pathways that couple these processes are poorly understood. Thus, to better understand the cross-communication between these two organelles we initially investigated whether, in addition to targeting mitochondria, HG and IL-1β can also perturb ER function. Therefore, we measured gene and protein expression of several ER stress markers, such as ATF4, CHOP, XBP1, GADD34 and GRP78.

Using NRVMs as a model, we were unable to detect prominent ER stress at different time points (3 h, 6 h, 12 h, 24 h and 48 h) following treatment with HG or the combination of HG and IL-1β. IL-1β alone led to a mild but significant increase in the expression of ATF4, CHOP and spliced XBP1 marking the occurrence of ER stress after 48h (Figure 18A). Unlike IL-1β, HG did not show any significant changes in ER stress markers, whereas the combination of HG and IL-1β led to an increase only in spliced XBP1 levels. Pargyline completely prevented this increase suggesting that MAO-generated ROS formation contributes to UPR activation (Figure 18B).

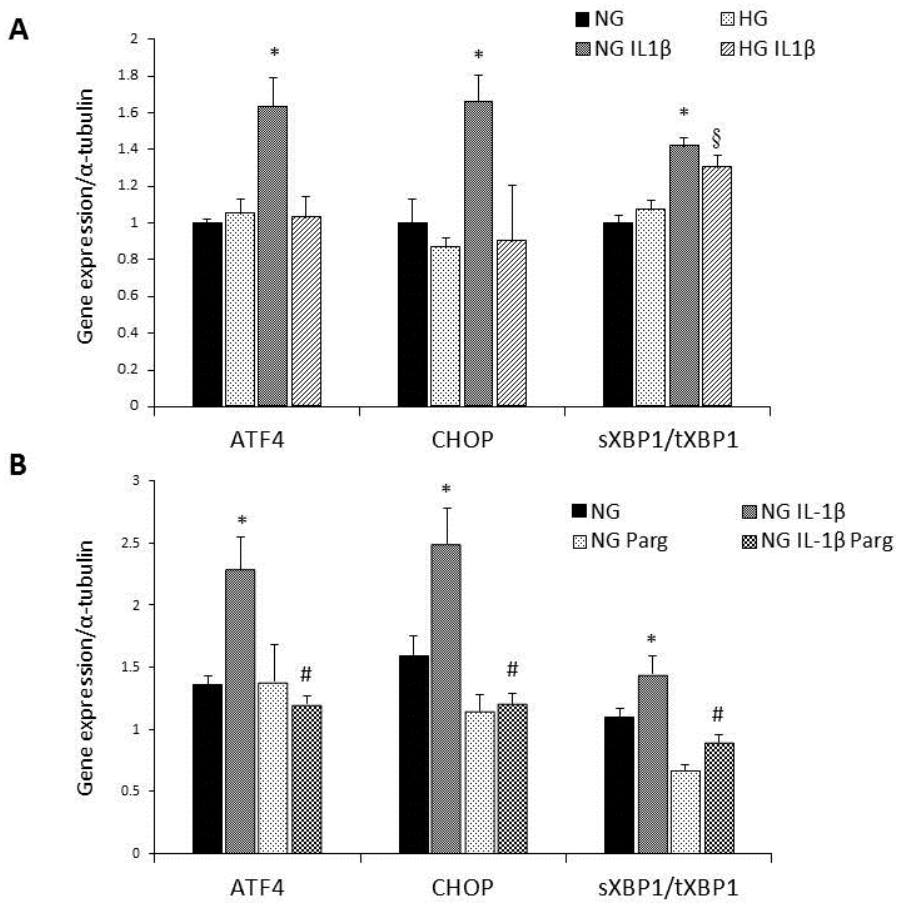

Figure 18. UPR in NRVMs exposed to HG and pro-inflammatory cytokine IL-1β. (A) Gene expression of ER stress markers involved in UPR was assessed in NRVMs treated in different conditions after 48h. (B) Effects of pargyline on IL-1β-induced gene expression of ER stress markers in NRVMs. *§p<0.05 vs NG, #p<0.05 vs NG+IL-1β. UPR: unfolded protein response, NG: normal glucose, HG: high glucose, NRVMs: neonatal rat ventricular myocytes, IL-1β: interleukin-1β, ER: endoplasmic reticulum.

On the other hand, exposure of adult cardiomyocytes to HG resulted in stronger induction of ER stress. Expression levels of ER chaperone GRP78/BiP was ~3 fold upregulated in presence of HG and HG-IL1β as shown in Figure 19. GRP78 is the central regulator of ER stress and it binds to the luminal domains of three ER transmembrane proteins, namely IRE1α, PERK and ATF6, thereby keeping them inactive. Upon ER stress, GRP78 dissociates from these sensor proteins resulting in their activation [138]. Accordingly, phosphorylation levels of IRE1α, an ER transmembrane kinase, were also increased in these cells further confirming the activation of UPR. We also assessed the expression of other proteins downstream of GRP78, such as transcription factor ATF4 and growth arrest and DNA damage-inducible protein GADD34. Both ATF4 and GADD34 were also upregulated by HG and IL-1β treatment as shown in Figure 19. Interestingly, MAO inhibition completely

prevented the activation of UPR induced by HG and IL-1β in adult cardiomyocytes. These results indicate that MAO-dependent ROS formation not only targets mitochondria to induce mitochondrial dysfunction, but it can also perturb ER homeostasis leading to the activation of UPR. In addition, we show that mitochondrial ROS formation and dysfunction are upstream of ER stress, at least in these conditions.

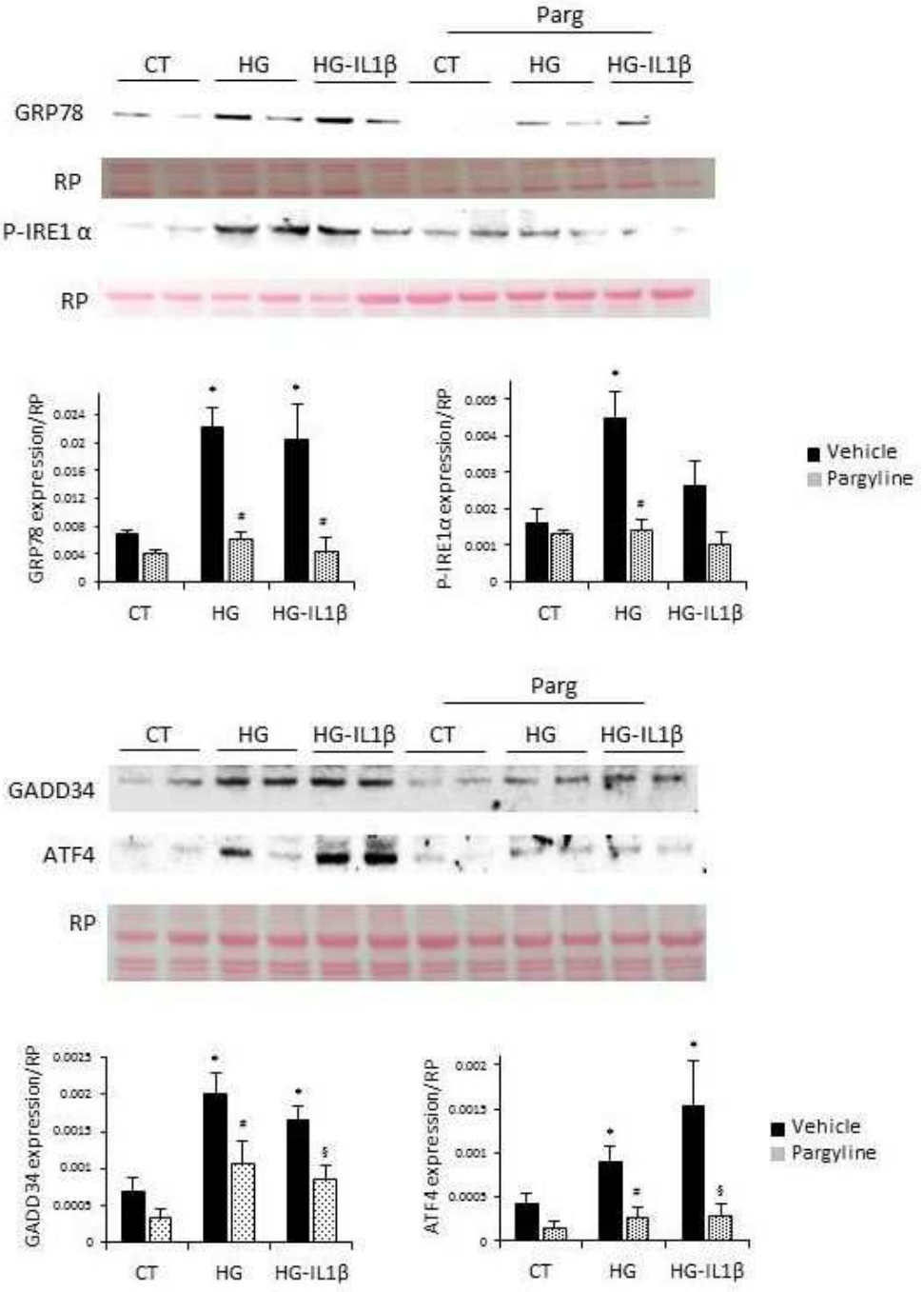

Figure 19. ER stress in adult cardiomyocytes exposed to HG and/or IL-1β. Protein expression of ER stress markers, GRP78, GADD34, ATF4 and phosphorylation levels of IRE1α were assessed in adult cardiomyocytes after 48 h of treatment with HG and/or IL-1β with or without pargyline (100 μM). Protein expression was normalized to total protein determined by Red Ponceau staining. *p<0.005 vs NG vehicle, #p<0.005 vs HG-IL1β vehicle. ER: endoplasmic reticulum, NG: normal glucose, HG: high glucose, IL-1β: interleukin-1β, GRP78: 78 kDa glucose-regulated protein, GADD34: growth arrest and DNA damage-inducible protein, ATF4: activating transcription factor, IRE1α: inositol-requiring enzyme 1α.

7.4 ER stress induced by tunicamycin and thapsigargin is MAO independent

Considering that MAO-generated ROS formation appears to be upstream of ER stress when cells are treated with HG and pro-inflammatory stimuli, we next examined whether direct induction of ER stress in NRVMs with tunicamycin or thapsigargin can affect mitochondrial ROS formation and function in a MAO-dependent manner. Tunicamycin inhibits the synthesis of glycoproteins in the lumen of ER leading to the accumulation of unfolded proteins and UPR activation [133]. Thapsigargin instead causes a reduction in ER calcium levels due to the inhibition of SERCA. This results in the loss of activity of calcium-dependent ER chaperones, such as calnexin, and accumulation of unfolded proteins. Initially, a dose dependent curve was performed to find the optimal concentration of tunicamycin and thapsigargin required to induce ER stress. We found that 1 μg/ml tunicamycin and 1 μM thapsigargin induced maximum ER stress after overnight incubation. Gene expression of transcription factor ATF4 and pre-apoptotic gene CHOP was 4 fold upregulated in these conditions, indicating the activation of PERK/eIF2α/ATF4 pathway (Figure 20 A). Furthermore, the ratio of spliced/unspliced XBP1 was ~4 fold higher in the cells treated with tunicamycin and thapsigargin. All of the UPR markers were significantly reduced by the chemical chaperone TUDCA (Figure 20B). We also observed that ER stress was accompanied by ROS formation in these conditions. Tunicamycin and thapsigargin both led to a significant increase in ROS formation measured with MTR (Figure 20C, D). As expected, this severe ER stress also led to a 40% decrease in cell viability (Figure 20E, F). To investigate whether MAO plays any role in ER stress-induced cell damage cells were co-treated with MAO inhibitor pargyline in these conditions. We found that MAO inhibition did not have any effect on thapsigargin induced cell damage. However, tunicamycin induced ROS formation was partially reduced upon pargyline treatment (Figure 20C) with no effects observed on ER stress markers and cell death (Figure 20B, E).

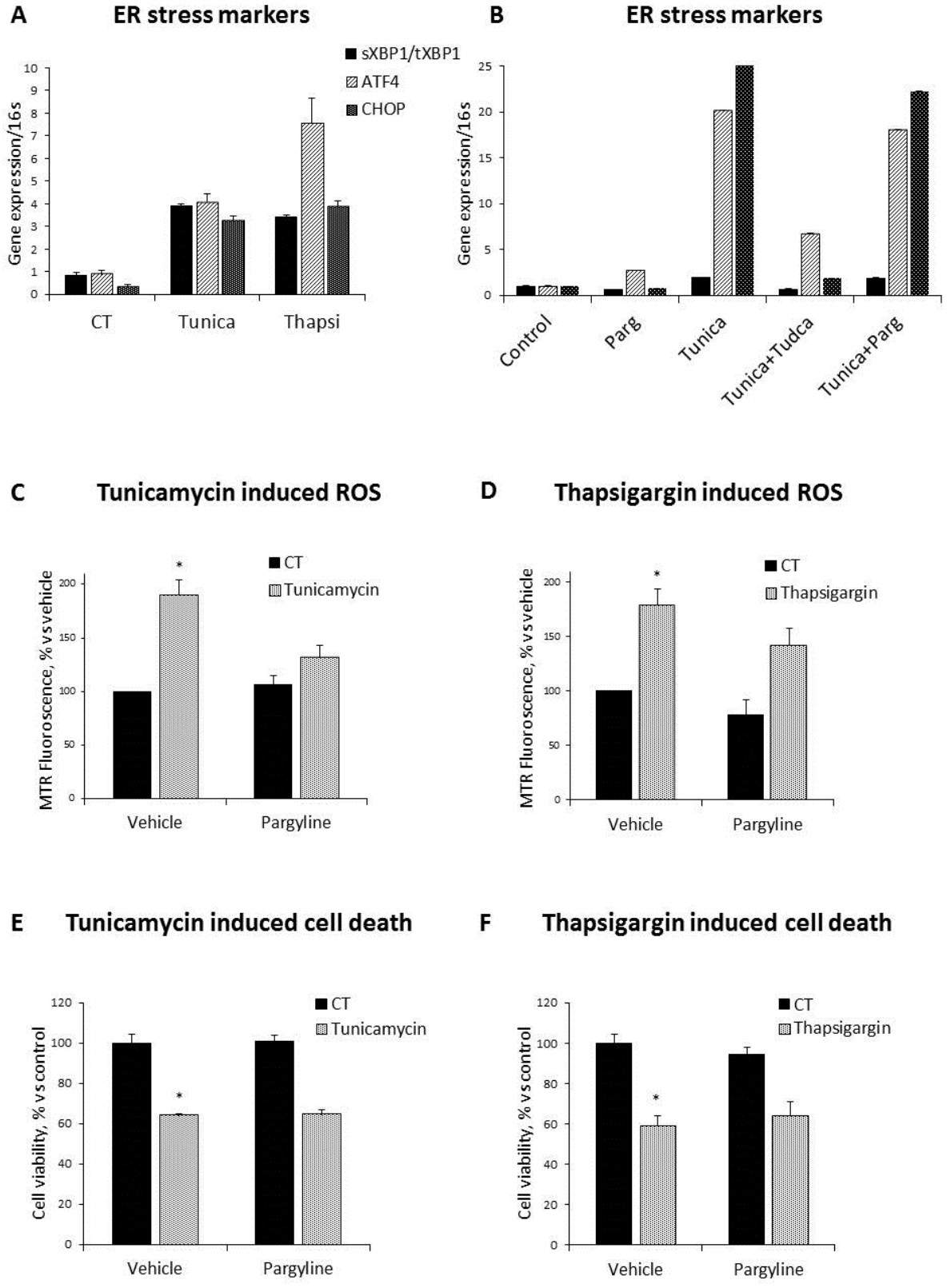

Figure 20. Tunicamycin and thapsigargin induced cell damage in NRVMs. (A) Gene expression of ER stress markers, ATF4, CHOP and sXBP1/tXBP1. (B) Effects of pargyline and TUDCA on tunicamycin-induced ER stress markers. (C-D) Cell viability and (E-F) ROS formation induced by tunicamycin (1 µg/ml) and thapsigargin (1 µM) in NRVMs with and without pargyline (100 µM).

Chemical chaperone TUDCA was used as a positive control. *p<0.005 vs control vehicle. NRVMs; neonatal rat ventricular myocytes, ER: endoplasmic reticulum, ATF4: activating transcription factor, CHOP: CCAAT-enhancer-binding protein homologous protein, s/tXBP1: spliced/total X-box binding protein 1, TUDCA: tauroursodeoxycholic acid, ROS: reactive oxygen species.

7.5 MAO contributes to LV diastolic dysfunction in STZ-induced T1D mice

Cardiovascular complications are one of the most common causes of death among diabetic patients. Several studies have characterized a number of functional changes that develop early in the course of diabetic cardiomyopathy. To investigate whether MAO contributes to oxidative stress and cardiac dysfunction occurring in diabetes, we used STZ-induced T1D mice. C57BL6/J male mice were anesthetized and injected intraperitoneally (i.p) with STZ (50 mg/kg) for 5 consecutive days to induce T1D. STZ causes pancreatic β-cell necrosis and thus inhibits glucose-induced insulin secretion leading to the development of T1D [204]. After 12 weeks of STZ treatment, we assessed LV function in these mice via PV relationships, as shown in Figure 21A.

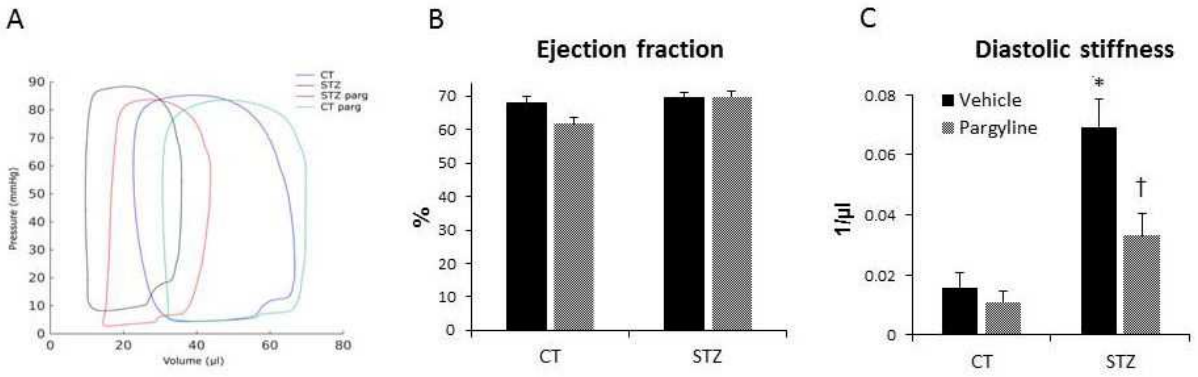

Figure 21. Characterization of LV function in STZ-induced T1D mice. (A) Representative pressure-volume loops from control (blue), STZ (black), control+pargyline (green) and STZ+pargyline (red) treated mice. (B) Ejection fraction and (C) Diastolic stiffness measurement in vehicle or pargyline treated control and STZ mice. *p<0.005 vs CT vehicle, †p<0.005 vs STZ vehicle. LV: left ventricle, STZ: streptozotocin, T1D: type 1 diabetes.

Heart rate and cardiac output remained unchanged between the experimental groups (Table 1). Moreover, we found that ejection fraction, an index of systolic function, was also unaffected in STZ-mice (Figure 21B). dP/dt_{max} and dP/dt_{min}, indexes of contractility and relaxation, showed a trend to decrease in STZ-treated mice but these changes were not statistically significant (Table 1). This suggests that, although systolic function still appears unaffected, STZ mice are likely to undergo systolic dysfunction with prolonged treatment. Interestingly, diastolic stiffness, an index of diastolic dysfunction, was 4.6-fold increased in diabetic mice (Figure 21C). These findings are consistent with clinical reports showing that

LV diastolic dysfunction is one of the earliest signs of cardiac complications in diabetic patients, followed by systolic dysfunction only at later stages [27, 205]. To assess whether MAO activity might play a role in the development of diabetic cardiomyopathy, cardiac function was evaluated also in STZ-mice that were administered MAO inhibitor pargyline. Importantly, MAO inhibition did not affect any of the LV functional parameters in the control group, as indicated in Table 1. However, pargyline administration significantly reduced diastolic stiffness in STZ-mice, indicating a pivotal role of these flavoenzymes in LV dysfunction in diabetic cardiomyopathy.

	Control (n=6)	**Control+Parg (n=4)**	**STZ (n=8)**	**STZ+Parg (n=10)**
Glucose (mmol/l)	10.20±1.40	8.60±0.40	32.20±30*	32.10±3.10*
Body weight (g)	33.10±2.70	32.40±2.00	25.50±4.30	24.20±5.30
Heart rate (bpm)	380.56±20.42	446.59±21.90	350.57±16.58	343.83±1.94
EDV (µl)	65.66±9.43	70.50±2.60	47.62±3.52*	50.70±2.87*
ESV (µl)	21.50±4.28	27.00±1.41	14.87±1.74	15.30±1.49
SV (µl)	44.16±5.31	43.50±2.38	32.87±2.12*	35.20±2.11*
EF (%)	68.01±2.06	61.75±2.07	69.34±1.76	69.82±1.88
Diast stiff (1/µl)	0.0158±0.005	0.010±0.004	0.069±0.009*	0.0331±0.007†
ESP (mmHg)	82.66±2.39	91.63±5.72	67.47±5.67	76.20±1.94
EDP (mmHg)	8.58±1.53	5.98±1.79	9.21±2.20	10.32±1.75
dP/dt_{max} (mmHg/s)	5487.40±430.94	7120.29±522.16	4101.85±645.78	4713.28±316.7

dP/dt_{min} (mmHg/s)	-5930.80±389.2	-7161.70±804.36	-4001.30±886.90	-4500.29±885.7
Eff (%)	73.35±4.15	70.37±17.02	76.22±6.62	74.06±5.36

Table 1. Glycemic and hemodynamic parameters measured in T1D mice. EDV: end-diastolic volume, ESV: end-systolic volume, SV: stoke volume, EF: ejection fraction, CO: cardiac output, ESP: end-systolic pressure, EDP: end diastolic pressure, Eff: efficiency. *$p<0.005$ vs Control, †$p<0.005$ vs STZ. T1D: type 1 diabetes.

7.6 MAO contributes to oxidative stress and impairs ER homeostasis in diabetic hearts

Accumulating evidence supports the role of oxidative stress and ER stress in diastolic dysfunction occurring in both diabetic patients and animal models. Thus, we investigated whether oxidative stress and impaired ER function might contribute to LV diastolic dysfunction also in our T1D model. To measure oxidative stress in T1D hearts we assessed the levels of 4-HNE, a product of lipid peroxidation. 4-HNE is a highly reactive aldehyde that modifies proteins, phospholipids and nucleic acids. Thus, it is widely used as an oxidative stress marker. As expected, we found that levels of 4-HNE were significantly increased in T1D hearts indicating the occurrence of oxidative stress in these mice (Figure 22).

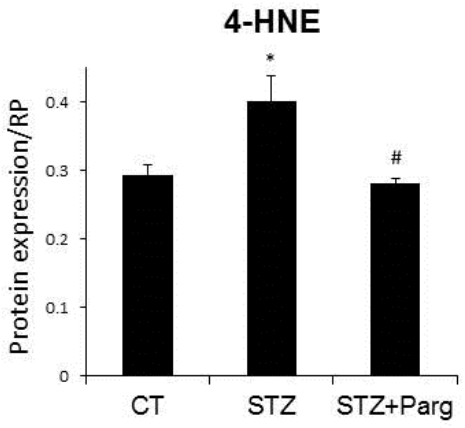

Figure 22. Oxidative stress in STZ-induced T1D mice. 4-HNE staining was performed on heart tissue lysates extracted from vehicle- or pargyline-treated control and STZ mice. 4-HNE levels were normalized to total protein content determined by Red Ponceau. *p<0.05 vs control, #p<0.05 vs STZ. STZ: streptozotocin, T1D: type 1 diabetes, 4-HNE: 4-hydroxy-2-nonenal.

Moreover, oxidative stress was accompanied by impaired ER homeostasis in STZ-mice as demonstrated by induction of UPR associated proteins, including ATF4 and GADD34 (Figure 23). In line with our in vitro data, pargyline administration to diabetic mice completely prevented these alterations. These results suggest that hyperglycemia-induced changes in diabetic hearts lead to the enhanced MAO activity resulting in oxidative stress. As a consequence, misfolded proteins accumulate in the ER leading to the activation of UPR.

This data further support previous studies suggesting that oxidative and ER stress contribute to the pathogenesis of diabetic cardiomyopathy [93, 206].

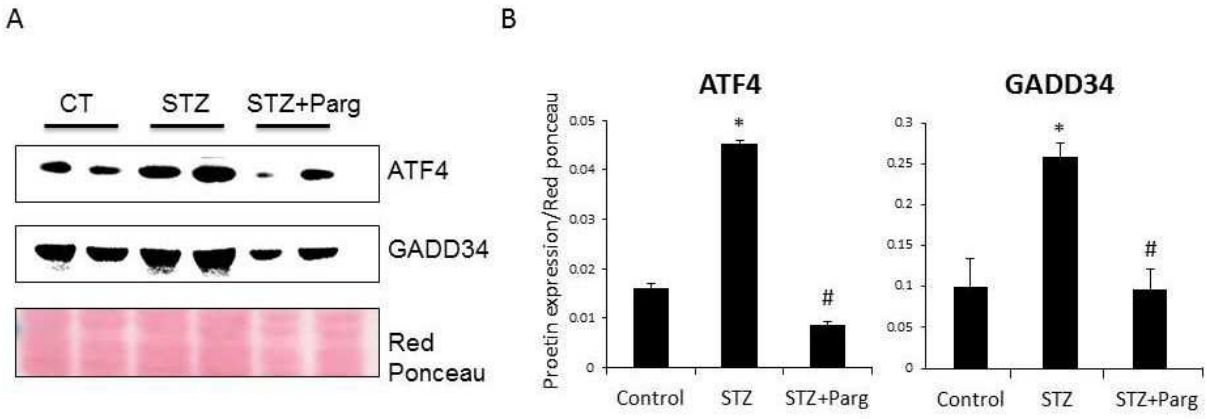

Figure 23. ER stress in STZ-induced T1D mice. (A) Representative western blot and (B) quantification of ATF4 and GADD34 band intensities in heart tissue lysates of control, STZ and STZ+pargyline treated mice. *p<0.05 vs control, #p<0.05 vs STZ. ER: endoplasmic reticulum, T1D: type 1 diabetes, STZ: streptozotocin, ATF4: activating transcription factor 4, GADD34: growth arrest and DNA damage-inducible protein.

We also investigated whether the increase in oxidative stress was due to changes in MAO protein expression in diabetic conditions. In agreement with our in vitro data, the protein expression of MAO-B, predominant isoform in the mouse heart, was not significantly different in STZ hearts as compared to controls (Figure 24).

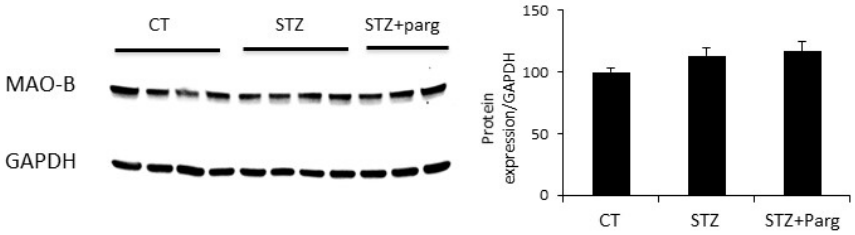

Figure 24. MAO-B protein expression in heart tissue lysates. MAO-B protein expression in heart tissue lysates of control, STZ and STZ+pargyline treated mice. MAO: monoamine oxidase, STZ: streptozotocin.

7.7 MAO activity triggers mast cell degranulation and cardiac fibrosis in T1D mice in vivo

Cardiac fibrosis is one of the underlying causes of diastolic dysfunction and a major feature of diabetic cardiomyopathy [24, 37]. Collagen synthesis is enhanced, whereas its degradation is limited in pathological conditions, creating a net excess of collagen deposition [207]. An over-production of collagen is known to increase myocardial stiffness and consequent cardiac dysfunction, ultimately resulting in cardiac failure [37, 208]. Hence, we assessed collagen levels in our diabetic model using Masson's Trichrome staining. Indeed, we found a 4-fold increase in collagen deposition in STZ-hearts as shown in Figure 25. Surprisingly, pargyline treated mice showed complete absence of these histological alterations suggesting that MAO plays a crucial role in the development of fibrosis in these animals.

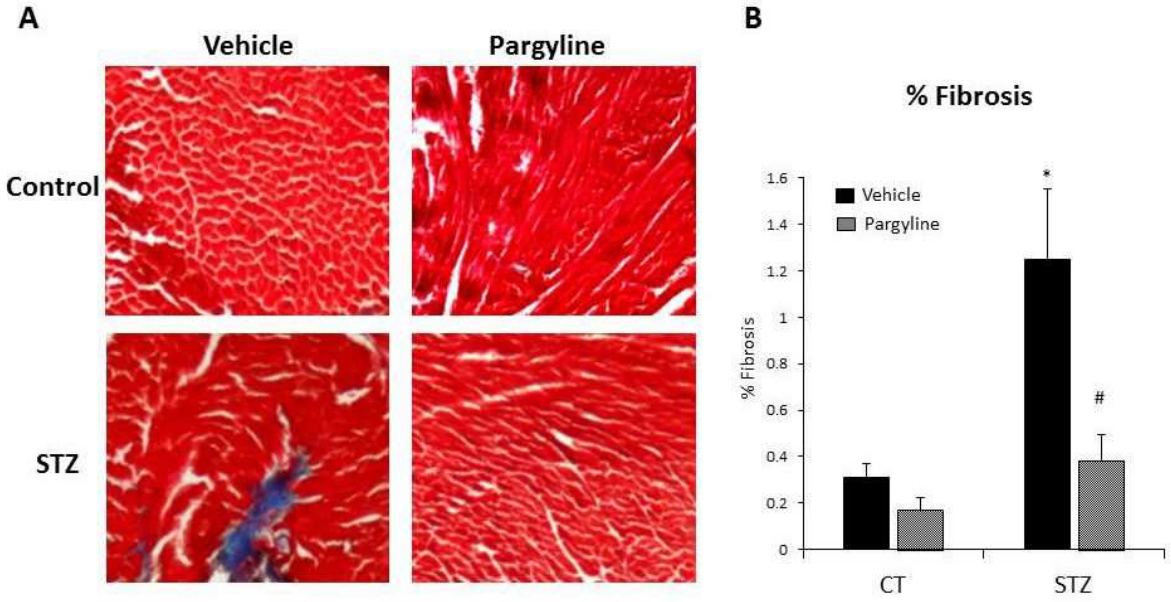

Figure 25. Cardiac fibrosis in T1D mice. (A) Representative images of Masson's trichrome staining from control and STZ mice, showing collagen deposition in blue. (B) The quantification data is expressed as percentage of fibrotic vs total cardiac tissue. *$p<0.05$ vs control vehicle, $^{\#}p<0.05$ vs control vehicle. T1D: type 1 diabetes, STZ: streptozotocin.

One of the mechanisms leading to the development of fibrosis is mast cell degranulation [209]. Mast cells are known to play a key role in the inflammatory processes and, when stimulated, can undergo degranulation to release a number of pro-inflammatory

and pro-fibrotic factors [210]. Several studies linked increased ROS production and mast cell degranulation in pathological conditions [163-165]. Indeed, multiple studies have demonstrated that incubation of mast cells with H_2O_2 lead to a dose-dependent increase in mast cell degranulation in vitro [165]. Moreover, Luo et al. and Gan et al. have shown that specific inhibition of ROS-generating enzyme

oxidase by apocynin in a model of intestinal ischemia−reperfusion-induced acute lung injury completely abolished the activation of mast cells [164, 165]. However, whether mitochondria and ROS are involved in triggering cardiac mast cell degranulation in diabetic cardiomyopathy is not yet clear. Thus, to understand whether mast cell degranulation is triggering fibrosis and if MAO activity is involved in this inflammatory process, we assessed cardiac mast cell density and level of degranulation in STZ mice. No significant difference was observed in the density of mast cell between STZ hearts and control mice (Figure 26B). However, mast cell degranulation was 1.8-fold higher in diabetic mice as compared to control (Figure 26C). Interestingly, pargyline treatment prevented mast cell degranulation in T1D mice. Taken together, these results suggest that MAO is involved in the activation of cardiac mast cells thereby leading to the remodeling of the extracellular matrix, fibrosis and, ultimately, LV dysfunction. These findings complement previous studies reporting that myocardial remodeling is associated with cardiac mast cell activation in diabetic cardiomyopathy [211]. However, further investigation is required to elucidate how the activity of these flavoenzymes triggers mast cell degranulation.

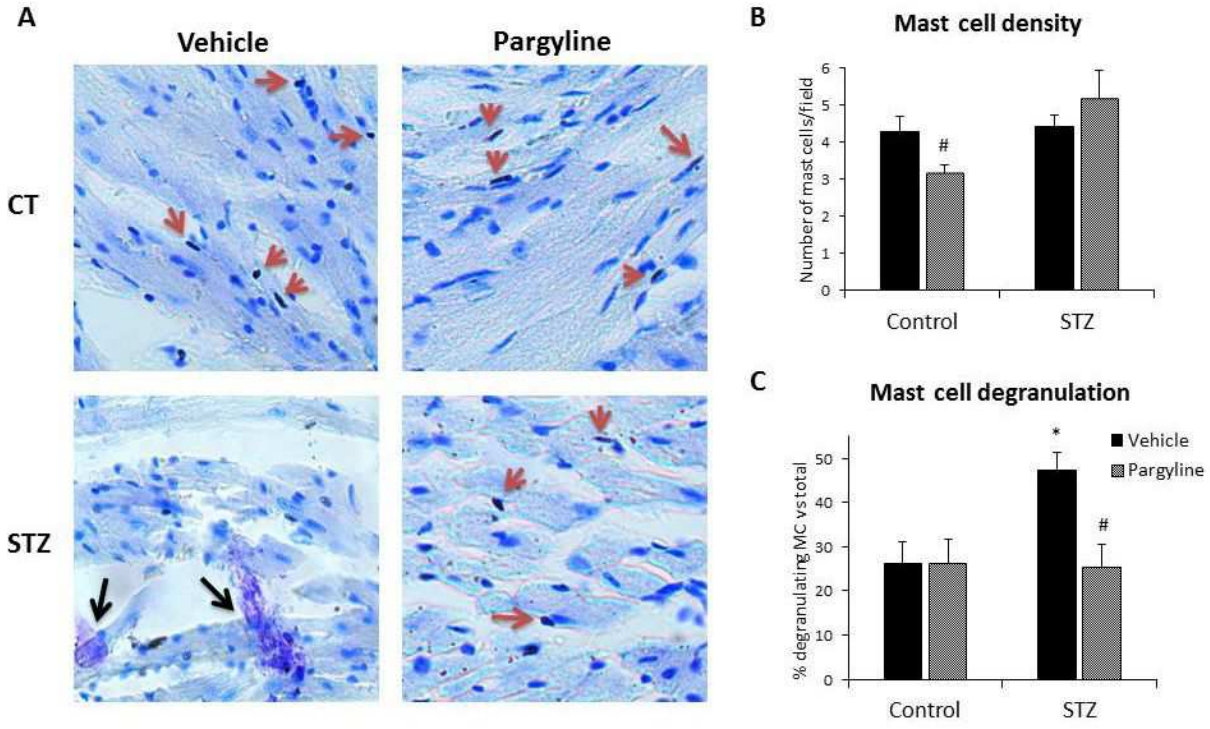

Figure 26. Mast cell degranulation in STZ-induced T1D mice. (A) Representative images of toluidine blue staining of cardiac tissue from indicated experimental groups. Red arrows indicate intact mast cells, while black arrows indicate actively degranulating mast cells. Quantification of (B) mast cell density and (C) mast cell degranulation. Results are expressed as number of mast cells per field and percentage of degranulating mast cells vs total number of mast cells, respectively.*$p<0.05$ vs control vehicle, $^{\#}p<0.05$ vs STZ vehicle. STZ: streptozotocin, T1D: type 1 diabetes.

8. DISCUSSION AND CONCLUSIONS

This study demonstrates that MAOs play a prominent role in HG and/or IL-1β induced mitochondrial ROS formation and dysfunction in vitro, and cardiac damage in T1D mice in vivo. We also show that ROS produced by these flavoenzymes can also perturb ER function leading to the activation of UPR in diabetic conditions. Furthermore, we describe the novel role of MAO in the activation of cardiac mast cells thereby providing an important link between MAO activity, inflammation and fibrosis in diabetic cardiomyopathy.

Several hypotheses for the mechanism underlying hyperglycemia-induced cardiac impairment include an increase in polyol pathway flux, intracellular AGE formation or increased flux through the hexosamine pathway [212, 213]. Many alterations of cellular and mitochondrial metabolism observed during the development of diabetic cardiomyopathy are associated with increased ROS levels. Multiple studies indicated that cardiac impairment is not caused by hyperglycemia *per se*, but rather it is the oxidative stress and inflammation that lead to cardiovascular complications. Moreover, clinical studies validated IL-1β, a pro-inflammatory cytokine, as a target to improve glucose metabolism and cardiac complications in patients with both T1D and T2D [214-216]. It is well known that mitochondrial ROS formation and dysfunction lead to the production of IL-1β via inflammasome pathway [186, 217], but whether and how IL-1β can induce mitochondrial ROS formation has never been investigated. Here, we show for the first time that IL-1β, in combination with HG, is able to induce mitochondrial ROS formation and, importantly, this occurs in a MAO-dependent manner. We demonstrate that MAO-induced ROS formation is remarkably increased when cells are treated with the combination of HG and IL-1β, as compared to either of them alone. The exacerbated ROS formation in these conditions is more evident in NRVMs as compared to adult cardiomyocytes. The reason behind this discrepancy is likely due to technical limitations of the MTR probe, as mentioned in the Results section. Overall, our in vitro results indicate that adult cardiomyocytes are more susceptible to HG and pro-inflammatory stimuli as compared to NRVMs. This is supported by the observation that HG led to a mild increase in ROS formation in NRVMs after 48 h, whereas adult cardiomyocytes displayed a 2-fold increase in ROS formation within 2 hours of treatment. Moreover, NRVMs did not display any change in $\Delta\Psi m$ even after 48 h of treatment with HG, while adult cardiomyocytes show a 2-fold and 9-fold reduction in $\Delta\Psi m$ in presence of HG and HG-IL1β,

respectively. Finally, we also observed that NRVMs do not show remarkable changes in the expression of ER stress markers, whereas adult cardiomyocytes underwent strong impairment of ER homeostasis and upregulation of UPR markers. This discrepancy might be due to the glycolytic phenotype of neonatal cardiomyocytes or due to the differences in the antioxidant defense system between these two cultures [193, 218]. Thus, it is important to take these notions into consideration when choosing the adequate model for the assessment of the effects following exposure to the diabetic milieu.

MAO-generated H_2O_2 is not only confined to mitochondria, but also occurs in the cytosol in HG- and/or IL-1β- treated cardiomyocytes. In recent years, it has been shown that mitochondrial impairment can induce cytosolic ROS formation and vice-versa. Maharjan et al. demonstrated that proteasome inhibition causes an increase in mitochondrial ROS formation and dysfunction leading to cytosolic oxidative stress [219]. On the other hand, Coughlan et al. reported that exposure of primary renal cells to AGEs leads to an increase in cytosolic ROS formation which facilitated the production of mitochondrial superoxide and deficiency of mitochondrial complex I [220]. Thus, it remains an open question whether in our experimental model mitochondrial ROS occurs prior to cytosolic oxidative stress. However, previous data obtained in our laboratory suggest that in cardiomyocytes MAO-induced ROS formation occurs firstly in mitochondria and then in the cytosol [120].

It is important to understand why and how the activity of MAO is upregulated in diabetic conditions. Although MAO protein expression remains unchanged both in vitro and in vivo, increased substrate availability and/or post-translational modifications might account for the enhanced activity of these enzymes. Indeed, our laboratory has previously demonstrated that enhanced MAO-A-dependent norepinephrine degradation contributes to oxidative stress and transition from compensated hypertrophy to heart failure in pressure overloaded mice [117]. However, catecholamines are mainly stored in the sympathetic nerve endings and, at present, it still remains to be elucidated whether these or other MAO substrates may also be stored in cardiac myocytes.

We also demonstrated that MAO is involved in HG and pro-inflammatory stimuli induced mitochondrial dysfunction. It has been previously shown in a model of Parkinson's disease that increased MAO activity can affect mitochondrial function by decreasing mitochondrial complex I activity, thus impairing electron transport chain [221]. Our data

demonstrate that MAO-generated H_2O_2 leads to reduced $\Delta\Psi m$, most likely due to the impairment of the mitochondrial respiratory chain. Besides H_2O_2 formation, these flavoenzymes also produce aldehydes and ammonia [110, 115, 123]. Recent studies have focused on the deleterious effects of reactive aldehydes in cardiac diseases. It has been demonstrated that aldehydes can perturb mitochondrial function by directly targeting pyruvate dehydrogenase and complex I-associated proteins [222]. Moreover, Zhang et al. showed that mitochondrial ALDH2, improves mitochondrial function and reduces apoptosis in STZ-induced T1D hearts [223]. Thus, it might be possible that MAO-induced mitochondrial dysfunction in cardiomyocytes is a combined effect of increased ROS levels and aldehydes upon HG and IL-1β exposure.

Our data demonstrate that in addition to oxidative stress and mitochondrial dysfunction, MAO activity also leads to the impairment of ER homeostasis and activation of UPR in both in vitro and in vivo model of diabetes, highlighting the novel role of these flavoenzymes in the interplay between ER and mitochondria. Persistent protein misfolding is known to play predominant roles in the pathogenesis of multiple cardiovascular diseases including diabetes, heart failure, and ischemia/reperfusion injury [144, 224, 225]. Although many studies have shown an association between oxidative and ER stress, whether mitochondrial ROS formation is upstream of ER stress or vice-versa is not clear. It has been demonstrated that activation of UPR under stress conditions led to impaired calcium and redox homeostasis. As a consequence, oxidative stress is increased leading to impaired mitochondrial function [226, 227]. Although the exact mechanism of how protein misfolding can trigger ROS formation is not yet fully understood, several possible mechanisms have been proposed. First, under stress conditions misfolded proteins bind to ER chaperone GRP78; this process requires ATP that may stimulate mitochondria to generate more ATP through oxidative phosphorylation leading to the production of ROS as a byproduct [227]. Second, ROS may be produced as a consequence of disulfide bond formation. ER oxidoreductase proteins oxidize cysteine residues of nascent proteins, helping them in the formation and isomerization of correct disulfide bonds. Reduced folding enzymes are re-oxidized by ERO-1, the enzyme which reduces molecular oxygen leading to the production of H_2O_2 [228]. On the other hand, Malhotra et al. suggested that both ROS and unfolded proteins are required to activate UPR in the cell. They further demonstrated that reducing ROS by the antioxidant butylated hydroxyanisole improves protein folding and cell survival [229]. Furthermore, two independent studies reported that inhibition of oxidative stress by MitoTEMPO and ER stress

by TUDCA prevented diabetes-induced cardiac damage in rodents [145, 230]. These findings suggest the crucial need for understanding the pathological mechanisms that alter both organelles in pathological conditions, and particularly the mechanisms that coordinate the interplay between mitochondrial dysfunction and ER stress. In the present study we show that HG- and inflammation-induced ROS formation and mitochondrial dysfunction are upstream of ER stress in cardiomyocytes. Importantly, MAO contributes to perturbed ER function in HG/IL1β-treated NRVMs in vitro and in T1D mice in vivo. These findings indicate the novel role of these flavoenzymes in the vicious cycle between excessive ROS formation and ER stress. However, MAO inhibition is not sufficient to protect the cell from damage when ER stress is induced directly and occurs upstream of mitochondrial ROS formation (Figure 20). This might be due to the fact that both tunicamycin and thapsigargin led to severe ER stress as demonstrated by the 20-fold increase in gene expression of ATF4 and pre-apoptotic gene CHOP. This increase is much higher compared to our in vitro diabetic model where we observed a 3-fold upregulation of ER stress markers (Figure 19). On the other hand, it is possible that tunicamycin- and thapsigargin-induced ER stress cause mitochondrial dysfunction, oxidative stress and cell death in a MAO-independent manner. Indeed, it has been shown that ER stress can cause mitochondria to produce more ROS causing cell death via induction of mitochondrial permeability transition, induced upon entry of excessive amounts of Ca^{2+} into the mitochondrial matrix [133].

Besides the functional link between mitochondria and ER, the sites of physical communication between these organelles, known as mitochondria associated membranes (MAMs), have recently earned considerable attention. Indeed, some studies proposed that MAMs are involved in the maintenance of lipid and calcium homeostasis, in the initiation of autophagy and mitochondrial division, and in sensing metabolic shifts inside the cell [231-235]. One study has highlighted the role of MAMs in diabetes demonstrating that obesity drives an abnormal increase in MAMs formation in the liver, resulting in increased Ca^{2+} flux from the ER to mitochondria [236]. Downregulation of PACS-2, a protein important for ER-mitochondria tethering, prevented these changes [236]. Moreover, it has been shown that ER stress led to a remarkable increase in MAMs both in vitro and in the liver of obese mice in vivo [232, 236]. Mitofusin 2, a molecular tether between ER and mitochondria, has been shown to play a role in ER-mitochondria calcium cross-talk in cardiomyocytes and to be one of the factors that regulate events orchestrated by mitochondrial calcium uptake, such as metabolism, opening of the mitochondrial permeability transition pore (MPTP), and

programmed cardiomyocyte death [237]. In addition to that, recent studies have shown that ER-mitochondria tethering enables ER proteins to associate directly with proteins and lipids of the OMM. It is therefore tempting to hypothesize that MAO, localized at the OMM, might interact with some of the ER proteins and also play a role in ER-mitochondria tethering. A coherent understanding of the bidirectional communication existing between these two organelles will certainly aid in the development of specific therapeutic strategies to treat diseases associated with oxidative stress, UPR and inflammation such as obesity, diabetic cardiomyopathy and neurological disorders.

Oxidative stress and mitochondrial dysfunction are widely accepted to play an important role in the development and progression of LV dysfunction in diabetic cardiomyopathy [37, 39, 238]. Recent studies documented mitochondrial dysfunction in human diabetic hearts showing an increased mitochondrial oxidative stress and increased sensitivity to calcium-induced opening of the MPTP in atrial tissue of patients [37, 85]. Here we provide strong evidence that diastolic dysfunction occurring in STZ mice is completely prevented upon MAO inhibition. These findings are of major importance because of their clinical relevance. Diastolic dysfunction detected at the initial stages of diabetes falls into the category of HFpEF, a condition that occurs in approximately 50% of patients with heart failure. The mechanisms of this modality are poorly understood because of the limited availability of animal models with HFpEF. Although the role of MAO in TAC-induced heart failure has already been reported [117], current data strongly suggests that targeting MAO activity might be particularly interesting in diabetic patients with HFpEF.

Mitochondrial ROS formation is believed to be the primary cause for LV diastolic dysfunction [198, 238]. In this regard, Dai et al have shown that specific inhibition of mitochondrial ROS formation by synthetic Szeto-Schiller peptide SS-31prevented LV diastolic dysfunction, whereas non-targeted ROS scavenging with N-acetyl cysteine (NAC) had no effect [239]. A recent study emphasized that already in prediabetic conditions ROS levels are elevated in subsarcolemmal mitochondria, further indicating that mitochondrial ROS production is one the earliest events to trigger cardiac pathological changes well before major metabolic derangements occur [240]. Within this scenario, we provide strong evidence that specific inhibition of MAO activity in T1D results in improved cardiac function. Nevertheless, it remains to be elucidated whether MAO inhibition affords protection also when inhibitors are administered after the onset of diastolic dysfunction.

It appears that increased diastolic stiffness in STZ mice is the result of MAO-induced cardiac fibrosis, one of the major features of diabetic cardiomyopathy. Several factors have been reported to contribute to cardiac fibrosis, including cytokines, growth factors, infiltration of inflammatory cells monocyte/macrophages and degranulation of mast cells. In our T1D model, we found that MAO activity triggers mast cell degranulation that might be contributing to cardiac fibrosis and thus diastolic dysfunction. Although several studies hint to the link between mast cell and oxidative stress in different pathological disorders [161, 163, 164, 209, 241], up to date no study has identified the specific source of ROS responsible for mast cell degranulation in diabetic cardiomyopathy. Here, we report for the first time that MAO activity triggers mast cell degranulation in STZ-mice, thus providing a mechanistic link between these mitochondrial flavoenzymes, inflammation and fibrosis in diabetic cardiomyopathy. Nevertheless, it still remains to be elucidated whether it is MAO-generated ROS formation in cardiomyocytes or in mast cells themselves that is triggering this inflammatory response.

Since oxidative stress is known to play a major role in the development of cardiovascular complications in diabetes, several therapies aimed at reducing ROS formation and enhancing antioxidant defense have been employed to improve cardiac dysfunction in rodents. In contrast, large-scale clinical trials using antioxidant therapies for the treatment of these pathological disorders have been ineffective [242, 243]. Collectively, these studies point towards a serious need to develop therapeutic strategies aimed at inhibiting specific sources of ROS in pathological conditions. We demonstrate that MAO contributes to increased ROS formation and ER stress in HG and IL-1β treated cardiomyocytes in vitro and in T1D model in vivo. Moreover, we show that these enzymes further activate cardiac mast cells, leading to fibrosis and ultimately diastolic dysfunction. These results point to MAO inhibition as a potential therapy in diabetic cardiomyopathy. Moreover, as mentioned before, besides the generation of H_2O_2 these flavoenzymes also produce reactive aldehydes that, *per se*, are deleterious for the heart. Thus, therapy employing MAO inhibition in cardiac dysfunction will not only aim at reducing oxidative stress but also abolishing the detrimental effects of these reactive aldehydes.

9. REFERENCES

1. Hotamisligil, G.S., *Inflammatory pathways and insulin action.* Int J Obes Relat Metab Disord, 2003. **27 Suppl 3**: p. S53-5.
2. Daneman, D., *Type 1 diabetes.* Lancet, 2006. **367**(9513): p. 847-58.
3. Rewers, M. and J. Ludvigsson, *Environmental risk factors for type 1 diabetes.* Lancet, 2016. **387**(10035): p. 2340-8.
4. Atkinson, M.A. and G.S. Eisenbarth, *Type 1 diabetes: new perspectives on disease pathogenesis and treatment.* Lancet, 2001. **358**(9277): p. 221-9.
5. Lu, J., Q. Xia, and Q. Zhou, *How to make insulin-producing pancreatic beta cells for diabetes treatment.* Sci China Life Sci, 2016.
6. Shapiro, A.M., et al., *Islet transplantation in seven patients with type 1 diabetes mellitus using a glucocorticoid-free immunosuppressive regimen.* N Engl J Med, 2000. **343**(4): p. 230-8.
7. Chari, S. and S. Mao, *Timeline: iPSCs--The First Decade.* Cell Stem Cell, 2016. **18**(2): p. 294.
8. Shiba, Y., et al., *Human ES-cell-derived cardiomyocytes electrically couple and suppress arrhythmias in injured hearts.* Nature, 2012. **489**(7415): p. 322-5.
9. Ning, G., *Decade in review-type 2 diabetes mellitus: At the centre of things.* Nat Rev Endocrinol, 2015. **11**(11): p. 636-8.
10. Kahn, S.E., M.E. Cooper, and S. Del Prato, *Pathophysiology and treatment of type 2 diabetes: perspectives on the past, present, and future.* Lancet, 2014. **383**(9922): p. 1068-83.
11. Ikezaki, H., et al., *Ethnic Differences in Glucose Homeostasis Markers between the Kyushu-Okinawa Population Study and the Framingham Offspring Study.* Sci Rep, 2016. **6**: p. 36725.
12. Forslund, K., et al., *Disentangling type 2 diabetes and metformin treatment signatures in the human gut microbiota.* Nature, 2015. **528**(7581): p. 262-6.
13. Harada, N. and N. Inagaki, *Role of sodium-glucose transporters in glucose uptake of the intestine and kidney.* J Diabetes Investig, 2012. **3**(4): p. 352-3.
14. Shah, K., S. Desilva, and T. Abbruscato, *The role of glucose transporters in brain disease: diabetes and Alzheimer's Disease.* Int J Mol Sci, 2012. **13**(10): p. 12629-55.
15. Bryant, N.J., R. Govers, and D.E. James, *Regulated transport of the glucose transporter GLUT4.* Nat Rev Mol Cell Biol, 2002. **3**(4): p. 267-77.
16. Huang, S. and M.P. Czech, *The GLUT4 glucose transporter.* Cell Metab, 2007. **5**(4): p. 237-52.

17. Lizcano, J.M. and D.R. Alessi, *The insulin signalling pathway.* Curr Biol, 2002. **12**(7): p. R236-8.

18. Saltiel, A.R. and C.R. Kahn, *Insulin signalling and the regulation of glucose and lipid metabolism.* Nature, 2001. **414**(6865): p. 799-806.

19. Huang, W., et al., *Kinetic analysis of PI3K reactions with fluorescent PIP2 derivatives.* Anal Bioanal Chem, 2011. **401**(6): p. 1881-8.

20. Mackenzie, R.W. and B.T. Elliott, *Akt/PKB activation and insulin signaling: a novel insulin signaling pathway in the treatment of type 2 diabetes.* Diabetes Metab Syndr Obes, 2014. **7**: p. 55-64.

21. Chang, L., S.H. Chiang, and A.R. Saltiel, *Insulin signaling and the regulation of glucose transport.* Mol Med, 2004. **10**(7-12): p. 65-71.

22. Jorgensen, S.B., E.A. Richter, and J.F. Wojtaszewski, *Role of AMPK in skeletal muscle metabolic regulation and adaptation in relation to exercise.* J Physiol, 2006. **574**(Pt 1): p. 17-31.

23. Forbes, J.M. and M.E. Cooper, *Mechanisms of diabetic complications.* Physiol Rev, 2013. **93**(1): p. 137-88.

24. Bugger, H. and C. Bode, *The vulnerable myocardium. Diabetic cardiomyopathy.* Hamostaseologie, 2015. **35**(1): p. 17-24.

25. Schannwell, C.M., et al., *Left ventricular diastolic dysfunction as an early manifestation of diabetic cardiomyopathy.* Cardiology, 2002. **98**(1-2): p. 33-9.

26. Nadeau, K.J., et al., *Insulin resistance in adolescents with type 1 diabetes and its relationship to cardiovascular function.* J Clin Endocrinol Metab, 2010. **95**(2): p. 513-21.

27. Maharaj, R., *Diastolic dysfunction and heart failure with a preserved ejection fraction: Relevance in critical illness and anaesthesia.* J Saudi Heart Assoc, 2012. **24**(2): p. 99-121.

28. Michalski, B., et al., *The differences in the relationship between diastolic dysfunction, selected biomarkers and collagen turn-over in heart failure patients with preserved and reduced ejection fraction.* Cardiol J, 2016.

29. Boyer, J.K., et al., *Prevalence of ventricular diastolic dysfunction in asymptomatic, normotensive patients with diabetes mellitus.* Am J Cardiol, 2004. **93**(7): p. 870-5.

30. Alpert, M.A., J. Omran, and B.P. Bostick, *Effects of Obesity on Cardiovascular Hemodynamics, Cardiac Morphology, and Ventricular Function.* Curr Obes Rep, 2016.

31. Smiseth, O.A., *Assessment of ventricular diastolic function.* Can J Cardiol, 2001. **17**(11): p. 1167-76.

32. Chan, E., et al., *Exercise training in heart failure patients with preserved ejection fraction: a systematic review and meta-analysis.* Monaldi Arch Chest Dis, 2016. **86**(1-2): p. 759.

33. Fukuta, H. and W.C. Little, *The cardiac cycle and the physiologic basis of left ventricular contraction, ejection, relaxation, and filling.* Heart Fail Clin, 2008. **4**(1): p. 1-11.

34. Little, W.C. and R.J. Applegate, *Congestive heart failure: systolic and diastolic function.* J Cardiothorac Vasc Anesth, 1993. **7**(4 Suppl 2): p. 2-5.

35. Elnady, B.M., et al., *The implication of tissue Doppler echocardiography and cardiopulmonary exercise in early detection of cardiac dysfunction in systemic lupus erythematosus patients.* Eur J Rheumatol, 2016. **3**(3): p. 109-117.

36. Zile, M.R. and D.L. Brutsaert, *New concepts in diastolic dysfunction and diastolic heart failure: Part I: diagnosis, prognosis, and measurements of diastolic function.* Circulation, 2002. **105**(11): p. 1387-93.

37. Bugger, H. and E.D. Abel, *Molecular mechanisms of diabetic cardiomyopathy.* Diabetologia, 2014. **57**(4): p. 660-71.

38. Teupe, C. and C. Rosak, *Diabetic cardiomyopathy and diastolic heart failure -- difficulties with relaxation.* Diabetes Res Clin Pract, 2012. **97**(2): p. 185-94.

39. Bugger, H. and E.D. Abel, *Mitochondria in the diabetic heart.* Cardiovasc Res, 2010. **88**(2): p. 229-40.

40. Bandeira Sde, M., et al., *Characterization of blood oxidative stress in type 2 diabetes mellitus patients: increase in lipid peroxidation and SOD activity.* Oxid Med Cell Longev, 2012. **2012**: p. 819310.

41. Huynh, K., et al., *Diabetic cardiomyopathy: mechanisms and new treatment strategies targeting antioxidant signaling pathways.* Pharmacol Ther, 2014. **142**(3): p. 375-415.

42. Spycher, S.E., et al., *Aldose reductase induction: a novel response to oxidative stress of smooth muscle cells.* FASEB J, 1997. **11**(2): p. 181-8.

43. Brownlee, M., *Biochemistry and molecular cell biology of diabetic complications.* Nature, 2001. **414**(6865): p. 813-20.

44. Tang, W.H., K.A. Martin, and J. Hwa, *Aldose reductase, oxidative stress, and diabetic mellitus.* Front Pharmacol, 2012. **3**: p. 87.

45. Kaneko, M., et al., *Aldose reductase and AGE-RAGE pathways: key players in myocardial ischemic injury.* Ann N Y Acad Sci, 2005. **1043**: p. 702-9.

46. Bhadada, S.V., V.K. Vyas, and R.K. Goyal, *Protective effect of Tephrosia purpurea in diabetic cataract through aldose reductase inhibitory activity.* Biomed Pharmacother, 2016. **83**: p. 221-228.

47. Vedantham, S., et al., *Human aldose reductase expression accelerates atherosclerosis in diabetic apolipoprotein E-/- mice.* Arterioscler Thromb Vasc Biol, 2011. **31**(8): p. 1805-13.

48. Dzib-Guerra, W.D., et al., *Anti-Advanced Glycation End-product and Free Radical Scavenging Activity of Plants from the Yucatecan Flora.* Pharmacognosy Res, 2016. **8**(4): p. 276-280.

49. Sung, S.K., et al., *Sildenafil Ameliorates Advanced Glycation End Products-Induced Mitochondrial Dysfunction in HT-22 Hippocampal Neuronal Cells.* J Korean Neurosurg Soc, 2016. **59**(3): p. 259-68.

50. Wautier, M.P., et al., *Activation of NADPH oxidase by AGE links oxidant stress to altered gene expression via RAGE.* Am J Physiol Endocrinol Metab, 2001. **280**(5): p. E685-94.

51. Rahbar, S. and J.L. Figarola, *Novel inhibitors of advanced glycation endproducts.* Arch Biochem Biophys, 2003. **419**(1): p. 63-79.

52. Bucciarelli, L.G., et al., *RAGE blockade stabilizes established atherosclerosis in diabetic apolipoprotein E-null mice.* Circulation, 2002. **106**(22): p. 2827-35.

53. Williams, M.D. and J.L. Nadler, *Inflammatory mechanisms of diabetic complications.* Curr Diab Rep, 2007. **7**(3): p. 242-8.

54. Nishikawa, T., et al., *Normalizing mitochondrial superoxide production blocks three pathways of hyperglycaemic damage.* Nature, 2000. **404**(6779): p. 787-90.

55. Newton, A.C., *Protein kinase C: structure, function, and regulation.* J Biol Chem, 1995. **270**(48): p. 28495-8.

56. Pinton, P., et al., *Protein kinase C beta and prolyl isomerase 1 regulate mitochondrial effects of the life-span determinant p66Shc.* Science, 2007. **315**(5812): p. 659-63.

57. Haller, M., et al., *Novel Insights into the PKCbeta-dependent Regulation of the Oxidoreductase p66Shc.* J Biol Chem, 2016.

58. Roul, D. and F.A. Recchia, *Metabolic alterations induce oxidative stress in diabetic and failing hearts: different pathways, same outcome.* Antioxid Redox Signal, 2015. **22**(17): p. 1502-14.

59. Du, X.L., et al., *Hyperglycemia-induced mitochondrial superoxide overproduction activates the hexosamine pathway and induces plasminogen activator inhibitor-1 expression by increasing Sp1 glycosylation.* Proc Natl Acad Sci U S A, 2000. **97**(22): p. 12222-6.

60. Kim, Y.S., et al., *Differential behavior of mesangial cells derived from 12/15-lipoxygenase knockout mice relative to control mice.* Kidney Int, 2003. **64**(5): p. 1702-14.

61. Reddy, M.A., et al., *The oxidized lipid and lipoxygenase product 12(S)-hydroxyeicosatetraenoic acid induces hypertrophy and fibronectin transcription in*

vascular smooth muscle cells via p38 MAPK and cAMP response element-binding protein activation. Mediation of angiotensin II effects. J Biol Chem, 2002. **277**(12): p. 9920-8.

62. Antonipillai, I., et al., *A 12-lipoxygenase product, 12-hydroxyeicosatetraenoic acid, is increased in diabetics with incipient and early renal disease.* J Clin Endocrinol Metab, 1996. **81**(5): p. 1940-5.

63. Chattopadhyay, R., et al., *12/15-Lipoxygenase-dependent ROS production is required for diet-induced endothelial barrier dysfunction.* J Lipid Res, 2015. **56**(3): p. 562-77.

64. Scribner, K.A., et al., *Masoprocol decreases serum triglyceride concentrations in rats with fructose-induced hypertriglyceridemia.* Metabolism, 2000. **49**(9): p. 1106-10.

65. Cesselli, D., et al., *Oxidative stress-mediated cardiac cell death is a major determinant of ventricular dysfunction and failure in dog dilated cardiomyopathy.* Circ Res, 2001. **89**(3): p. 279-86.

66. Varga, Z.V., et al., *Interplay of oxidative, nitrosative/nitrative stress, inflammation, cell death and autophagy in diabetic cardiomyopathy.* Biochim Biophys Acta, 2015. **1852**(2): p. 232-42.

67. Boudina, S., et al., *Contribution of impaired myocardial insulin signaling to mitochondrial dysfunction and oxidative stress in the heart.* Circulation, 2009. **119**(9): p. 1272-83.

68. Pitocco, D., et al., *Oxidative stress in diabetes: implications for vascular and other complications.* Int J Mol Sci, 2013. **14**(11): p. 21525-50.

69. Matsuda, M. and I. Shimomura, *Increased oxidative stress in obesity: implications for metabolic syndrome, diabetes, hypertension, dyslipidemia, atherosclerosis, and cancer.* Obes Res Clin Pract, 2013. **7**(5): p. e330-41.

70. Braunersreuther, V., et al., *Role of NADPH oxidase isoforms NOX1, NOX2 and NOX4 in myocardial ischemia/reperfusion injury.* J Mol Cell Cardiol, 2013. **64**: p. 99-107.

71. Santos, C.X., S. Raza, and A.M. Shah, *Redox signaling in the cardiomyocyte: From physiology to failure.* Int J Biochem Cell Biol, 2016. **74**: p. 145-51.

72. Kayama, Y., et al., *Diabetic Cardiovascular Disease Induced by Oxidative Stress.* Int J Mol Sci, 2015. **16**(10): p. 25234-63.

73. Zhang, M., et al., *NADPH oxidase-4 mediates protection against chronic load-induced stress in mouse hearts by enhancing angiogenesis.* Proc Natl Acad Sci U S A, 2010. **107**(42): p. 18121-6.

74. Kuroda, J., et al., *NADPH oxidase 4 (Nox4) is a major source of oxidative stress in the failing heart.* Proc Natl Acad Sci U S A, 2010. **107**(35): p. 15565-70.

75. Maalouf, R.M., et al., *Nox4-derived reactive oxygen species mediate cardiomyocyte injury in early type 1 diabetes.* Am J Physiol Cell Physiol, 2012. **302**(3): p. C597-604.

76. Rodino-Janeiro, B.K., et al., *Current status of NADPH oxidase research in cardiovascular pharmacology.* Vasc Health Risk Manag, 2013. **9**: p. 401-28.

77. Privratsky, J.R., et al., *AT1 blockade prevents glucose-induced cardiac dysfunction in ventricular myocytes: role of the AT1 receptor and NADPH oxidase.* Hypertension, 2003. **42**(2): p. 206-12.

78. Balteau, M., et al., *NADPH oxidase activation by hyperglycaemia in cardiomyocytes is independent of glucose metabolism but requires SGLT1.* Cardiovasc Res, 2011. **92**(2): p. 237-46.

79. Nishio, S., et al., *Activation of CaMKII as a key regulator of reactive oxygen species production in diabetic rat heart.* J Mol Cell Cardiol, 2012. **52**(5): p. 1103-11.

80. Saliaris, A.P., et al., *Chronic allopurinol administration ameliorates maladaptive alterations in Ca2+ cycling proteins and beta-adrenergic hyporesponsiveness in heart failure.* Am J Physiol Heart Circ Physiol, 2007. **292**(3): p. H1328-35.

81. Amado, L.C., et al., *Xanthine oxidase inhibition ameliorates cardiovascular dysfunction in dogs with pacing-induced heart failure.* J Mol Cell Cardiol, 2005. **39**(3): p. 531-6.

82. Rajesh, M., et al., *Xanthine oxidase inhibitor allopurinol attenuates the development of diabetic cardiomyopathy.* J Cell Mol Med, 2009. **13**(8B): p. 2330-41.

83. Downey, J.M., et al., *Xanthine oxidase is not a source of free radicals in the ischemic rabbit heart.* J Mol Cell Cardiol, 1987. **19**(11): p. 1053-60.

84. Eddy, L.J., et al., *Free radical-producing enzyme, xanthine oxidase, is undetectable in human hearts.* Am J Physiol, 1987. **253**(3 Pt 2): p. H709-11.

85. Anderson, E.J., et al., *Substrate-specific derangements in mitochondrial metabolism and redox balance in the atrium of the type 2 diabetic human heart.* J Am Coll Cardiol, 2009. **54**(20): p. 1891-8.

86. Shen, X., et al., *Protection of cardiac mitochondria by overexpression of MnSOD reduces diabetic cardiomyopathy.* Diabetes, 2006. **55**(3): p. 798-805.

87. Kukidome, D., et al., *Activation of AMP-activated protein kinase reduces hyperglycemia-induced mitochondrial reactive oxygen species production and promotes mitochondrial biogenesis in human umbilical vein endothelial cells.* Diabetes, 2006. **55**(1): p. 120-7.

88. Chen, Q., et al., *Ischemic defects in the electron transport chain increase the production of reactive oxygen species from isolated rat heart mitochondria.* Am J Physiol Cell Physiol, 2008. **294**(2): p. C460-6.

89. Chen, Y.R. and J.L. Zweier, *Cardiac mitochondria and reactive oxygen species generation.* Circ Res, 2014. **114**(3): p. 524-37.

90. Kaludercic, N., et al., *Monoamine oxidases as sources of oxidants in the heart.* J Mol Cell Cardiol, 2014. **73**: p. 34-42.

91. Murphy, E., et al., *Mitochondrial Function, Biology, and Role in Disease: A Scientific Statement From the American Heart Association.* Circ Res, 2016. **118**(12): p. 1960-91.

92. Chouchani, E.T., et al., *Ischaemic accumulation of succinate controls reperfusion injury through mitochondrial ROS.* Nature, 2014. **515**(7527): p. 431-5.

93. Shah, M.S. and M. Brownlee, *Molecular and Cellular Mechanisms of Cardiovascular Disorders in Diabetes.* Circ Res, 2016. **118**(11): p. 1808-29.

94. Ye, G., et al., *Catalase protects cardiomyocyte function in models of type 1 and type 2 diabetes.* Diabetes, 2004. **53**(5): p. 1336-43.

95. Schriner, S.E., et al., *Extension of murine life span by overexpression of catalase targeted to mitochondria.* Science, 2005. **308**(5730): p. 1909-11.

96. Sivitz, W.I. and M.A. Yorek, *Mitochondrial dysfunction in diabetes: from molecular mechanisms to functional significance and therapeutic opportunities.* Antioxid Redox Signal, 2010. **12**(4): p. 537-77.

97. Banerjee, P.S., J. Ma, and G.W. Hart, *Diabetes-associated dysregulation of O-GlcNAcylation in rat cardiac mitochondria.* Proc Natl Acad Sci U S A, 2015. **112**(19): p. 6050-5.

98. Anderson, E.J., et al., *Monoamine oxidase is a major determinant of redox balance in human atrial myocardium and is associated with postoperative atrial fibrillation.* J Am Heart Assoc, 2014. **3**(1): p. e000713.

99. Di Lisa, F., et al., *New aspects of p66Shc in ischemia reperfusion injury and cardiovascular diseases.* Br J Pharmacol, 2016.

100. Di Lisa, F., et al., *Mitochondrial pathways for ROS formation and myocardial injury: the relevance of p66(Shc) and monoamine oxidase.* Basic Res Cardiol, 2009. **104**(2): p. 131-9.

101. Carpi, A., et al., *The cardioprotective effects elicited by p66(Shc) ablation demonstrate the crucial role of mitochondrial ROS formation in ischemia/reperfusion injury.* Biochim Biophys Acta, 2009. **1787**(7): p. 774-80.

102. Min, W., et al., *The signal transduction pathway of PKC/NF-kappa B/c-fos may be involved in the influence of high glucose on the cardiomyocytes of neonatal rats.* Cardiovasc Diabetol, 2009. **8**: p. 8.

103. Rota, M., et al., *Diabetes promotes cardiac stem cell aging and heart failure, which are prevented by deletion of the p66shc gene.* Circ Res, 2006. **99**(1): p. 42-52.

104. Youdim, M.B., D. Edmondson, and K.F. Tipton, *The therapeutic potential of monoamine oxidase inhibitors.* Nat Rev Neurosci, 2006. **7**(4): p. 295-309.

105. Edmondson, D.E., et al., *Structure and mechanism of monoamine oxidase.* Curr Med Chem, 2004. **11**(15): p. 1983-93.

106. Kopin, I.J., *Monoamine oxidase and catecholamine metabolism.* J Neural Transm Suppl, 1994. **41**: p. 57-67.

107. Hardebo, J.E. and C. Owman, *Barrier mechanisms for neurotransmitter monoamines and their precursors at the blood-brain interface.* Ann Neurol, 1980. **8**(1): p. 1-31.

108. Shih, J.C., K. Chen, and M.J. Ridd, *Monoamine oxidase: from genes to behavior.* Annu Rev Neurosci, 1999. **22**: p. 197-217.

109. Kitahama, K., et al., *Monoamine oxidase: distribution in the cat brain studied by enzyme- and immunohistochemistry: recent progress.* Prog Neurobiol, 1994. **42**(1): p. 53-78.

110. Kaludercic, N., et al., *Monoamine oxidases (MAO) in the pathogenesis of heart failure and ischemia/reperfusion injury.* Biochim Biophys Acta, 2011. **1813**(7): p. 1323-32.

111. Gorkin, V.Z. and T.A. Moskvitina, *[Monoamine oxidases of the brain and problems of central nervous system pathology (review)].* Zh Nevropatol Psikhiatr Im S S Korsakova, 1985. **85**(7): p. 1062-4.

112. Caraci, F., et al., *Neuroprotective effects of the monoamine oxidase inhibitor tranylcypromine and its amide derivatives against Abeta(1-42)-induced toxicity.* Eur J Pharmacol, 2015. **764**: p. 256-63.

113. Fabbri, M., et al., *Clinical pharmacology review of safinamide for the treatment of Parkinson's disease.* Neurodegener Dis Manag, 2015. **5**(6): p. 481-96.

114. Perez-Lloret, S. and O. Rascol, *The safety and efficacy of safinamide mesylate for the treatment of Parkinson's disease.* Expert Rev Neurother, 2016. **16**(3): p. 245-58.

115. Mialet-Perez, J., et al., *New insights on receptor-dependent and monoamine oxidase-dependent effects of serotonin in the heart.* J Neural Transm (Vienna), 2007. **114**(6): p. 823-7.

116. Vindis, C., et al., *Monoamine oxidase B induces ERK-dependent cell mitogenesis by hydrogen peroxide generation.* Biochem Biophys Res Commun, 2000. **271**(1): p. 181-5.

117. Kaludercic, N., et al., *Monoamine oxidase A-mediated enhanced catabolism of norepinephrine contributes to adverse remodeling and pump failure in hearts with pressure overload.* Circ Res, 2010. **106**(1): p. 193-202.

118. Lairez, O., et al., *Genetic deletion of MAO-A promotes serotonin-dependent ventricular hypertrophy by pressure overload.* J Mol Cell Cardiol, 2009. **46**(4): p. 587-95.

119. Kong, S.W., et al., *Genetic expression profiles during physiological and pathological cardiac hypertrophy and heart failure in rats.* Physiol Genomics, 2005. **21**(1): p. 34-42.

120. Kaludercic, N., et al., *Monoamine oxidase B prompts mitochondrial and cardiac dysfunction in pressure overloaded hearts.* Antioxid Redox Signal, 2014. **20**(2): p. 267-80.

121. Chen, C.H., L. Sun, and D. Mochly-Rosen, *Mitochondrial aldehyde dehydrogenase and cardiac diseases.* Cardiovasc Res, 2010. **88**(1): p. 51-7.

122. Chen, C.H., et al., *Targeting aldehyde dehydrogenase 2: new therapeutic opportunities.* Physiol Rev, 2014. **94**(1): p. 1-34.

123. Bianchi, P., et al., *Oxidative stress by monoamine oxidase mediates receptor-independent cardiomyocyte apoptosis by serotonin and postischemic myocardial injury.* Circulation, 2005. **112**(21): p. 3297-305.

124. Kunduzova, O.R., et al., *Hydrogen peroxide production by monoamine oxidase during ischemia/reperfusion.* Eur J Pharmacol, 2002. **448**(2-3): p. 225-30.

125. Pchejetski, D., et al., *Oxidative stress-dependent sphingosine kinase-1 inhibition mediates monoamine oxidase A-associated cardiac cell apoptosis.* Circ Res, 2007. **100**(1): p. 41-9.

126. Villeneuve, C., et al., *p53-PGC-1alpha pathway mediates oxidative mitochondrial damage and cardiomyocyte necrosis induced by monoamine oxidase-A upregulation: role in chronic left ventricular dysfunction in mice.* Antioxid Redox Signal, 2013. **18**(1): p. 5-18.

127. Santin, Y., et al., *Oxidative Stress by Monoamine Oxidase-A Impairs Transcription Factor EB Activation and Autophagosome Clearance, Leading to Cardiomyocyte Necrosis and Heart Failure.* Antioxid Redox Signal, 2016. **25**(1): p. 10-27.

128. Umbarkar, P., et al., *Monoamine oxidase-A is an important source of oxidative stress and promotes cardiac dysfunction, apoptosis, and fibrosis in diabetic cardiomyopathy.* Free Radic Biol Med, 2015. **87**: p. 263-73.

129. Xu, C., B. Bailly-Maitre, and J.C. Reed, *Endoplasmic reticulum stress: cell life and death decisions.* J Clin Invest, 2005. **115**(10): p. 2656-64.

130. Ron, D. and P. Walter, *Signal integration in the endoplasmic reticulum unfolded protein response.* Nat Rev Mol Cell Biol, 2007. **8**(7): p. 519-29.

131. Luo, T., et al., *Attenuation of ER stress prevents post-infarction-induced cardiac rupture and remodeling by modulating both cardiac apoptosis and fibrosis.* Chem Biol Interact, 2015. **225**: p. 90-8.

132. Inagi, R., Y. Ishimoto, and M. Nangaku, *Proteostasis in endoplasmic reticulum--new mechanisms in kidney disease.* Nat Rev Nephrol, 2014. **10**(7): p. 369-78.

133. Oslowski, C.M. and F. Urano, *Measuring ER stress and the unfolded protein response using mammalian tissue culture system.* Methods Enzymol, 2011. **490**: p. 71-92.

134. Santos, C.X., et al., *Mechanisms and implications of reactive oxygen species generation during the unfolded protein response: roles of endoplasmic reticulum*

oxidoreductases, mitochondrial electron transport, and NADPH oxidase. Antioxid Redox Signal, 2009. **11**(10): p. 2409-27.

135. Liu, Z., et al., *Protein kinase R-like ER kinase and its role in endoplasmic reticulum stress-decided cell fate.* Cell Death Dis, 2015. **6**: p. e1822.

136. Sha, H.B., et al., *The IRE1 alpha-XBP1 Pathway of the Unfolded Protein Response Is Required for Adipogenesis.* Cell Metabolism, 2009. **9**(6): p. 556-564.

137. Chen, L., et al., *Cab45S inhibits the ER stress-induced IRE1-JNK pathway and apoptosis via GRP78/BiP.* Cell Death Dis, 2014. **5**: p. e1219.

138. Lee, A.S., *The ER chaperone and signaling regulator GRP78/BiP as a monitor of endoplasmic reticulum stress.* Methods, 2005. **35**(4): p. 373-81.

139. Dally, S., et al., *Compartmentalized expression of three novel sarco/endoplasmic reticulum Ca2+ATPase 3 isoforms including the switch to ER stress, SERCA3f, in non-failing and failing human heart.* Cell Calcium, 2009. **45**(2): p. 144-54.

140. Li, Z., et al., *Involvement of endoplasmic reticulum stress in myocardial apoptosis of streptozocin-induced diabetic rats.* J Clin Biochem Nutr, 2007. **41**(1): p. 58-67.

141. Hoyer-Hansen, M., et al., *Control of macroautophagy by calcium, calmodulin-dependent kinase kinase-beta, and Bcl-2.* Mol Cell, 2007. **25**(2): p. 193-205.

142. Jung, C.H., et al., *ULK-Atg13-FIP200 complexes mediate mTOR signaling to the autophagy machinery.* Mol Biol Cell, 2009. **20**(7): p. 1992-2003.

143. Younce, C.W., K. Wang, and P.E. Kolattukudy, *Hyperglycaemia-induced cardiomyocyte death is mediated via MCP-1 production and induction of a novel zinc-finger protein MCPIP.* Cardiovasc Res, 2010. **87**(4): p. 665-74.

144. Kouroku, Y., et al., *ER stress (PERK/eIF2alpha phosphorylation) mediates the polyglutamine-induced LC3 conversion, an essential step for autophagy formation.* Cell Death Differ, 2007. **14**(2): p. 230-9.

145. Miki, T., et al., *Endoplasmic reticulum stress in diabetic hearts abolishes erythropoietin-induced myocardial protection by impairment of phospho-glycogen synthase kinase-3beta-mediated suppression of mitochondrial permeability transition.* Diabetes, 2009. **58**(12): p. 2863-72.

146. Ji, Y., et al., *Liraglutide alleviates diabetic cardiomyopathy by blocking CHOP-triggered apoptosis via the inhibition of the IRE-alpha pathway.* Mol Med Rep, 2014. **9**(4): p. 1254-8.

147. Souders, C.A., S.L. Bowers, and T.A. Baudino, *Cardiac fibroblast: the renaissance cell.* Circ Res, 2009. **105**(12): p. 1164-76.

148. Krenning, G., E.M. Zeisberg, and R. Kalluri, *The origin of fibroblasts and mechanism of cardiac fibrosis.* J Cell Physiol, 2010. **225**(3): p. 631-7.

149. Liu, R.M. and K.A. Gaston Pravia, *Oxidative stress and glutathione in TGF-beta-mediated fibrogenesis.* Free Radic Biol Med, 2010. **48**(1): p. 1-15.

150. Weber, K.T., *Fibrosis and hypertensive heart disease.* Curr Opin Cardiol, 2000. **15**(4): p. 264-72.

151. Anderson, K.R., M.G. Sutton, and J.T. Lie, *Histopathological types of cardiac fibrosis in myocardial disease.* J Pathol, 1979. **128**(2): p. 79-85.

152. Isoyama, S. and Y. Nitta-Komatsubara, *Acute and chronic adaptation to hemodynamic overload and ischemia in the aged heart.* Heart Fail Rev, 2002. **7**(1): p. 63-9.

153. Han, D.C., et al., *High glucose stimulates proliferation and collagen type I synthesis in renal cortical fibroblasts: mediation by autocrine activation of TGF-beta.* J Am Soc Nephrol, 1999. **10**(9): p. 1891-9.

154. Russo, I. and N.G. Frangogiannis, *Diabetes-associated cardiac fibrosis: Cellular effectors, molecular mechanisms and therapeutic opportunities.* J Mol Cell Cardiol, 2016. **90**: p. 84-93.

155. Neumann, S., et al., *Aldosterone and D-glucose stimulate the proliferation of human cardiac myofibroblasts in vitro.* Hypertension, 2002. **39**(3): p. 756-60.

156. Asbun, J., A.M. Manso, and F.J. Villarreal, *Profibrotic influence of high glucose concentration on cardiac fibroblast functions: effects of losartan and vitamin E.* Am J Physiol Heart Circ Physiol, 2005. **288**(1): p. H227-34.

157. Asbun, J. and F.J. Villarreal, *The pathogenesis of myocardial fibrosis in the setting of diabetic cardiomyopathy.* J Am Coll Cardiol, 2006. **47**(4): p. 693-700.

158. Conway, B.R., et al., *Tight blood glycaemic and blood pressure control in experimental diabetic nephropathy reduces extracellular matrix production without regression of fibrosis.* Nephrology (Carlton), 2014. **19**(12): p. 802-13.

159. Venkatachalam, K., et al., *WISP1, a pro-mitogenic, pro-survival factor, mediates tumor necrosis factor-alpha (TNF-alpha)-stimulated cardiac fibroblast proliferation but inhibits TNF-alpha-induced cardiomyocyte death.* J Biol Chem, 2009. **284**(21): p. 14414-27.

160. Biernacka, A., M. Dobaczewski, and N.G. Frangogiannis, *TGF-beta signaling in fibrosis.* Growth Factors, 2011. **29**(5): p. 196-202.

161. Zhang, J. and G.P. Shi, *Mast cells and metabolic syndrome.* Biochim Biophys Acta, 2012. **1822**(1): p. 14-20.

162. Hara, M., et al., *Evidence for a role of mast cells in the evolution to congestive heart failure.* J Exp Med, 2002. **195**(3): p. 375-81.

163. Zhao, W., et al., *Propofol prevents lung injury after intestinal ischemia-reperfusion by inhibiting the interaction between mast cell activation and oxidative stress.* Life Sci, 2014. **108**(2): p. 80-7.

164. Luo, C., et al., *Sevoflurane ameliorates intestinal ischemia-reperfusion-induced lung injury by inhibiting the synergistic action between mast cell activation and oxidative stress.* Mol Med Rep, 2015. **12**(1): p. 1082-90.

165. Gan, X., et al., *Propofol Attenuates Small Intestinal Ischemia Reperfusion Injury through Inhibiting NADPH Oxidase Mediated Mast Cell Activation.* Oxid Med Cell Longev, 2015. **2015**: p. 167014.

166. Iwasaki, Y., et al., *Dehydroepiandrosterone-sulfate inhibits nuclear factor-kappaB-dependent transcription in hepatocytes, possibly through antioxidant effect.* J Clin Endocrinol Metab, 2004. **89**(7): p. 3449-54.

167. Purnomo, Y., et al., *Oxidative stress and transforming growth factor-beta1-induced cardiac fibrosis.* Cardiovasc Hematol Disord Drug Targets, 2013. **13**(2): p. 165-72.

168. Aragno, M., et al., *Oxidative stress triggers cardiac fibrosis in the heart of diabetic rats.* Endocrinology, 2008. **149**(1): p. 380-8.

169. Zhao, L.M., et al., *Advanced glycation end products promote proliferation of cardiac fibroblasts by upregulation of KCa3.1 channels.* Pflugers Arch, 2012. **464**(6): p. 613-21.

170. Schram, K., et al., *Regulation of MT1-MMP and MMP-2 by leptin in cardiac fibroblasts involves Rho/ROCK-dependent actin cytoskeletal reorganization and leads to enhanced cell migration.* Endocrinology, 2011. **152**(5): p. 2037-47.

171. Barouch, L.A., et al., *Disruption of leptin signaling contributes to cardiac hypertrophy independently of body weight in mice.* Circulation, 2003. **108**(6): p. 754-9.

172. Mozaffari, M.S., et al., *Mechanisms of load dependency of myocardial ischemia reperfusion injury.* Am J Cardiovasc Dis, 2013. **3**(4): p. 180-96.

173. Jahng, J.W., E. Song, and G. Sweeney, *Crosstalk between the heart and peripheral organs in heart failure.* Exp Mol Med, 2016. **48**: p. e217.

174. Shaver, A., et al., *Role of Serum Biomarkers in Early Detection of Diabetic Cardiomyopathy in the West Virginian Population.* Int J Med Sci, 2016. **13**(3): p. 161-8.

175. Ferdinandy, P., et al., *Peroxynitrite is a major contributor to cytokine-induced myocardial contractile failure.* Circ Res, 2000. **87**(3): p. 241-7.

176. Westermann, D., et al., *Tumor necrosis factor-alpha antagonism protects from myocardial inflammation and fibrosis in experimental diabetic cardiomyopathy.* Basic Res Cardiol, 2007. **102**(6): p. 500-7.

177. Donath, M.Y., *Targeting inflammation in the treatment of type 2 diabetes: time to start.* Nat Rev Drug Discov, 2014. **13**(6): p. 465-76.

178. Liu, Z., et al., *Circulating interleukin-1beta promotes endoplasmic reticulum stress-induced myocytes apoptosis in diabetic cardiomyopathy via interleukin-1 receptor-associated kinase-2.* Cardiovasc Diabetol, 2015. **14**: p. 125.

179. Palomer, X., et al., *An overview of the crosstalk between inflammatory processes and metabolic dysregulation during diabetic cardiomyopathy.* Int J Cardiol, 2013. **168**(4): p. 3160-72.

180. Yeung, F., et al., *Modulation of NF-kappaB-dependent transcription and cell survival by the SIRT1 deacetylase.* EMBO J, 2004. **23**(12): p. 2369-80.

181. Luo, B., et al., *NLRP3 gene silencing ameliorates diabetic cardiomyopathy in a type 2 diabetes rat model.* PLoS One, 2014. **9**(8): p. e104771.

182. Wang, Y., et al., *Pirfenidone attenuates cardiac fibrosis in a mouse model of TAC-induced left ventricular remodeling by suppressing NLRP3 inflammasome formation.* Cardiology, 2013. **126**(1): p. 1-11.

183. Wen, H., et al., *Fatty acid-induced NLRP3-ASC inflammasome activation interferes with insulin signaling.* Nat Immunol, 2011. **12**(5): p. 408-15.

184. Fujiu, K. and R. Nagai, *Contributions of cardiomyocyte-cardiac fibroblast-immune cell interactions in heart failure development.* Basic Res Cardiol, 2013. **108**(4): p. 357.

185. Miki, T., et al., *Diabetic cardiomyopathy: pathophysiology and clinical features.* Heart Fail Rev, 2013. **18**(2): p. 149-66.

186. Usui, F., et al., *Inflammasome activation by mitochondrial oxidative stress in macrophages leads to the development of angiotensin II-induced aortic aneurysm.* Arterioscler Thromb Vasc Biol, 2015. **35**(1): p. 127-36.

187. Esposito, K., R. Marfella, and D. Giugliano, *Stress hyperglycemia, inflammation, and cardiovascular events.* Diabetes Care, 2003. **26**(5): p. 1650-1.

188. Halter, J.B., et al., *Diabetes and cardiovascular disease in older adults: current status and future directions.* Diabetes, 2014. **63**(8): p. 2578-89.

189. Mandrup-Poulsen, T., L. Pickersgill, and M.Y. Donath, *Blockade of interleukin 1 in type 1 diabetes mellitus.* Nat Rev Endocrinol, 2010. **6**(3): p. 158-66.

190. Maedler, K., et al., *Interleukin-1 beta targeted therapy for type 2 diabetes.* Expert Opin Biol Ther, 2009. **9**(9): p. 1177-88.

191. Buckman, J.F., et al., *MitoTracker labeling in primary neuronal and astrocytic cultures: influence of mitochondrial membrane potential and oxidants.* J Neurosci Methods, 2001. **104**(2): p. 165-76.

192. Kaludercic, N., S. Deshwal, and F. Di Lisa, *Reactive oxygen species and redox compartmentalization.* Front Physiol, 2014. **5**: p. 285.

193. Kuznetsov, A.V., et al., *H9c2 and HL-1 cells demonstrate distinct features of energy metabolism, mitochondrial function and sensitivity to hypoxia-reoxygenation.* Biochim Biophys Acta, 2015. **1853**(2): p. 276-84.

194. Milerova, M., et al., *Neonatal cardiac mitochondria and ischemia/reperfusion injury.* Mol Cell Biochem, 2010. **335**(1-2): p. 147-53.

195. Bombicino, S.S., et al., *Diabetes impairs heart mitochondrial function without changes in resting cardiac performance.* Int J Biochem Cell Biol, 2016.

196. de Carvalho, A.K., et al., *Prior Exercise Training Prevent Hyperglycemia in STZ Mice by Increasing Hepatic Glycogen and Mitochondrial Function on Skeletal Muscle.* J Cell Biochem, 2016.

197. Rolo, A.P. and C.M. Palmeira, *Diabetes and mitochondrial function: role of hyperglycemia and oxidative stress.* Toxicol Appl Pharmacol, 2006. **212**(2): p. 167-78.

198. Boudina, S., et al., *Reduced mitochondrial oxidative capacity and increased mitochondrial uncoupling impair myocardial energetics in obesity.* Circulation, 2005. **112**(17): p. 2686-95.

199. Duncan, J.G., et al., *Insulin-resistant heart exhibits a mitochondrial biogenic response driven by the peroxisome proliferator-activated receptor-alpha/PGC-1alpha gene regulatory pathway.* Circulation, 2007. **115**(7): p. 909-17.

200. Boudina, S., et al., *Mitochondrial energetics in the heart in obesity-related diabetes: direct evidence for increased uncoupled respiration and activation of uncoupling proteins.* Diabetes, 2007. **56**(10): p. 2457-66.

201. Inoue, M., et al., *Role of ATP decrease in secretion induced by mitochondrial dysfunction in guinea-pig adrenal chromaffin cells.* J Physiol, 2002. **539**(Pt 1): p. 145-55.

202. Xu, J., et al., *Endoplasmic reticulum stress and diabetic cardiomyopathy.* Exp Diabetes Res, 2012. **2012**: p. 827971.

203. Wu, T., et al., *Valsartan protects against ER stress-induced myocardial apoptosis via CHOP/Puma signaling pathway in streptozotocin-induced diabetic rats.* Eur J Pharm Sci, 2011. **42**(5): p. 496-502.

204. Wu, K.K. and Y. Huan, *Streptozotocin-induced diabetic models in mice and rats.* Curr Protoc Pharmacol, 2008. **Chapter 5**: p. Unit 5 47.

205. Chaudhary, A.K., et al., *Study on Diastolic Dysfunction in Newly Diagnosed Type 2 Diabetes Mellitus and its Correlation with Glycosylated Haemoglobin (HbA1C).* J Clin Diagn Res, 2015. **9**(8): p. OC20-2.

206. Yang, R., et al., *[Effect of hydrogen sulfide on oxidative stress and endoplasmic reticulum stress in diabetic cardiomyopathy].* Zhongguo Ying Yong Sheng Li Xue Za Zhi, 2016. **32**(1): p. 8-12.

207. Qi, X., et al., *Cardiac damage and dysfunction in diabetic cardiomyopathy are ameliorated by Grx1.* Genet Mol Res, 2016. **15**(3).

208. Liu, X., et al., *Inhibition of Pin1 alleviates myocardial fibrosis and dysfunction in STZ-induced diabetic mice.* Biochem Biophys Res Commun, 2016. **479**(1): p. 109-15.

209. Summers, S.A., et al., *Mast cell activation and degranulation promotes renal fibrosis in experimental unilateral ureteric obstruction.* Kidney Int, 2012. **82**(6): p. 676-85.

210. Levick, S.P., et al., *Cardiac mast cells mediate left ventricular fibrosis in the hypertensive rat heart.* Hypertension, 2009. **53**(6): p. 1041-7.

211. Huang, Z.G., et al., *Myocardial remodeling in diabetic cardiomyopathy associated with cardiac mast cell activation.* PLoS One, 2013. **8**(3): p. e60827.

212. Brownlee, M., *The pathobiology of diabetic complications: a unifying mechanism.* Diabetes, 2005. **54**(6): p. 1615-25.

213. Giacco, F. and M. Brownlee, *Oxidative stress and diabetic complications.* Circ Res, 2010. **107**(9): p. 1058-70.

214. Donath, M.Y., et al., *Inflammation in obesity and diabetes: islet dysfunction and therapeutic opportunity.* Cell Metab, 2013. **17**(6): p. 860-72.

215. Aharon-Hananel, G., et al., *Antidiabetic Effect of Interleukin-1beta Antibody Therapy Through beta-Cell Protection in the Cohen Diabetes-Sensitive Rat.* Diabetes, 2015. **64**(5): p. 1780-5.

216. Owyang, A.M., et al., *XOMA 052, an anti-IL-1{beta} monoclonal antibody, improves glucose control and {beta}-cell function in the diet-induced obesity mouse model.* Endocrinology, 2010. **151**(6): p. 2515-27.

217. Krakauer, T., *Inflammasome, mTORC1 activation, and metabolic derangement contribute to the susceptibility of diabetics to infections.* Med Hypotheses, 2015. **85**(6): p. 997-1001.

218. Frank, L., J.R. Bucher, and R.J. Roberts, *Oxygen toxicity in neonatal and adult animals of various species.* J Appl Physiol Respir Environ Exerc Physiol, 1978. **45**(5): p. 699-704.

219. Maharjan, S., et al., *Mitochondrial impairment triggers cytosolic oxidative stress and cell death following proteasome inhibition.* Sci Rep, 2014. **4**: p. 5896.

220. Coughlan, M.T., et al., *RAGE-induced cytosolic ROS promote mitochondrial superoxide generation in diabetes.* J Am Soc Nephrol, 2009. **20**(4): p. 742-52.

221. Wang, J. and D.E. Edmondson, *Topological probes of monoamine oxidases A and B in rat liver mitochondria: inhibition by TEMPO-substituted pargyline analogues and inactivation by proteolysis.* Biochemistry, 2011. **50**(13): p. 2499-505.

222. Vaishnav, R.A., et al., *Lipid peroxidation-derived reactive aldehydes directly and differentially impair spinal cord and brain mitochondrial function.* J Neurotrauma, 2010. **27**(7): p. 1311-20.

223. Zhang, Y., et al., *Mitochondrial aldehyde dehydrogenase (ALDH2) protects against streptozotocin-induced diabetic cardiomyopathy: role of GSK3beta and mitochondrial function.* BMC Med, 2012. **10**: p. 40.

224. Liu, Z., et al., *Protein kinase RNA-like endoplasmic reticulum kinase (PERK)/calcineurin signaling is a novel pathway regulating intracellular calcium accumulation which might be involved in ventricular arrhythmias in diabetic cardiomyopathy.* Cell Signal, 2014. **26**(12): p. 2591-600.

225. Liu, Z., et al., *Circulating interleukin-1beta promotes endoplasmic reticulum stress-induced myocytes apoptosis in diabetic cardiomyopathy via interleukin-1 receptor-associated kinase-2.* Cardiovasc Diabetol, 2015. **14**(1): p. 125.

226. Plaisance, V., et al., *Endoplasmic Reticulum Stress Links Oxidative Stress to Impaired Pancreatic Beta-Cell Function Caused by Human Oxidized LDL.* PLoS One, 2016. **11**(9): p. e0163046.

227. Tu, B.P. and J.S. Weissman, *Oxidative protein folding in eukaryotes: mechanisms and consequences.* J Cell Biol, 2004. **164**(3): p. 341-6.

228. Sevier, C.S., et al., *Modulation of cellular disulfide-bond formation and the ER redox environment by feedback regulation of Ero1.* Cell, 2007. **129**(2): p. 333-44.

229. Malhotra, J.D., et al., *Antioxidants reduce endoplasmic reticulum stress and improve protein secretion.* Proc Natl Acad Sci U S A, 2008. **105**(47): p. 18525-30.

230. Luo, M., et al., *Diabetes increases mortality after myocardial infarction by oxidizing CaMKII.* J Clin Invest, 2013. **123**(3): p. 1262-74.

231. Sood, A., et al., *A Mitofusin-2-dependent inactivating cleavage of Opa1 links changes in mitochondria cristae and ER contacts in the postprandial liver.* Proc Natl Acad Sci U S A, 2014. **111**(45): p. 16017-22.

232. Bravo, R., et al., *Increased ER-mitochondrial coupling promotes mitochondrial respiration and bioenergetics during early phases of ER stress.* J Cell Sci, 2011. **124**(Pt 13): p. 2143-52.

233. Csordas, G., et al., *Structural and functional features and significance of the physical linkage between ER and mitochondria.* J Cell Biol, 2006. **174**(7): p. 915-21.

234. Rizzuto, R., et al., *Close contacts with the endoplasmic reticulum as determinants of mitochondrial Ca2+ responses.* Science, 1998. **280**(5370): p. 1763-6.

235. Rowland, A.A. and G.K. Voeltz, *Endoplasmic reticulum-mitochondria contacts: function of the junction.* Nat Rev Mol Cell Biol, 2012. **13**(10): p. 607-25.

236. Arruda, A.P., et al., *Chronic enrichment of hepatic endoplasmic reticulum-mitochondria contact leads to mitochondrial dysfunction in obesity.* Nat Med, 2014. **20**(12): p. 1427-35.

237. Dorn, G.W., 2nd, M. Song, and K. Walsh, *Functional implications of mitofusin 2-mediated mitochondrial-SR tethering.* J Mol Cell Cardiol, 2015. **78**: p. 123-8.

238. Konig, A., C. Bode, and H. Bugger, *Diabetes mellitus and myocardial mitochondrial dysfunction: bench to bedside.* Heart Fail Clin, 2012. **8**(4): p. 551-61.

239. Dai, D.F., et al., *Mitochondrial targeted antioxidant Peptide ameliorates hypertensive cardiomyopathy.* J Am Coll Cardiol, 2011. **58**(1): p. 73-82.

240. Koncsos, G., et al., *Diastolic dysfunction in prediabetic male rats: Role of mitochondrial oxidative stress.* Am J Physiol Heart Circ Physiol, 2016. **311**(4): p. H927-H943.

241. Zheng, J., et al., *Chymase mediates injury and mitochondrial damage in cardiomyocytes during acute ischemia/reperfusion in the dog.* PLoS One, 2014. **9**(4): p. e94732.

242. Garcia-Diaz, D.F., et al., *Vitamin C in the treatment and/or prevention of obesity.* J Nutr Sci Vitaminol (Tokyo), 2014. **60**(6): p. 367-79.

243. Debreceni, B. and L. Debreceni, *Why do homocysteine-lowering B vitamin and antioxidant E vitamin supplementations appear to be ineffective in the prevention of cardiovascular diseases?* Cardiovasc Ther, 2012. **30**(4): p. 227-33.